HAWASSA UNIVRSITY

INSTITUTE OF TECHNOLOGY

FACULTY OF ELECTRICAL ENGINEERING

DEPARTMENT OF ELECTRICAL AND COMPUTER ENGINEERING

Performance Analysis of High Speed Fiber Optic Communication Systems with Optical OFDM and Dispersion Compensation Technique

By: Girma Hasena Hinsene

Advisor: Demissie Jobir (PhD)

Co- Advisor: Abraham Lule (MSc)

A Thesis Submitted to the Department of Electrical and Computer Engineering in Partial Fulfillment of the Requirements for the Degree of Masters of Science in Communication Engineering and Networking

January, 2022

Hawassa, Ethiopia

PERFORMANCE ANALYSIS OF HIGH SPEED FIBER OPTIC COMMUNICATION WITH OPTICAL OFDM AND DISPERSION COMPENSATION TECHNIQUE

GIRMA HASENA HINSENE

ADVISOR: Dr. DEMISSIE JOBIR GALMECHA

CO-ADVISOR: Mr. ABRAHAM LULE(M.Sc.)

A THESIS SUBMITTED TO THE DEPARTMENT OF ELECTRICAL AND COMPUTER ENGINEERING, IN PARTIAL FULFILMENT OF THE REQUIREMENT FOR THE DEGREE OF MASTER OF SCIENCE IN COMMUNICATION ENGINEERING AND NETWORKING

January, 2022

ADVISORS' APPROVAL SHEET

SCHOOL OF GRADUARE STUDIES

HAWASSA UNIVERSITY ADVISORS' APPROVAL SHEET

(Submission Sheet-I)

This is to certify that the thesis entitled **PERFORMANCE ANALYSIS OF HIGH SPEED FIBER OPTIC COMMUNICATION SYSTEMS WITH OPTICAL OFDM AND DISPERSION COMPENSATION TECHNIQUE** submitted in partial fulfillment of the requirements for the degree of masters of science in communication engineering and networking, the graduate program of the department of electrical and computer engineering and has been carried out by **GIRMA HASSENA HINSENE** Id. No. PGComW/009/09 under our supervision. Therefore, we recommend that the student has fulfilled the requirements and hence hereby can submit the thesis to the department.

Dr. Demissie Jobir		_____
Name of advisor	Signature	Date
Abraham Lule (MSc.)	_____	_____
Name of co-Advisor	Signature	Date

Declaration

I, the undersigned, declare that this MSc. thesis is my own original work and has not been presented for a degree in this or any other university and any materials used from other sources has been clearly identified, properly acknowledged and cited.

Girma Hassena	_____	_____
Name	Signature	Date

Date of Submission: _____

Place: Hawassa, Ethiopia

This thesis has been submitted for examination by the approval of Advisor and co-Advisors:

Dr. Demissie Jobir		_____
Advisor	Signature	Date
Mr. Abraham Lule	_____	_____
Co- Advisor	Signature	Date

January, 2022

Hawassa University, Hawassa, Ethiopia

EXAMINERS' APPROVAL SHEET

SCHOOL OF GRADUATE STUDIES

HAWASS UNIVERSITY EXAMINERS' APPROVAL SHEET

(Submission sheet-II)

We, the undersigned, members of the board of examiners of the final open defense by Girma Hasena have read and evaluated his thesis entitled "PERFORMANCE ANALYSIS OF HIGH SPEED FIBER OPTIC COMMUNICATION SYSTEMS WITH OPTICAL OFDM AND DISPERSION COMPENSATION TECHNIQUE" and examined the candidate. This is therefore to certify that the thesis has been accepted in partial fulfillment of the requirements for the degree.

Dejene Hurissa (MSc.)	_____	_____
Name of Chair person	Signature	Date
Demissie Jobir (PhD.)		_____
Name of main advisor	Signature	Date
Abraham Lule (MSc.)	_____	_____
Name of co- advisor	Signature	Date
Shanko Chura (MSc.)	_____	_____
Name of Internal Examiner	Signature	Date
Sultan Feisso (PhD.)		_____
Name of External Examiner	Signature	Date

Final approval and acceptance of the contingent upon the submission of the final copy of the thesis to the School of Graduate Studies (SGS) through the Department/ School Graduate Committee (DGC/SGC) of the candidate department.

_____	_____
Stamp of SGS	Date

Acknowledgment

I praise you God, for who you are and for everything. Let everything that has breath praise the God.

First and foremost, I am appreciative to my advisor, Dr. Demissei Jobir, for his excellent guidance, consistent support, and patience during the process of this research. His vast knowledge and depth of experience have assisted me throughout my academic career and everyday life.

Next, I would like to thank my co-advisor Mr. Abraham Lule, for his meaningful and constructive feedbacks, and unreserved support. I also would like to thank Mr. Fitsum Zerfu and Mr. Alemayehu Cheru for their valuable feedback and recommendation.

I would like to extend my heartfelt gratitude to friends and classmate students for their technical support on my study. Finally, I'd like to thank my entire family, especially my mother Luku Burka, my partner Shegu Safawo, and my daughter, Firiftu. It would have been difficult for me to finish my studies without their wonderful understanding and inspiration throughout the last few years.

Abstract

Several designers are employing fiber optics instead of copper wire to transport information between data ports to fulfill the high-speed requirements of today's communication systems since it offers several advantages such as high transmission capacity and low losses. Limitations and flaws such as chromatic dispersion hamper the performance of optical fiber communication systems. Tolerating the effects of chromatic dispersion in optical communication systems, various classic dispersion compensation techniques such as Dispersion Compensation Fiber (DCF) and Fiber Bragg Grating (FBG) have been used. Advanced modulation schemes, such as orthogonal frequency division multiplexing (OFDM), are excellent candidates for improving spectrum efficiency in communication systems by reducing chromatic dispersion effects. That is FBG uses the principle of recompression of light signals with different wavelengths to reduce the effect of chromatic dispersion. And OFDM uses the orthogonality principle between subcarriers with the insertion of cyclic prefix and guard bands to reduce the effect of chromatic dispersion. The performance of a high-speed optical fiber communication system was investigated using coherent optical OFDM (Co-O-OFDM) and Fiber Bragg grating (FBG) as dispersion compensation techniques in this thesis study. The system models were simulated using Optisystem simulation software, and the output was plotted using MATLAB. Performance measuring metrics such as optical signal to noise ratio (OSNR), bit error rate (BER) and Quality-factor were used to thoroughly examine the results. RF spectrum, optical spectrum, and constellation diagram of the signal were examined at different distances to see the effect of chromatic dispersion. The performance of both DP-16QAM Co-O-OFDM and FBG integrated DP-16QAM Co-O-OFDM systems declined as the signal propagated long distances of fiber optic for four different rates due effect of chromatic dispersion, and FBG integrated DP-16QAM Co-O-OFDM system performed better for the same rate and distance due to integration of FBG.

Key Words: Orthogonal Frequency Division Multiplexing, Chromatic Dispersion, Fiber Bragg Grating, Optical Signal to Noise Ratio, Bit error rate, Quality factor

Table of Contents

List of Figures

List of Abbreviations

A/D	Analog to Digital
ADC	Analogue-to-Digital Converter
APD	Avalanche Photo Diode
ASK	Amplitude Shift Keying
BER	Bit Error Rate
CAM	Constellation Adjustment Method
CATV	Cable Television
CD	Chromatic Dispersion
CMA	Constant Modulus Algorithm
Co-O-OFDM	Coherent Optical OFDM
CP	Cyclic Prefix
CR	Compensation Ratio
CW-Laser	Continues Wave Laser
D/A	Digital to Analog
DAC	Digital to Analog Conversion
DCF	Dispersion Compensation Fiber
DCIs	Data Center Interconnections
DD-LMS	Decision Direct Least Mean Square
DD-O-OFDM	Direct Detection Optical OFDM
DFB	Distributed Feedback
DFE	Decision Feedback Equalizers
DFT	Discrete Fourier Transform
DP-16QAM	Dual Polarization 16 Quadrature Amplitude Modulation
DP-QPSK	Dual Polarization Quadrature Phase Shift Keying
DQPSK	Dual Quadrature Phase Shift Keying
DSP	Digital Signal Processing
EDC	Electronics Dispersion Compensation
EDFA	Erbium Doped Fiber Amplifier
FBG	Fiber Bragg Grating
FDE	Frequency Domain Equalizer
FDM	Frequency Division Multiplexing
FEC	Forward Error Correction
FFE	Feed Forward Equalizer
FFT	Fast Fourier Transform
FPL	Fabry-Perot Laser
ICI	Inter Carrier Interference
IDFT	Inverse Discrete Fourier Transform
IF	Intermediate Frequency
IFFT	Inverse Fast Fourier Transform
IMDD	Intensity Modulated-Direct Detection
IQM	In phase Quadrature Modulator

ISI	Inter Symbol Interference
ITU-T	International Telecommunication Union -Telecommunication
LAN	Local Area Network
LD	Laser Diode
LED	Light Emitting Diode
LMS	Least Mean Square
LO	Local Oscillator
LPF	Low Pass Filter
LSD	Least Significant Dibit
MAN	Metropolitan Area Network
MIMO	Multiple Input Multiple Output
MMF	Multi-Mode Fiber
MMSE	Minimum Mean Square Error
MSD	Most Significant Dibit (MSD) and the least significant dibit (LSD).
MZM	Mach-Zehnder Modulator
NRZ	Non-Return to Zero
OA	Optical Amplifier
OFDM	Orthogonal Frequency Division Multiplexing
O-OFDM	Optical OFDM
OOK	On Off Keying
OPC	Optical Phase Conjugate
OS	Optical Spectrum
OSNR	Optical Signal to Noise Ratio
PDM	Polarization Division Multiplexed
PMC-SH	Polarization Multiplexed Carrier based Self-Homodyne
PMD	Polarization Mode Dispersion
PON	Passive Optical Network
PRBS	Psuedo Random Binary Sequence
PRM/CAM	Phase Rotation Method/Constellation Adjustment Method
QAM	Quadrature Amplitude Modulation
Q-factor	Quality Factor
QPSK	Quadrature Phase Shift Keying
RF	Radio Frequency
RoF	Radio Over Fiber
SMF	Single Mode Fiber
SNR	Signal to Noise Ratio
SSB	Single Side band
SSMF	Standard Single Mode Fiber
TAE	Tunable Adaptive Equalizer
TDM	Time Division Multiplexing
VCSEL	Vertical-Cavity Surface-Emitting Laser
WDMSCM-OFDM	Wave Division Multiplexing Subcarrier Multiplexing OFDM

CHAPTER ONE

Introduction

1.1. Background

The growth of human civilization has been aided by information transmission. A communication system's major goal is to transfer the most data bits per second across the shortest distance possible with the lowest errors[1]. As shown in Figure 1.1, the demand for high-capacity communication systems is growing at an exponential rate as a result of the introduction of various new applications such as video conferencing and broadband wireless communication[2]. As a result, the next generation of access networks, such as 5G, is hastening the need for wired and wireless services to be converged in order to provide end customers with more choice, convenience, and diversity in a more efficient manner. To put it another way, new telecommunications systems necessitate huge transmission bandwidth and dependable mobility.

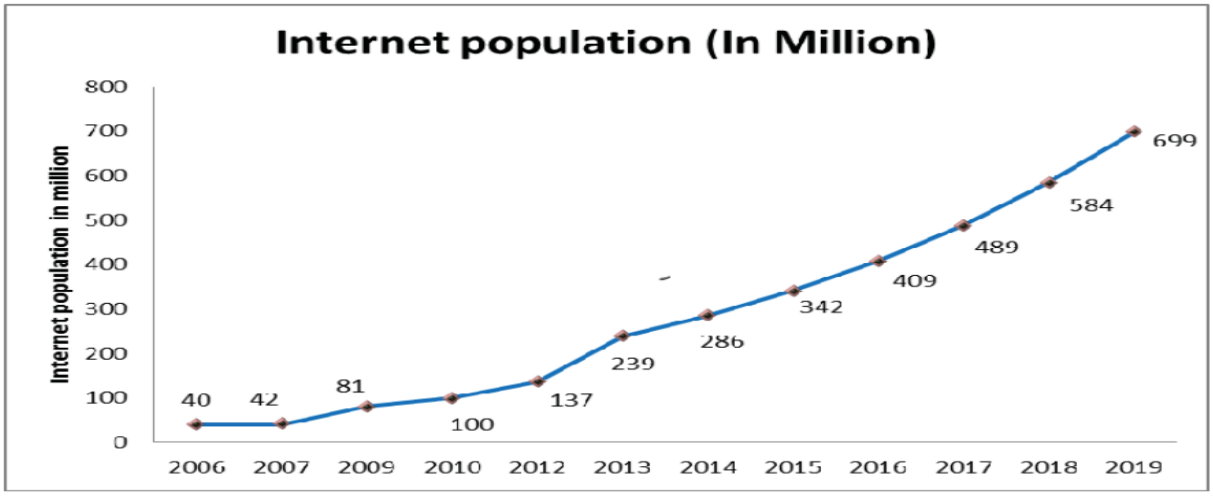

Figure 1. 1: Increase in internet users [2]

These enormous bandwidth and high speed communication system requirements can only be met by optical fiber connection, therefore the evolution of optical communication must continue to meet the ever-increasing bandwidth demands of consumers from the backbone side[3]. These factors have prompted the researcher to devise and test various strategies for increasing the transmission capacity of optical terrestrial and wireless networks.

1.2. Optical Fiber Communication System

Fiber optic communication systems were introduced into the telecommunication system because of the growing demands for high data rates in modern communication systems, as mentioned above. Fiber optic communication is a means of transferring light pulses over an optical fiber to transport data from one location to another. Light is a modulated electromagnetic carrier wave that carries information[4, 5]. The availability of a large optical spectrum for communication is what makes optical communication appealing. Optical fiber has mainly supplanted copper wire communications in core networks and long transmission systems due to its benefits over electrical transmission.

1.2.1. Linear Effects in Optical Fiber Communication system

Distinct linear effects caused the majority of the signal transmission losses in optical fibers. Linear effects include dispersion and numerous optical signal losses such as attenuation [9].

1.2.1.1. Fiber Loss

Transmission loss is defined as a decrease in the number of signal pulses or signal strength as the signal length grows. Impurities are the primary cause of optical fiber loss in silica-based materials. Because of infrared photon absorption, the loss rises at shorter wavelengths. Material absorption, scattering, mode coupling, leak modes, fiber bending and design, radiation induced attenuation, poor construction losses, inversion square law losses, transmission losses, core and cladding losses, and radiation induced attenuation are some of the multiple sources of loss. Even while fiber attenuation is quite low in current fiber optics (0.2dB/km), it is still a major element for linear effect, which gradually reduces signal power and necessitates signal amplification over a certain distance to compensate for these losses.

1.2.1.2. Fiber Dispersion

In an optical communication system, the accuracy and reliability of data transmission is influenced not only by the performance of the optical transmitter and receiver, but also by the influence of dispersion. Dispersion is the spreading of a light pulse as it travels along the length of an optical cable, as seen in figure 1.2. Dispersion limits the bandwidth or information carrying capacity of a fiber. This causes the pulse to overlap with the nearby pulses, making it difficult to precisely

reconstruct the original signal[6]. Inter-symbol interference (ISI) is caused by dispersion, which affects the correct assessment of optical pulse signals at the receiving end, degrades BER performance, and even changes sent data.

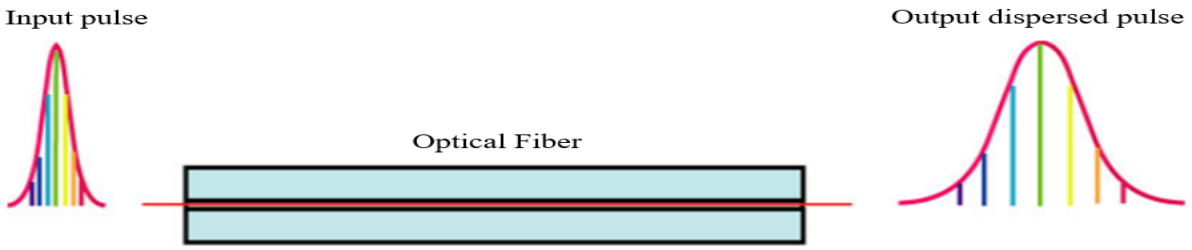

Figure 1. 2: Effect of dispersion on an optical pulse in a fiber link [56]

The light pulse that enters a fiber is made up of numerous different wavelength light waves. As a result, each wave passes through the medium at a different speed. The pulses become advanced and delayed as a result of this, causing the pulse to spread. Chromatic dispersion is the name given to this sort of dispersion[7, 8]. Single mode fiber (SMF) is dominated by polarization mode dispersion in areas where chromatic dispersion is minimal. This occurs when waves of different polarization propagate at different speeds, causing the pulse to spread.

1.2.2. Nonlinear Effects in Optical Fiber Communication system

Fiber nonlinearities can degrade the performance of an optical communication system. As a result, the existence of this nonlinear effect in an optical communication system might cause communication between two receiving locations to be disrupted. The Kerr effect and stimulated scattering are examples of nonlinear effects generated by the intensity dependence of the refractive index[17].

The Kerr nonlinearity occurs when the transmitted signal strength affects the refractive index in fiber optics. The stimulated elastic scattering effect is another sort of optical fiber nonlinear phenomenon that aids in the transfer of energy from the optical field to the medium.

Nonlinear impairments in glass might affect signal transmission quality to the desired site. Nonlinearity is frequently confused with dispersion. Optical fiber nonlinearity effects cause channel interaction when multiple channels are examined. These nonlinear impairments can be mitigated with good system design.

1.3. Optical Fiber Communication System and OFDM

So, why do optical fiber communication systems require orthogonal frequency division multiplexing (OFDM)? To match the world's growing demand for high communication capacity, next-generation optical fiber communication systems are expected to operate at rates of 1Tb/s and higher, either in a single channel or multichannel configuration[9, 10]. The spectral efficiency (SE), which is a ratio of bit rate to used bandwidth, is a metric for determining how efficiently we are utilizing the fiber's usable spectrum. The performance of optical fiber communication systems is degraded for two primary reasons. The first is a mishandling of a large optical spectrum that will be used in optical fiber communication systems. That is a poor choice or a rash combination of different approaches, such as modulation techniques, for both single and multichannel applications. For example, if a single carrier system is modulated using the On Off Keying (OOK) modulation scheme[11, 12], the system's SE will be about 0.2 bit/s/Hz, which is excessively low.

The second reason is the effect of multipath fading, like dispersion, as previously explained. In Fiber optics communication systems, dispersion is a major issue that restricts the quality of the transmitted signal's performance. It generates pulse distortion and signal widening, which increases the bit error rate and signal deterioration. In an optical fiber link, it also restricts the number of channels. Traditional dispersion compensation techniques, such as Dispersion Compensating Fiber(DCF), are available. These traditional dispersion correction procedures, on the other hand, become expensive and time-consuming as data rates increase[13, 14], and it is difficult to accurately compensate the dispersion.

For the above two reasons and others, multi-carrier modulation like orthogonal frequency division multiplexing (OFDM) is introduced to optical communication. OFDM is a modulation scheme that offers a high data rate while also being resistant to multipath fading. The baseband data in OFDM is spread across numerous carriers, resulting in a data symbol that is lengthy enough to overcome any signal delay spread.

1.4. Statement of the problem

One of the most important considerations in the process of realizing high-speed fiber optic communication systems to meet users' growing demand for systems with more bandwidth and spectral efficiency is to choose the best method and technique for reducing the influence of chromatic dispersion in optical fiber communication links. Chromatic dispersion which consists of both wave guide and material dispersions, is the pulse broadening that occurs in a single mode fiber due to finite spectral width of the optical sources. Chromatic dispersion distorts signal and degrades performance of fiber optic communication system. Both traditional dispersion compensation techniques and optical OFDM have the ability to combat the effect of chromatic dispersion in the optical link. But performance of these traditional dispersion compensation techniques decreased as transmission capacity of the system increases. So in this thesis work, the influence of chromatic dispersion on high speed fiber optic communication was analyzed using optical OFDM and integration of optical OFDM and dispersion compensation technique.

1.5. Objectives

1.5.1. General Objective

- General objectives of this thesis is performance analysis of high speed fiber optic communication system using optical orthogonal frequency division multiplexing (O-OFDM) and dispersion compensation technique.

1.5.2. Specific Objectives

- Performance analysis of 100Gb/s, 200Gbits/s, 400Gbits/s and 1Tbits/s Co-O-OFDM systems over different propagation distances of SMF for single user
- Performance investigation of 100Gb/s, 200Gbits/s, 400Gbits/s and 1Tbits/s FBG integrated Co-O-OFDM systems over different propagation distances of SMF for single user

1.6. Research Contributions

This thesis work has the following contributions: -

- Selection and integration of optical OFDM and dispersion compensation technique types which can be suited to each other in working principle so that chromatic dispersion effect will be reduced efficiently in high speed fiber optic communication system. Chromatic dispersion mostly occurs and worth in SMF due to variation of phase and group velocities with wavelength, so based on this Co-O-OFDM and FBG are selected and integrated.
- Exploring the method to enhance the capacity of fiber optic communication system or spectral efficiency of fiber optic communication system by integrating multicarrier modulation system (i.e. Co-O-OFDM) with advanced single carrier dual polarization modulation (i.e. DP-16QAM) technique.

1.7. Significance of the Study

Coherent optical OFDM (Co-O-OFDM) is a new optical communications technology that combines the benefits of both coherent and OFDM systems into a single optical fiber. The Co-O-OFDM modulation system provides a high spectral efficiency and a wide bandwidth. Many optical fiber barriers, such as chromatic dispersion (CD) induced by inter-symbol interference(ISI), can be overcome with the Co-O-OFDM system (ISI). Independently, the Co-O-OFDM and FBG methods can provide high spectrum efficiency and boost receiver sensitivity by minimizing chromatic dispersion. Co-O-OFDM and FBG are important options for long-haul optical communication because of their ability to counteract chromatic (CD). The relevance of this research is that it inherits and integrates the benefits of Co-O-OFDM and FBG approaches for reducing chromatic dispersion in high-speed fiber optic communication systems, as well as demonstrating the novelty of the optical OFDM idea in fiber optic communication systems.

1.8. Scope and Limitations of the thesis

In this thesis performance of high speed fiber optic communication systems were analyzed and evaluated using Co-O-OFDM and integration of Co-O-OFDM and FBG. Here are scope and limitations of the thesis.

- 100Gbps, 200Gbps, 400Gbps and 1Tbps capacity Co-O-OFDM and Co-O-OFDM and FBG integrated systems were analyzed at different distances.
- DP-16QAM modulation technique was used for mapping and de-mapping of single carrier
- The performance evaluation was carried out for a single user with frequency 192.1 THz.
- Standard single mode fiber was used.
- Influence of fiber impairment called chromatic dispersion was analyzed in the two models.

1.9. Organization of the Study

This study is organized into six chapters as follow:

Chapter One covers the background, explanation of the problem, goals, specific objectives, significance of the study, scope of the study, and limitations of the study. The literature review and associated works are discussed in Chapter 2. Chapter 3 discusses methods and materials. The mathematical and system models of Co-O-OFDM, as well as the integration of Co-O-OFDM and FBG systems, are discussed in Chapter 4. Chapter 5 covers the setup of Co-O-OFDM parameters, simulation, results, and discussion, as well as the use of analytical tools to integrate Co-O-OFDM with the FBG system. The conclusion and next work recommendations are presented in Chapter 6.

CHAPTER TWO

Literature Review

2.1. Introduction

To fulfill the increased bit rate demand in future applications, efficient usage of communication resources is a fundamental challenge in modern communication technology. The performance of high-speed fiber optic communication networks has been evaluated in a number of research. In thesis work, a few articles are examined that are relevant to this work by the study's problem and the methodology utilized in the analysis, as listed below.

2.2. Related Works

The performance analysis of RoF links with and without optical OFDM for multichannel to reduce non-linearity impacts of the channel employed a hybrid wave division multiplexing subcarrier multiplexing (WDMSCM-OFDM) passive optical network (PON) architecture and radio over fiber (RoF) technology [15]. Different digital quadrature amplitude modulation techniques were used to evaluate the network's performance. 16 QAM-OFDM outperformed 4 QAM-OFDM and 64 QAM OFDM, according to the results. Furthermore, 64 QAM-OFDM has the largest noise ratio, with a little change in signal to ratio compared to 16 QAM-OFDM.

For the system with coherent optical OFDM, the Constellation Adjustment Method (CAM) was suggested to compensate both chromatic and residual dispersion efficiently after compensation [16]. Optisystem was used for 107-Gb/s single-channel transmission over 1000-km Standard Single Mode Fiber (SSMF) with polarization division multiplexing Four Quadrature Amplitude Multiplexing (4-QAM). In addition, simulations were run at various transmission distances. Non-Return to Zero (NRZ) systems have a lower Min. BER and a higher Max. Q factor than OFDM systems.

The author examined the performance study and simulation of high data rate employing direct and coherent optical OFDM for long haul transmission in [17]. The author begins with a single user and progresses to the implementation of a 100Gbit/s OFDM-WDM system. That is, three separate systems were modeled utilizing direct and coherent OFDM detection with different data rates. The

first was DD-O-OFDM, which employs a 7.5GHz frequency carrier. This system investigated different transmission lines with a data rate of 10Gbits/s and modulation type of 16-QAM, 256 subcarriers, and 512 FFT points. It has been discovered that as the transmission length increases, the Q-factor lowers, resulting in a lower BER value. The best BER value was 0. The second system was a Co-O-OFDM with SMF system with a data rate of 40 Gbits/s, 16-QAM modulation, 512 subcarriers, and 1024 FFT points. The transmission line was 150 kilometers long. This system was created and tested in order to get the best BER value of zero. WDM CO-OFDM with a 120km SMF-DCF transmission link was the final project. The carrier wave frequencies were adjusted from 193.05THz to 193.2THz with 50GH channel spacing, 512 subcarriers, and 1024 FFT points. This system was created and tested in order to get the best BER value of zero.

The authors in[18] discussed OFDM transmission over optical connections using good spectral efficiency by via high-order QAM modulation methods as a mapping mechanism before the OFDM multicarrier representation. They suggested a nonlinear electrical equalization system based on the Wiener-Hammerstein model to address coherent optical OFDM across long distances, which is influenced by nonlinear distortion produced by fiber nonlinearity. The Wiener Hammerstein model-based equalizer can dramatically minimize nonlinear distortion when compared to other prominent linear compensation approaches like the LMS (Least Mean Square) employed in a coherent OFDM system.

In performance investigation of 112 Gb/s PDM-QPSK and 224 Gb/s PDM-16-QAM systems, digital signal processing (DSP) based equalization algorithms for CD and PMD compensation were developed and optimized[19]. FDEs have been investigated and proposed as the most efficient option for CD compensation in long-haul fiber lines with high CD levels. The results demonstrated that a 1024-point FFT-based FDE can successfully correct for fiber CD up to 48000 ps/nm (i.e. 3000 km fiber link). Furthermore, MIMO equalization approaches for polarization DE multiplexing, PMD, and residual CD compensation have been researched and optimized. In this case, the update process' computational complexity is lowered by a factor of P, and the decision directed least mean square (DD-LMS) based MIMO equalizer outperforms the constant modulus algorithm (CMA)-QAM-based MIMO equalizer. In other words, in terms of performance and computing complexity, the PU-DD-LMS based MIMO equalizer is the most viable solution.

To mitigate inter-symbol interference owing to dispersion, a relative investigation of the optical communication system using 16-QAM modulation with and without OFDM was conducted in[20]. These include optical communication system design, modeling, simulation, and comparative performance analysis with and without OFDM for dispersion compensation. This study presents a new tunable dispersion compensation technique based on DD-O-OFDM. For long-haul high-data-rate transmission with high bandwidth utilization efficiency, OFDM has been shown to outperform in high-data-rate optical communication systems. As a result, the most efficient technique for next-generation long-haul high-capacity communication networks is integrating an optical system with OFDM.

Authors examined the performance of a hybrid optical OFDM system with high order dispersion compensation in[21]. This journal proposes a tunable adaptive equalizer (TAE) system at the receiver end to recover higher-order dispersion that is not compensated by DCF. It addressed a coherent OFDM system that used QAM modulation as a mapper and demapper, as well as a Mach-Zehnder modulator as an optical modulator, with a 25 Gbaud rate and passed OFDM in phase and quadrature to a low pass filter. It was demonstrated that the system may be used for both short and long distance transmission at very high data rates by combining the advantages of Coherent OFDM and QAM modulation. This increases system flexibility and delivers a vast coverage area for telecommunication networks without significantly raising the system's cost and complexity.

Two model systems, one with Phase Rotation Method/Constellation Adjustment Method (PRM/CAM) and the other without, were built to evaluate the BER performance of the system using Coherent OFDM dual polarization[22]. The compensation of chromatic dispersion (CD) and residual dispersion in long-haul optical fiber networks was demonstrated experimentally using both coherent and direct-detection optical OFDM. Advanced modulation formats (Quadrature phase keying and Quadrature amplitude modulations) were utilized in the simulations as a mapper and de-mapper. When the same parameters were utilized throughout the studies, Co-OFDM outperformed DDO-OFDM, according to the results. The results revealed that the model with PRM outperformed the model without PRM. Higher modulation methods, such as 256-QAM and 512-QAM, provide lower BER performance than QPSK and 4-QAM. The 4-QAM systems outperformed QPSK, 256-QAM, and 512-QAM systems by a factor of 10^{-2}, 10^{-4} and 10^{-5} respectively at a distance of around 1000 km.

The superchannel polarization division multiplexed coherent optical orthogonal frequency-division Multiplexing (PDM-Co-O-OFDM) system employing midway optical phase conjugation (OPC) demonstrated in [23]. The system was designed to show the optimum number of sub-carriers, amplifier spacing and the maximum achievement distance at data rate of 1Tb/s (10x100 Gb/s). The system was simulated with 10-WDM superchannel at 50 GHz channel spacing. From the simulation results, PDM-CO-OFDM, with midway OPC and the optimum system parameters, we can achieve the maximum reachable distance of 24,000 km at BER $4x10^{-3}$.

The authors presented in [24], analyzed high-capacity coherent data center interconnections (DCIs) using Pol-muxed carrier and LO-less Receiver to reduce higher complexity of receiver in coherent links and much power consumption of the system. It presented a polarization multiplexed carrier based self-homodyne (PMC-SH) system for DCIs that can handle faster data speeds while using the same amount of power as a PAM-4 system. The results satisfactorily evaluate the proposed system for a PMC-SH 16-ary quadrature amplitude modulation (16 QAM) link with a capacity of 200 Gbs (50 Gboud). A 32 Gboud (128 Gb/s) PMC-SH 16-QAM link for a normal single-mode fiber channel is also demonstrated. Analytically, the PMC-SH scheme produces a drastically reduced bit rate error for a given transmission bit rate or can double the data rate for a given electronics bandwidth (when compared with the PAM-4 system).

Selective QAM subcarrier method was proposed to release 50Gbs DD-O-OFDM transmission after 80km without dispersion compensation fiber (DCF) based on selective subcarrier-filling using an electronic-absorption modulator[25]. 64-QAM, 16-QAM and 4-QAM single carrier modulation were used to fit the fading channel and improve spectral efficiency. Using selective QAM subcarrier the power fading problem efficiently solved with 20-GHz bandwidth.

Based on dual polarization of signal in [26], author designed 100 Gb/s QAM modulated Co-O-OFDM to increase performance of conventional Co-O-OFDM. Performance of the system is assessed using QAM modulation format and suggested system using signal over 576 km optical link. In dual polarization multiplexed QAM modulated Co-O-OFDM system, the influence of dispersion is significantly compensated by post dispersion compensation technique. The spectral efficiency of the dual polarization multiplexed QAM modulated Co-O-OFDM is better as compared to conventional QAM modulated of Co-O-OFDM.

In [27], the authors suggested a coherent optical system that compensates for IQ imbalance and estimates channel. It looks into the effects of IQ mismatch on coherent optical transmission across a single-mode fiber on both the transmitter and receiver sides. It specifically explored alternative frequency domain methods for concurrently compensating the IQ mismatch and equalizing the optical fiber channel while accounting for the influence of chromatic dispersion. When compared to the traditional method of coherent optical OFDM, the proposed minimal mean square error (MMSE) compensation mechanism performs better.

To reduce cost of optical amplifier in the OFDM radio over fiber system authors in [28], proposed a system using direct detection Mach Zehnder Modulator (DD-MZM). This article addresses a 4-QAM and 16-QAM based OFDM-RoF system with an FBG based dispersion compensator and a direct detection Mach Zehnder Modulator (DD-MZM) capable of directly generating a single side band (SSB) signal at transmission distances of 70 and 50 kilometers, respectively. The spectral efficiency of a proposed system is quite impressive in the absence of optical amplifier. Although a 16-QAM system may function at a higher data rate than a 10Gbs system, symbol defects limit its performance.

The influence of chromatic dispersion was demonstrated experimentally and analyzed numerically using the Co-O-OFDM system in [29]. It looked at the effects of dispersion maps on the 10.7- and 42.8-Gb/s Co-O-OFDM systems. It also looked at the system's performance at 107 Gb/s with different dispersion compensation ratios (CR). The OFDM characteristics are as follows: 128 subcarriers with the middle 82 filled with data, four-quadrature amplitude modulation (4-QAM) encoding, guard interval of 1/8 of the observation period, and phase estimation using four pilot subcarriers. A Tektronix arbitrary waveform generator generates the analog signal. To create a multi-frequency optical source, two cascaded intensity modulators were used. Each OFDM sub-band is filled with exactly the same OFDM data. The optical OFDM signal is then sent into a polarization diversity transmitter, which consists of a polarization splitter/combiner with one OFDM symbol delayed on one branch. The optical signal from the recirculation loop is down-converted using a polarization diversity coherent receiver. When comparing the inline dispersion-compensated wavelength-division-multiplexing (WDM) systems to the non-compensated counterpart, it was observed that the DCF loss, DCF nonlinearity impact, and dispersion map influence are three factors to the reduction. The penalty from dispersion compensation for the data

rate of 10.7-, 42.8-, and 107-Gb/s WDM systems, respectively, is 2.7, 2.2, and 2.8 dB at the optimum launch power, according to simulation. That instance, for 10.7-, 42.8-, and 107-Gb/s WDM systems, the degradation from DCF impact is 2.7, 2.2, and 2.8 dB, respectively, at the optimum launch power.

In the presence of fiber optic dispersion, the performance of Orthogonal Frequency Division Multiplexing (OFDM) combined with Quadrature Amplitude Modulation (QAM) has been investigated [30]. With fiber lengths, bit rates, the number of channels, and source line-widths, the impact of dispersion on the OFDM spectrum is explored. The dispersion-induced broadening of the OFDM spectrum causes inter-channel interference. The system's power penalty is calculated using a bit error rate (BER) of 1×10^{-9} for a single mode fiber operating at 1.55 μm. In comparison to single bit transmission with the same bandwidth, the results obtained from the OFDM–QAM system shows that the effect of dispersion is lower in the OFDM–QAM spectrum.

As we have tried to review few related works, there are many papers investigating high-speed optical fiber communication systems and their superb robustness. However, there are gaps observed in the usage of multicarrier modulation techniques like optical OFDM with dispersion compensation techniques. So in this thesis work, performance of high speed fiber optic communication will be analyzed using both optical OFDM types and dispersion compensation technique.

CHAPTER THREE

Optical Communication System Overview

3.1. Basic Elements of Fiber Optic Transmission System

Both electrical and optical signal sources are used to transmit the optical signal from end to end. Transformation from the electrical to the optical domain requires the use of an optical source, whereas conversion from the optical to the electrical domain involves the use of an optical receiver. [31, 32]. Basic elements of Fiber optic link are Fiber, Transmitter, Receiver, Repeater and Optical amplifier as shown below with figure 3.1.

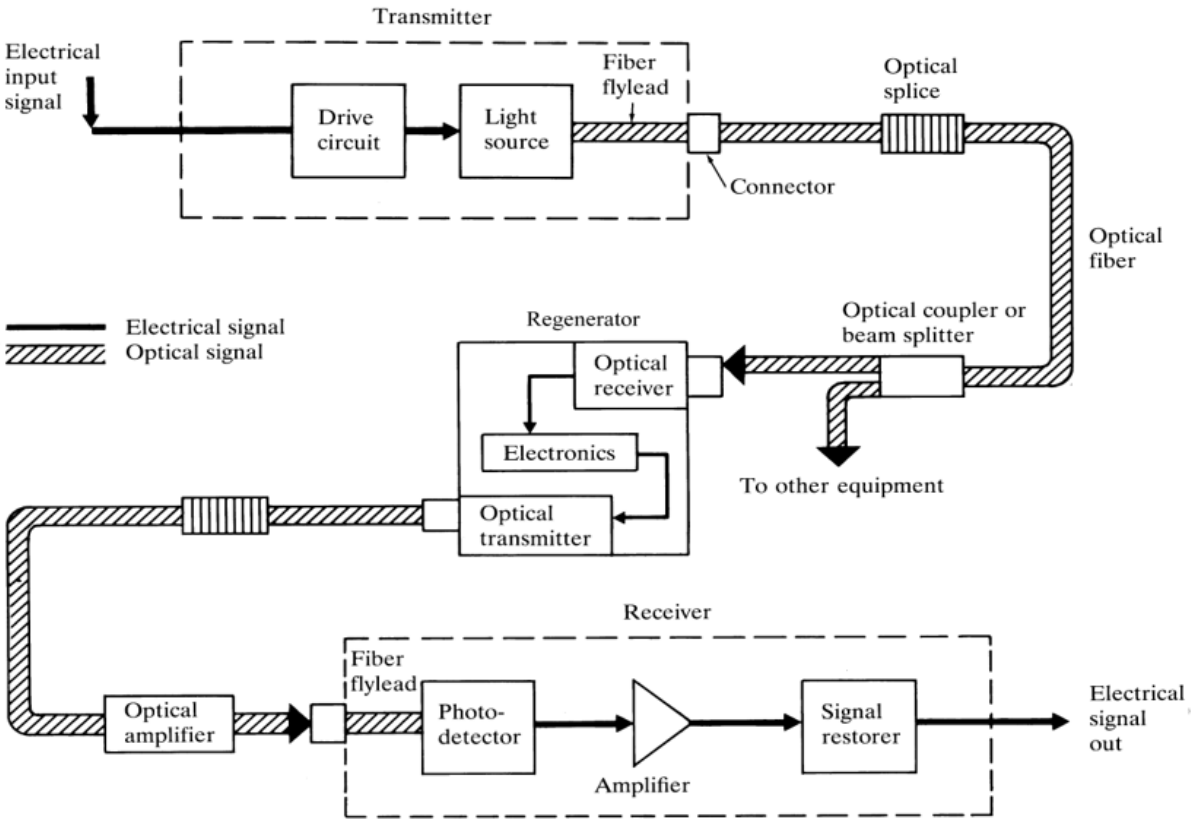

Figure 3. 1: Basic elements of Fiber Optic Link [5]

Optical fibers are used to transport optical signals from one location to another. Because of the enormous bandwidth and minimal loss, high-speed signals may be sent over long distances without the need for regeneration. An optical fiber is made up of two major layers: the core and the cladding, which are both covered by buffer coating. Based on electromagnetic mode exists, there

are two kinds of optical fiber[5, 33]: namely single mode fiber (SMF) and multimode fiber (MMF). SMF has only one mode, offers the highest bit rate and most widely utilized for long-haul distances transmission. MMF has multiple modes, hence it has higher dispersion due to multiple modes, cheaper than SMF and mostly used in local area networks.

A light source and related electronic circuits make up an optical transmitter. The source could be a light-emitting diode (LED) with spontaneous recombination predominant, or a semiconductor laser diode (LD) with stimulated emission dominating[34]. Setting the source operating point, managing light output stability, and altering the optical output in proportion to an electrically formatted information input signal are all done with electronic circuitry. An optical source's principal duty is to convert received electrical signals into optical forms before launching the modulated signal into an optical cable. For stimulated emission in optical systems, therefore, a variety of laser sources can be used[35]: Some examples are the Fabry-Perot laser (FPL), distributed feedback (DFB) laser, and vertical-cavity surface-emitting laser (VCSEL). The received information modulates the optical signal generated by a laser source in optical systems before being sent via an optical cable. This can be accomplished by directly modulating the semiconductor laser's bias current. External modulators apply the real data signal to be communicated[28, 36]. The most popular modulators are electro-optic optical modulators, such as Mach–Zehnder modulators (MZM), and electro-absorption modulators. The main purpose of these modulators is to increase the transmitted optical power in the fiber when high data rates are generated.

Output optical signal that comes from the end of an optical fiber is detected by a photodiode inside the receiver. The photodetector's main job is to receive the optical power generated from the fiber and transform it to electrical power in the form of electrical current. The avalanche photodiode (APD) and the pin photodiode (PIN) are two common photodiodes. PIN has poor performance, little internal gain, and is frequently utilized despite its low cost. APD has a high performance with internal(avalanche) gain.

Repeater receives weak light signal from optical fiber, cleans-up, amplifies and retransmits it. During this process first it converts optical signal to electrical signal and then it will convert electrical signal to optical signal before retransmit. Optical Amplifier amplifies light in fiber without conversion of signal forms.

3.2. Dispersion and its Compensation Techniques

Optical fiber communication system performance can be harmed for a variety of causes. Dispersion, which is described as pulse spreading in an optical cable, is one of the reasons. The spreading of a light pulse as it moves through a fiber is influenced by numerical aperture, core diameter, refractive index profile, wavelength, and laser linewidth[6].

Intersymbol Interference(ISI) is the total influence of dispersion on the performance of a fiber optic system. When dispersion causes the output pulses of a system to overlap and become undetected, this is known as intersymbol interference(ISI) [37]. Dispersion is generally divided into three categories: modal dispersion, chromatic dispersion and polarization mode dispersion.

The time delay between lower-order and higher-order modes causes modal dispersion, which is characterized as pulse spreading[38]. In multimode fiber, modal dispersion is a problem that limits bandwidth. Because the index of refraction of glass fiber is a wavelength-dependent parameter, chromatic dispersion (CD) is defined as pulses spreading owing to different wavelengths of light pulses travelling at somewhat different velocities through the fiber[7, 39]. Material dispersion and waveguide dispersion are the two components of chromatic dispersion. The changing of the refractive index of the core material of a fiber with the change of the optical wavelength causes material dispersion. Another type of chromatic dispersion is waveguide dispersion. The diameter of the fiber core determines waveguide dispersion, which causes signals of different wavelengths to travel at different speeds, spreading the pulse and causing it to overlap with surrounding pulses. Waveguide dispersion is not a large problem in a simple step-index profile fiber, but it can be substantial in fibers with more complex index profiles. This thesis study will go over chromatic dispersion in great detail. Polarization Mode Dispersion (PMD) is caused by birefringence along the fiber's length, which causes different polarization modes to travel at different speeds, resulting in polarization orientation rotation along the fiber[40] .

Dispersion is a major stumbling block in long-haul transmission systems that require higher speeds to increase transmission distance while ensuring quality. Replacing all of the existing optical wires with new ones is one of the finest ways to speed up optical communication networks. However, this is not a financially viable option. As a result, there must be another way to compensate for dispersion in fiber cables that have already been installed. The most crucial component required in an optical fiber communication system is dispersion compensation, which compensates for the

spreading of optical or light pulses. The following are the most often used classic dispersion compensating techniques: [20, 41]:

Dispersion Compensation Fibers (DCF)

A DCF is a fiber loop with negative dispersion equal to the transmitting fiber's dispersion. It can be placed between two optical amplifiers at either the beginning (pre-compensation techniques) or the end (post-compensation techniques). However, it results in significant footprint and insertion losses.

Electronics Dispersion Compensation (EDC)

EDC employs electronic equalization techniques. Linear distortions in the optical domain, such as chromatic dispersion, are transformed into non-linear distortions following optical-to-electrical conversion since there is direct detection at the receiver[42]. The concept of nonlinear cancellation and nonlinear channel modeling was developed for this purpose. Feed forward equalizer (FFE) and decision feedback equalizer (DFE) structures are primarily utilized for this. Because it slows down the digital to analog transfer, EDC slows down communication.

Fiber Bragg Grating (FBG)

Fiber Bragg Grating (FBG) has lately found a useful application in long-haul communication to compensate for dispersion-broadening. FBG is a tiny all-fiber passive device with minimal insertion loss that can be easily modified and is compatible with the transmission system[43]. For best performance, FBG should be placed in-line. Because of its advantages, such as a small footprint, low insertion loss, dispersion slope compensation, and minor non-linear effects, this approach is favored. However, the architectures that use FBG are complicated.

Digital Signal Processing (DSP)

The chromatic dispersion can be compensated using DSP. For wavelength division multiplexed systems, they provide fixed and adjustable dispersion compensation[41]. For fiber dispersion compensation, lossless all-pass optical filters are commonly utilized, as they may approximate any required phase response while preserving a constant, unity amplitude response. Bandpass filters, Gaussian filters, Super-Gaussian filters, Butterworth filters, and microwave photonic filters are some of the other filters utilized for dispersion compensation.

As data rates increase to 1Tbps and beyond, however, existing optical fiber dispersion compensation techniques become more expensive and time-consuming, making it difficult to compensate for dispersion accurately. Other ways must exist in which bitrates are kept low enough to ensure that pulses are spaced further apart and therefore larger dispersion can be tolerated. In optical communication systems, another form of dispersion compensation is to use advanced multicarrier modulation techniques like OFDM [13, 44, 45]. Complex operations in the frequency domain can be done due to the superior computational features of optical frequency division multiplexing (OFDM). Because the dispersion of optical fibers is adequately adjusted, OFDM technology, especially optical OFDM, is believed to be employed in optical communication

3.3. Fundamentals of OFDM and Optical OFDM

3.3.1. OFDM Blocks

As shown in figure 3.3, the OFDM system is comprised of two parts: a transmitter and a receiver. This section illustrates and discusses the transmitter and receiver, which are made up of a variety of sub-blocks. Let us have description of basic OFDM as follow and assume data with rate R.

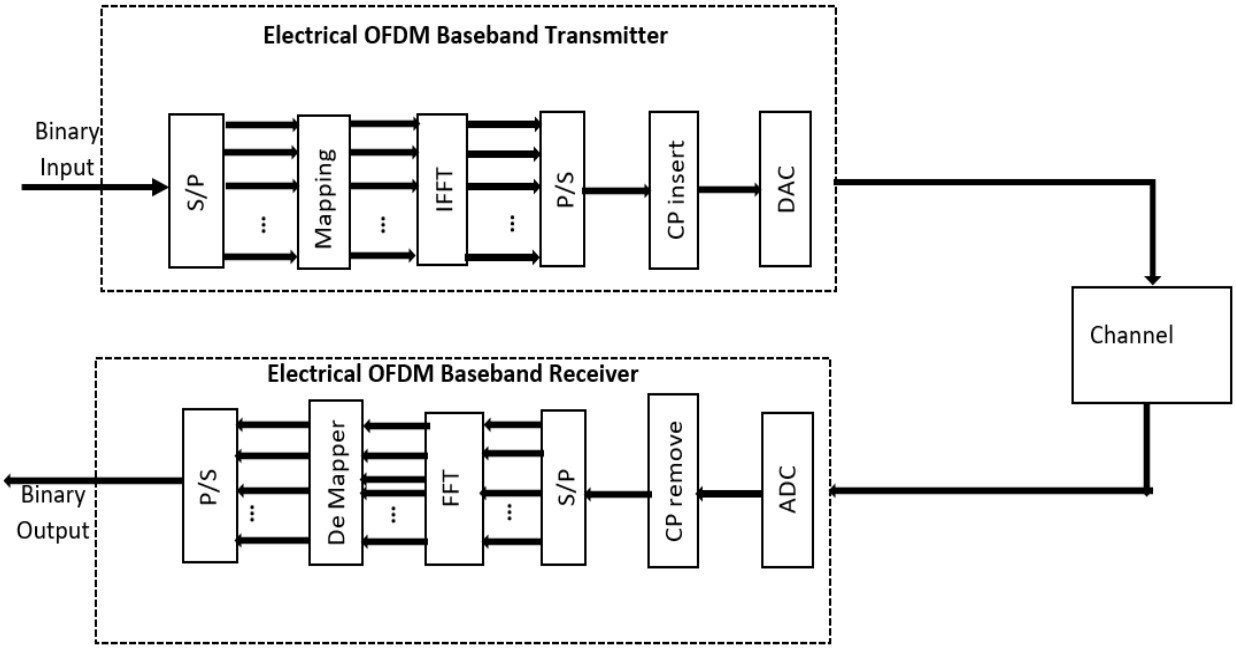

Figure 3. 2: OFDM Basic Block Diagram [55]

Serial to Parallel (S/P) and Parallel to Serial (P/S) Conversions

With a serial to parallel converter, a bit sequence with rate R is parallelized into N distinct subcarriers, each with its own frequency. At a rate of R/N, the whole bitrate is divided evenly among the channels. Each channel's data will be modulated to an information symbol before being multiplied by the frequency associated with that symbol. One OFDM symbol will be formed by adding these parallel information symbols[46, 47]. As a result, the time period of each OFDM symbol is N/R. As a result, the time domain OFDM signal s(t) can be represented as the sum of each information symbol $C_{i,k}$ being carried in the k^{th} subcarrier within the i^{th} OFDM symbol [46].

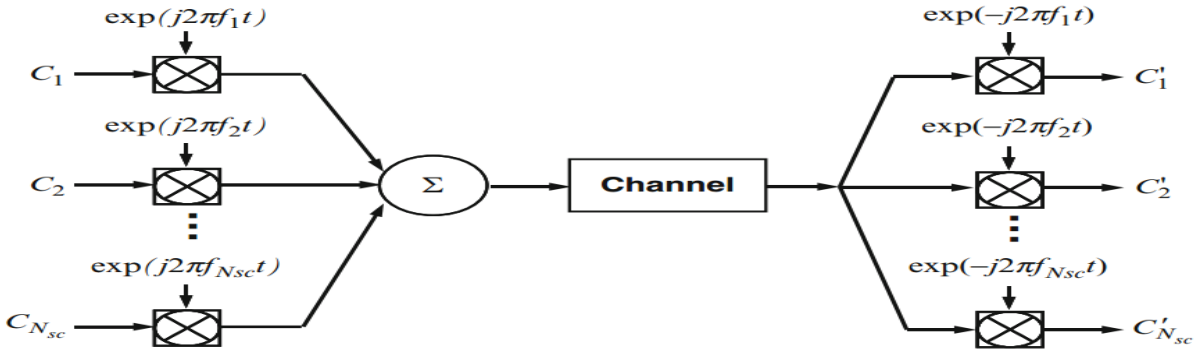

Figure 3. 3: Summation of information symbols [46]

$$S(t) = \sum_{i=-\infty}^{+\infty} \sum_{k=1}^{N_{sc}} C_{ki} S_{ki}(t - iT_s) \qquad 3.1$$

$$S_k(t) = \prod(t) e^{j2\pi f_k t} \qquad 3.2$$

$$\prod(t) = \begin{cases} 1, (0 < t \le T_s) \\ 0, (t < 0, t \le T_s) \end{cases} \qquad 3.3$$

where C_{ki} is the kth subcarrier's ith information symbol, S_k is kth subcarrier's waveform , N_{sc} is the number of subcarriers, f_k is subcarrier's frequency and T_s is the symbol period, $\prod(t)$ is the pulse shaping function of duration T_s. The OFDM symbol is multiplied by a square pulse in expression (3.1), which is one for a second period and zero otherwise. The square pulse's amplitude spectrum has the form sinc(f_s), with zeros for all frequencies f that are an integer multiple of 1/T_s.

Then, an OFDM symbol spectrum is made up of overlapping sinc functions, each one representing a subcarrier, with all other subcarriers having zeros at the frequency of the k^{th} subcarrier $1/T_s$.

A filter or a correlator that matches the subcarrier waveform could be used to create the best detector for each subcarrier. As a result, the received information symbol C'_{ki} at the correlator output is represented by

$$C'_{ki} = \frac{1}{T_s}\int_0^{T_s} r(t - iT_s)S_k^* dt = \frac{1}{T_s}\int_0^{T_s} r(t - iT_s)e^{-j2\pi f_k t} dt \qquad 3.4$$

where $r(t)$ is the detected time-domain signal. The orthogonality is derived from a straightforward correlation between any two subcarriers, which is given by [46]:

$$\delta_{kl} = \frac{1}{T_s}\int_0^{T_s} S_k S_l^* dt = \frac{1}{T_s}\int_0^{T_s} \exp(j2\pi(f_k - f_l)t) dt \qquad 3.5$$

$$= \exp(j\pi(f_k - f_l)T_s)\frac{\sin(\pi(f_k - f_l)T_s)}{\pi(f_k - f_l)T_s} \qquad 3.6$$

The two subcarriers are orthogonal to each other if the following condition is met, as shown by the preceding correlation formula.

$$f_k - f_l = m\frac{1}{T_s} \qquad 3.7$$

This means that, despite considerable signal spectral overlapping, these orthogonal subcarrier sets with frequencies separated at multiples of the inverse of the symbol rate may be retrieved with the matched filters without inter-carrier interference (ICI). The reciprocal baud rate 1/R determines the symbol period in single carrier systems. Because the symbol period in multicarrier systems like OFDM is N times longer, the influence of channel dispersion is often lower, and inter-symbol interference (ISI) is reduced. Furthermore, as shown in the following section, ISI can be nearly reduced by including a guard period in each OFDM symbol, ensuring that the majority of the dispersion generated by a multipath channel is contained inside the guard interval.

Mapping and DE mapping

The signal source's binary bits stream must be divided into many parallel data streams, each of which must be mapped or modulated into respective information symbols for the subcarriers in one OFDM symbol. Optical communication used to rely on the basic modulation technique On Off Keying (OOK), which is the optical equivalent of Amplitude shift Keying[48]. This technique utilizes more optical frequency grid bandwidth and requires mature electronics technology capable of operating at such a high rate. The alternative is to employ modern multi-level modulation techniques, which allow us to transmit more bits per symbol. We can reduce the symbol rate while preserving the same throughput using this strategy. As a result, optical transmission systems now use multi-level modulation techniques. Multi-level modulation encapsulates multiple bits in a single symbol. This reduces the system's symbol rate at the cost of higher transmitter and receiver complexity [49]. QPSK, DQPSK, 3ASK, and Mary QAM are just a few examples. Polarization division multiplexing is a new technology that was launched alongside multi-level modulation. Two signals that have already been modulated with multi-level modulation are placed in orthogonal polarization to each other, multiplexed, and delivered as a single entity using this technology. The system's capacity is doubled while the symbol rate and bandwidth remain same. Some examples of such a scenario are dual polarization QPSK (DP-QPSK) and DP-16QAM [50-52]. The DP-16QAM modulation is used to map bits into information symbols in one OFDM symbol in this thesis study.

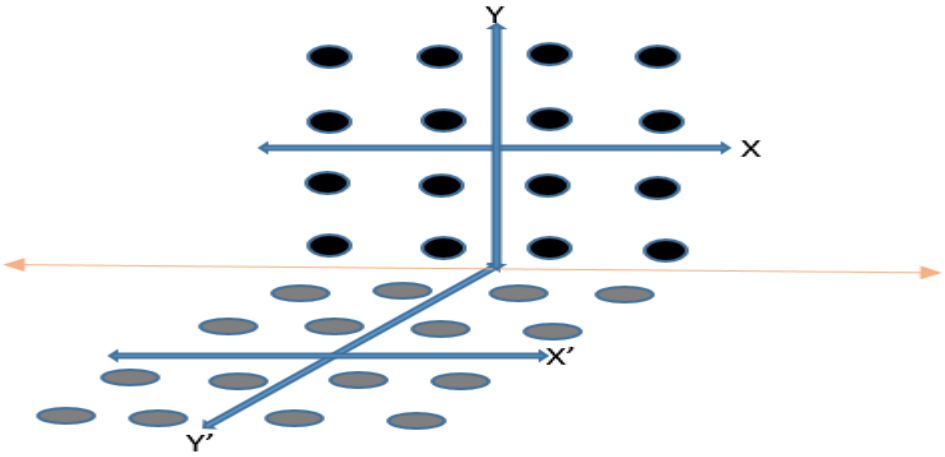

Figure 3. 5: Constellation mapping of DP-16QAM [56]

So, let's have a look at how this multilayer modulation approach maps each parallel bit.

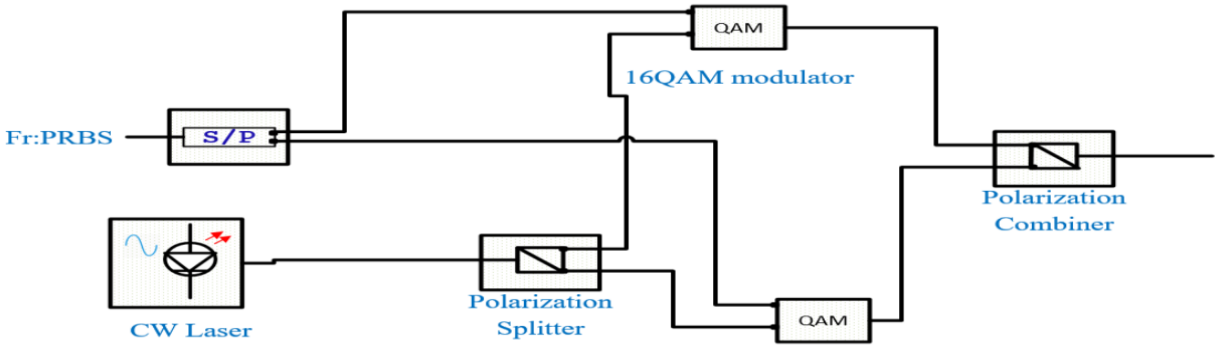

Figure 3. 6: General Architecture of DP-16QAM[63]

To clarify clearly, let us see general architecture of DP-16QAM depicted in figure 3.6 above. It is known that 16QAM is an M-ary technique where M =16 i.e. the input data are transferred on in groups of four (2^4 = 16). In QAM modulation, the carrier's phase and amplitude are both varied, unlike QPSK where only the phase of the carrier is varied[63].

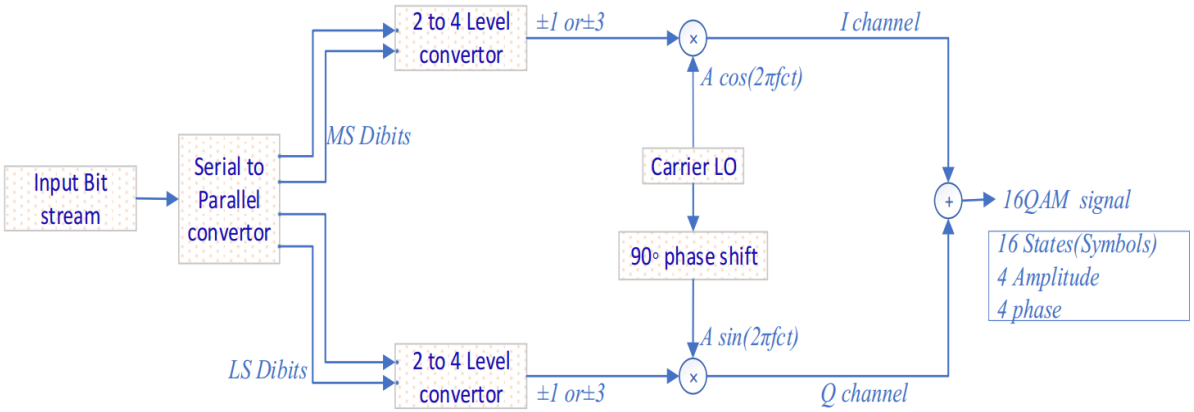

Figure 3. 7: 16QAM Modulator[63]

As illustrated in figure 3.7, the Serial to Parallel Converter divides the input data into a subset of quadbit each consisting of four bits. Then Serial to Parallel Converter produces one quadbit in parallel at each of its four outputs after four bits have been serially moved into its buffer. Each quadbit is made up of two dibits, the most significant dibit (MSD) and the least significant dibit (LSD). The MSD is then sent to the modulator's I-channel, whereas the LSD is sent to the modulator's Q-channel. Both I and Q channels work independently to process the data they receive.

The 2 to 4 Level Converter is a device that converts two levels into four levels. Each channel turns the dibit stream into a four-level (baseband) pulse stream that can be used as a single input to one of the mixers. Each of the four levels corresponds to a different dibit. As stated in tables 3.1 and 3.2, the four levels employed are equivalent to -3, -1, +1, and +3. As a result, the constellation points are distributed evenly. Each mixer modulates the sinusoidal carrier by multiplying it by the four-level data signal.

As a result, the mixer output signal is a bi-phase, bi-level sinusoidal waveform. The QAM signal is created by adding the two bi-phase, bi-level signals together. As a result of the usage of orthogonal carriers (in phase quadrature) to generate two bi-phase, bi-level signals, the signals themselves are orthogonal, and the QAM demodulator will be able to demodulate them individually.

Dibits	Output
00	-1
01	-3
10	+1
11	+3

Table 3. 1: Dibit to Pulse Level Mapping.

Quad bits	Amplitude and Phase	Quad bits	Amplitude and Phase
0000	$\sqrt{2}\ -135^0$	1000	$\sqrt{2}\ 135^0$
0001	$\sqrt{2}\ -165^0$	1001	$\sqrt{2}\ 165^0$
0010	$\sqrt{2}\ -45^0$	1010	$\sqrt{2}\ 45^0$
0011	$\sqrt{10}\ -15^0$	1011	$\sqrt{10}\ 15^0$
0100	$\sqrt{10}\ -105^0$	1100	$\sqrt{10}\ 105^0$
0101	$3\sqrt{2}\ -135^0$	1101	$3\sqrt{2}\ 135^0$
0110	$\sqrt{10}\ -75^0$	1110	$\sqrt{10}\ 75^0$
0111	$3\sqrt{2}\ -45^0$	1111	$3\sqrt{2}\ 45^0$

Table 3. 2: Mapping of Quad bits to Amplitude and phase for either Q or I channel.

For example, a quad bit 0000 is the input to modulator then the inputs for I channel product mixer will be -1 and $A\cos(2\pi f_c t)$

$$I=-A\cos(2\pi f_c t) \quad 3.8$$

Similarly for Q channel -1 and $A\sin(2\pi f_c t)$

$$Q=-A\sin(2\pi f_c t) \quad 3.9$$

The final output QAM signal will be the summation of I and Q channels' signals.

$$I+Q=-A\cos(2\pi f_c t)-A\sin(2\pi f_c t) \quad 3.10$$

Using Trigonometric identity this can be written as

$$I+Q=\sqrt{2}A\cos(2\pi f_c t-\frac{3}{4}\pi) \quad 3.11$$

In the most general sense, the output QAM signal can be represented by [63]:

$$S_n(t)=A_n g(t)\cos(2\pi f_c t+\theta_n) \quad \text{for n=1,...,M} \quad 3.12$$

where $g(t)$ is a pulse-shaping function.

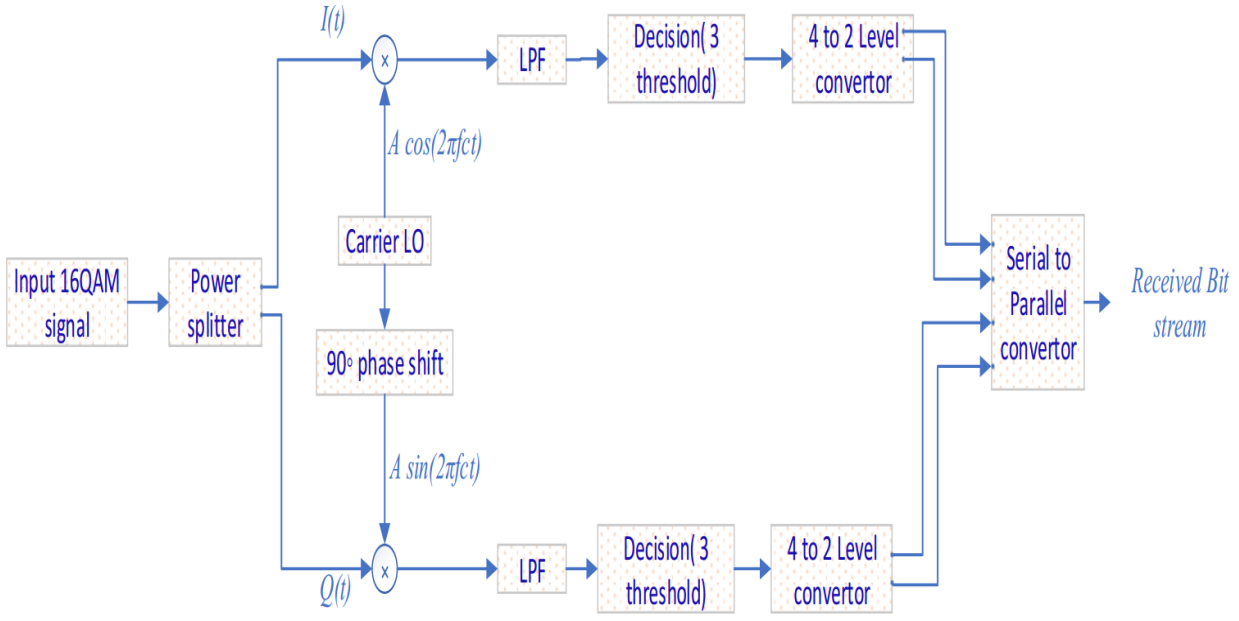

Figure 3. 8: 16QAM Demodualtor[63]

As shown in figure 3.8, the QAM demodulation process is done with two mixers and two carrier signals in phase and quadrature. Because the I and Q-channel signals that were mixed in the modulator are orthogonal, the demodulator can demodulate them independently. The following equation can be used to represent an idealized and received QAM waveform[63]:

$$s(t)=d_I\cos(2\pi f_c t)+d_Q\sin(2\pi f_c t) \quad 3.13$$

Where $s(t)$ is the QAM signal waveform, d_I is the I-channel four level pulse stream and d_Q is the Q-channel four level pulse stream. The I-channel component of this waveform is multiplied by the in-phase carrier $\cos(2\pi f_c t)$ as shown below

$$s_I(t)=[d_I\cos(2\pi f_c t)+d_Q\sin(2\pi f_c t)]\cos(2\pi f_c t) \quad 3.14$$

$$s_I(t) = d_I(\cos(2\pi f_c t))^2 + d_Q \sin(2\pi f_c t)\cos(2\pi f_c t) \quad 3.15$$

$$s_I(t) = \frac{1}{2}[d_I + d_I \cos(2(2\pi f_c t)) + d_I d_Q \sin(2(2\pi f_c t))] \quad 3.16$$

$$s_I(t) = \frac{1}{2}[d_I + d_I \cos(4\pi f_c t) + d_I d_Q \sin(4\pi f_c t)] \quad 3.17$$

The output of the I-channel mixer is an analog signal including four level data pulses d_I and high-frequency components $d_I \cos(4\pi f_c t)$ and $d_I d_Q \sin(4\pi f_c t)$, as shown in the last equation. The four-level data pulses d_Q and high frequency components are also included in the Q-channel mixer's output. The high-frequency components are removed by the LPF, leaving only the data pulses.

The detection circuit must sample these signals once every symbol period and then decide which state each sample represents because the integrated signal in each channel is a time-varying analog signal. To determine what levels each sampled level represents, the decision circuit compares it to three thresholds. This circuit produces a stream of bipolar data pulses with fixed amplitudes. This signal is converted to a digital signal via the 4 to 2 level Converter circuit. Each channel's dibits

are combined into a serial stream of data bits via the Parallel to Serial Converter. This data is identical if no errors occur during the modulation, transmission, and demodulation processes.

Fast Fourier Transform(FFT) and Inverse Fast Fourier Transform(IFFT)

The inverse fast Fourier transform (IFFT) is commonly used to superimpose independent modulated subcarriers, when the input channels are separated equivalently according to the orthogonality criterion. Because of the orthogonality condition, the OFDM receiver will calculate the spectrum values at those positions corresponding to the maximum of individuals' subcarriers as long as the channel is linear. Equation 1.1 can be rewritten as follow for one OFDM symbol[46]:

$$\tilde{S}(t) = \sum_{i=0}^{N-1} A_i \exp\, j2\pi \frac{i}{T} t, 0 \le t \le T \qquad 3.18$$

Equation 3.18 is the complex form of OFDM baseband signal.

When we sample the complex signal at a rate of N/T and apply a normalization factor of 1/N, we get

$$S_n = \frac{1}{N} \sum_{i=0}^{N-1} A_i \exp(j2\pi \frac{i}{N} n), n = 0,1,2,\ldots, N-1 \qquad 3.19$$

Where S_n is the n^{th} time domain sample. This is exactly how the inverse discrete Fourier transform (IDFT) is expressed. It means that IDFT can implement the OFDM baseband signal. The IDFT output is in the time domain, whereas the pre-coded signals are in the frequency domain. Similarly, the data is retrieved at the receiver using the discrete Fourier transform (DFT), which is provided by:

$$A_i = \sum_{i=0}^{N-1} R_n \exp(-j2\pi \frac{i}{N} n), n = 0,1,2,\ldots, N-1 \qquad 3.20$$

where R_n is the received sampled signal, and A_i is received information symbol for the i^{th} subcarrier.

The received subcarriers may then be demodulated without interference using an FFT operation, eliminating the requirement for analogue filtering to separate them, making OFDM not only

effective but also simple to implement in real-world transmission systems. As a result, the modulated OFDM signal can be generated by applying the IFFT operation to the symbols to transmit and then converting the digital signal into an analogue signal at sampling rate T_s using a DAC. Every temporal sample should be convolved by a sinc function in this D/A conversion. As seen in figure 3.9 below, this ideal shaping is converted into a completely rectangular filter that removes alias in the frequency domain.

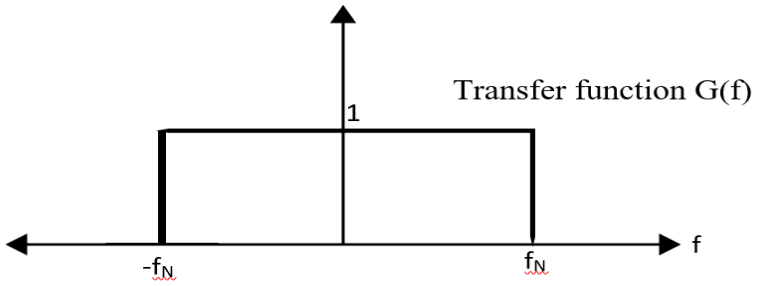

Figure 3. 9: Ideal filter at the DAC[64]

The alias caused by the sampling process will be removed by this ideal Filter, leaving the basic signal unaltered. The contribution of the distinct sinc pulses at each of the OFDM symbol samples results in a perfect square pulse of the OFDM symbol, and each of the subcarriers is represented in the frequency domain by a perfect sinc function. Similarly, the subcarriers forming the received signal r(t) are demodulated by an FFT operation after being transformed from analog to digital (A/D) and parallelized to generate the FFT block inputs.

D/A and A/D conversion

To convert the discrete value of (sample) to the continuous value of S(t), a digital-to-analogue converter (DAC) is required, and an analogue-to-digital converter (ADC) is required to convert the continuous received signal r(t) to discrete sample. Pulse shaping and oversampling with zero padding are the two major processes done in D/A and A/D conversion.

Pulse Shaping: - Symbols are applied to a transmitter filter inside the DAC, which results in a continuous-time signal that can be transmitted across the continuous-time channel[53]. A simple transmit filter has a rectangular impulse response, as illustrated in figure 3.10, which also represents a symbol sequence with two bits per symbol and its accompanying continuous-time signal.

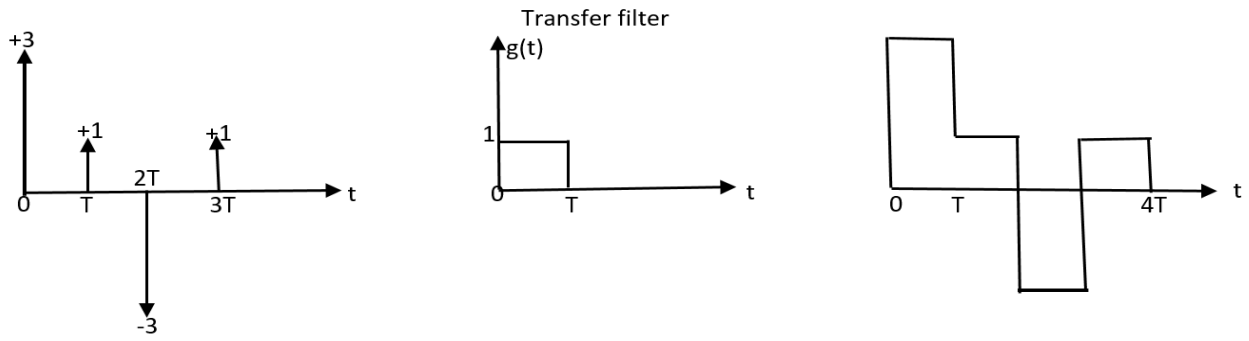

Figure 3. 10: Rectangular Impulse Response[64]

The pulse shape refers to the transmit filter's impulse response g(t). This filter's output is a convolution of the pulse shape with the symbol sequence, resulting in a signal that can be understood as a series of possibly overlapped pulses, each with a different amplitude defined by a symbol. There is no ISI in an ideal low-pass filter since the impulse response is a sinc function with equidistant zero-crossing at the sampling instants. This ideal filter, however, is not attainable. A increased cosine characteristic fitted to the ideal low-pass filter, which is a frequent pulse shape in OFDM, provides a feasible extension.

Oversampling by means of zero padding: - The DAC must sample the OFDM signal representing the analogue signal before it can be transmitted. The aliases produced by the sampling process would be right adjacent to the primary OFDM signal if they were sampled at a rate of $\frac{1}{T_s}$, making any reasonable filter impossible to separate them. However, as illustrated in figure 3.11, padding the right position of the IFFT input sequence with zeros can help to shift the aliases away from the OFDM signal.

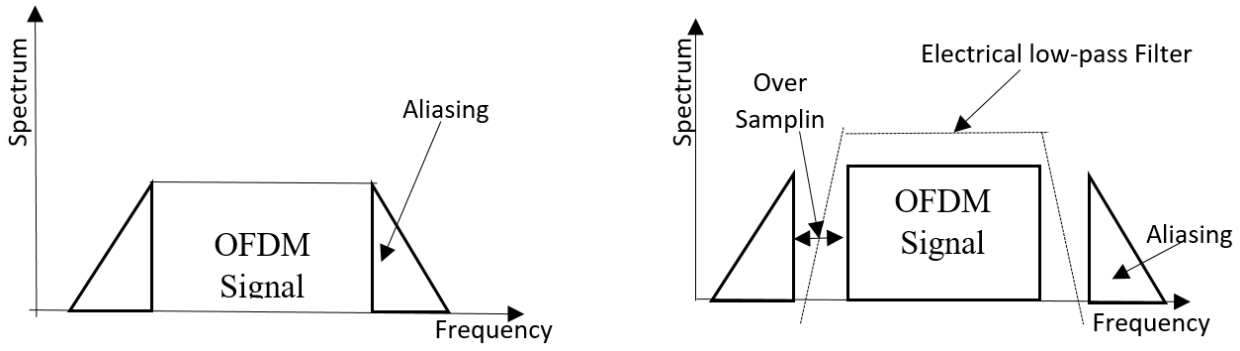

Figure 3. 11: Oversampling used to shift aliases away[64].

Cyclic Prefix

By dividing the data stream into N subcarriers, the symbol period is extended by N times, while the delay spread or chromatic dispersion relative to the symbol time is reduced, as stated in the previous section. After the IFFT, a guard time or interval is inserted for each OFDM symbol, which is cyclically extended inside this guard time, to reduce interference between OFDM symbols (meaning degrade influence of ISI) and also to diminish ICI. The cyclic prefix [46, 47, 54], is the name for this cyclical extension.

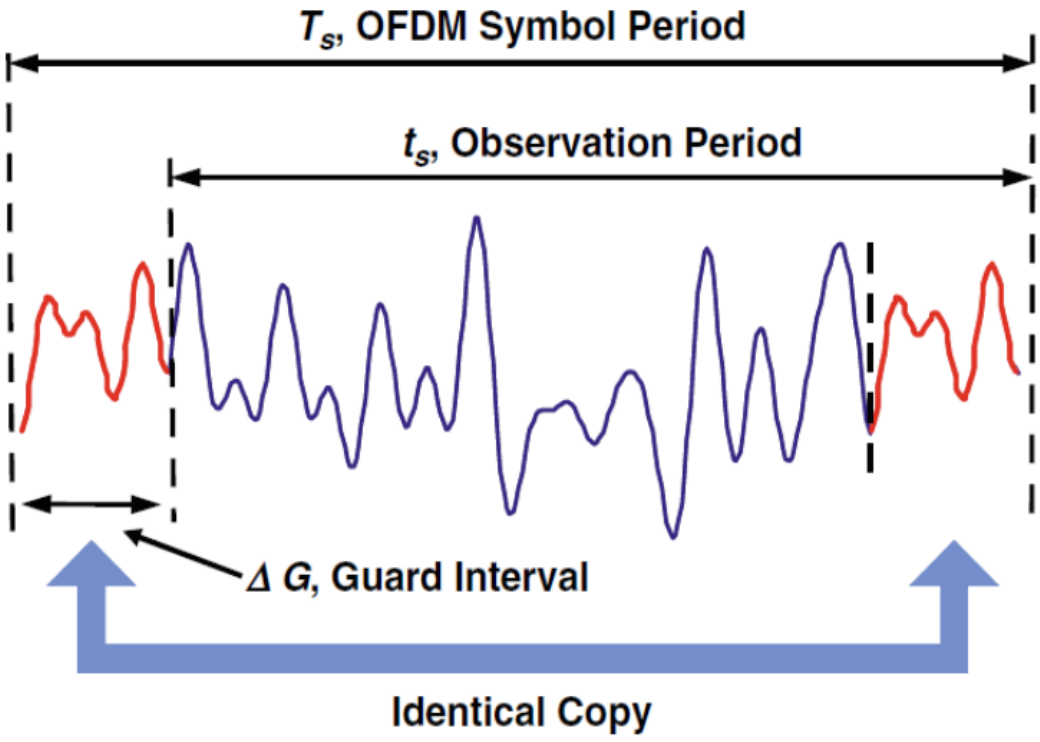

Figure 3. 12: CP insertion [46]

The influence of one symbol on its neighbors will be restricted to its cycle prefix corruption, without destroying the information, as long as the cyclic prefix time period or duration is equal to or longer than the maximum delay induced by channel impairments. The zero padding and cyclic prefix are removed at the receiver end in the reverse order that they were put at the transmitter.

3.3.3. Optical OFDM (O-OFDM)

The O-OFDM principle is identical to that of OFDM. The sole change is that the signal is transformed from an electrical domain to an optical domain. The structure block diagram of the O-OFDM system is presented in figure 3.13. Both the electrical OFDM baseband transmitter and receiver blocks are already discussed in the previous sections. Here under additional blocks: RF up and down conversion, optical modulation, the channel or fiber and optical detection are discussed. Up conversion and optical modulation are required to transfer this generated electrical signal across an optical channel[10, 46].

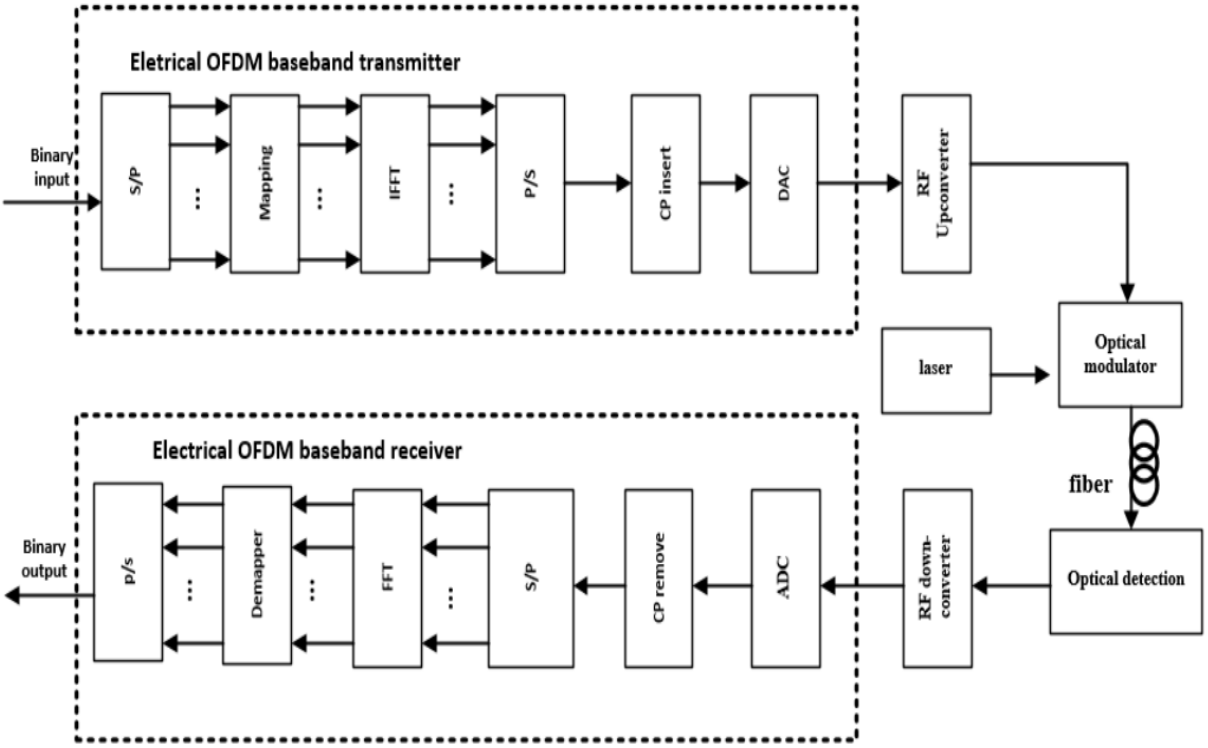

Figure 3.13: Basic Block Diagram of Optical OFDM [14]

In general, based on methods used to detect optical signal in the receiver side there are two scenarios of optical OFDMs [17, 27, 45]. The first scenario is direct-detection optical OFDM (DD-O-OFDM), which uses a single photodiode, and the second is coherent optical OFDM (Co-O-OFDM), which uses the principle of optical mixing with a local oscillator and an optical hybrid. Both methods have their merits. Although the DD-O-OFDM receiver is simple, some optical

frequencies must be left empty or guard band inserted between optical carrier and OFDM subcarrier to avoid undesirable mixing products causing interference [55]. However, using it that way possibly reduces the spectral efficiency. DD-O-OFDM also requires more transmitted optical power, as some power is required for the transmitted carrier. Because OFDM is sensitive to frequency offset and phase noise, Co-O-OFDM involves the use of very tiny linewidth lasers at the transmitter and receiver, as well as advanced tracking algorithms to track laser frequency and phase.

3.3.3.1. Up conversion and Down conversion

As shown in Figure 3.14, the up conversion approach converts the complex baseband OFDM signal s(t) generated with QAM subcarrier modulation into a passband signal centered at an intermediate frequency (IF). The frequency up conversion is done to establish a gap between the OFDM signal and the DC component, allowing the electrical spectrum to avoid the issues caused by the usage of analogue mixers and oscillators. After the IFFT operation, the real and imaginary components of the signal are processed by the two DACs.

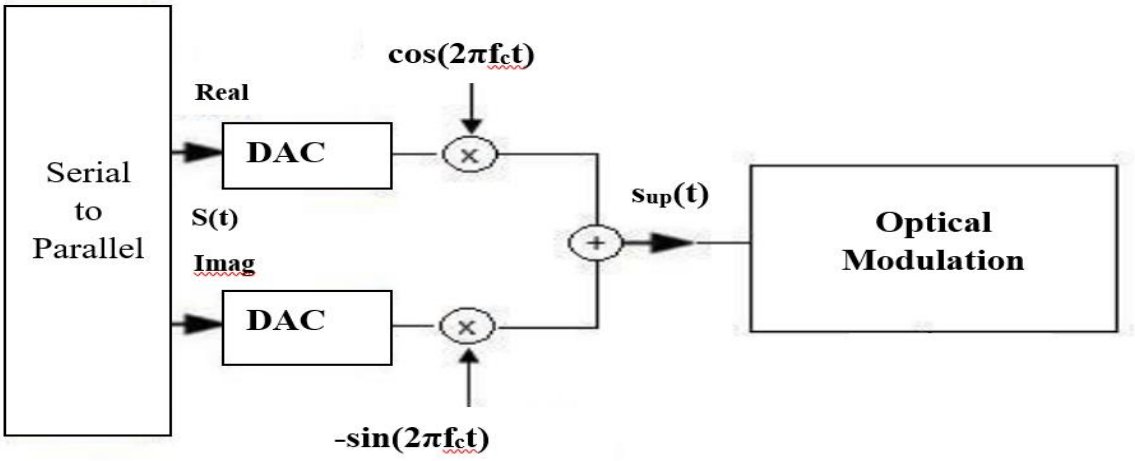

Figure 3.14: Up conversion block[64]

The signal's real and imaginary sections, which correspond to the signal's in-phase (I) and quadrature (Q) components, are then fed into an electrical IQ mixer for up conversion to an IF, f_c. For this reason, a 90^o phase shift is provided between the locally generated carrier at IF frequency

that multiplies the in-phase component and the one multiplying the quadrature component.

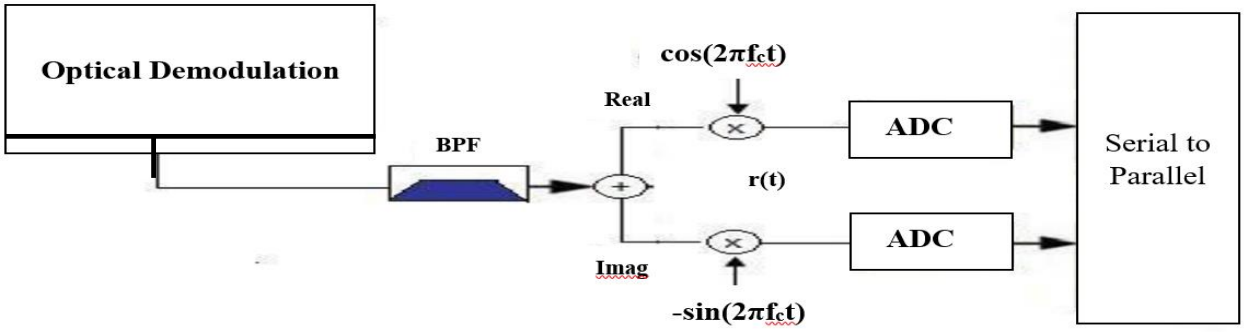

Figure 3.15: Down conversion block[64]

Another IQ mixer with the opposite function down converts the signal at the receiver, reverting the OFDM signal to baseband before extracting the CP and conducting the FFT procedure.

3.3.3.2. Optical Modulation

Optical modulation is necessary to transmit the signal generated in the RF up conversion stage across an optical channel [13, 28, 47]. Many various strategies could be used for this aim, but only two have been chosen for discussion. These are the directly modulated laser and the Mach Zehnder modulator, which is an external modulator (MZM).

3.3.3.2.1. Conventional Intensity Modulated / Direct Detection systems

As shown in figure 3.16, a laser diode is directly modulated by an electrical signal using its bias current. That means in direct modulation, the laser emits light when 1 is being transmitted and emits no light when 0 is being transmitted as [56]. This is the simplest way for sending data across optical fiber, as it relies on creating fluctuations in the bias current of a diode laser above a predetermined threshold.

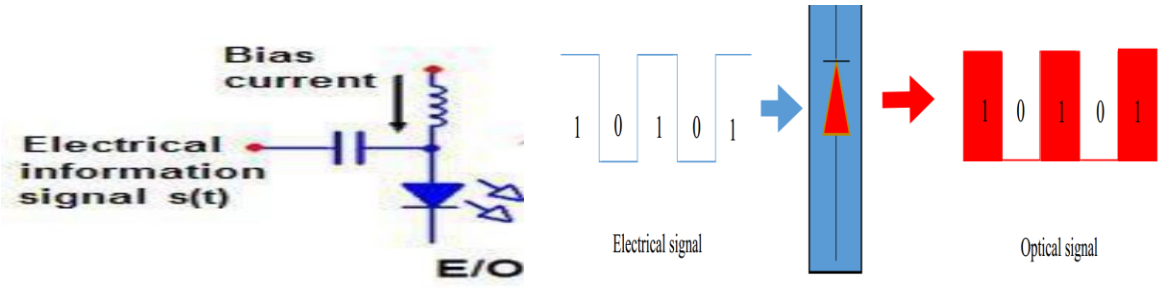

Figure 3. 16: Intensity Modulation/Direct Detection[56]

The current variations (I_m) cause proportional variations in the output optical power, which are detected by a PIN diode at the receiver end, allowing the supplied information signal s(t) to be recovered, as follows[56]:

$$P_{out} = P_o(1+m.s(t)) \quad 3.21$$

Where P_o is the power associated to the laser bias and *m* is the used modulation index, which is also related to the laser bias current as:

$$m = \frac{I_m}{I_0} \quad 3.22$$

Finally, given an ideal channel, the total received intensity is a function of the PIN diode's responsivity R and the varied gains of the reception amplifier devices (G):

$$I_R(t) = RGP_o(1+m.s(t)) \quad 3.23$$

The direct detection process is mathematically equivalent to applying the squared modulus:

$$I(t) \propto |s(t)|^2 \quad 3.24$$

The low-pass equivalent of the electrical field being transferred on the fiber can be calculated using the optical power at the laser output and the square root:

$$E_{out}(t) = \sqrt{P_0}\sqrt{1+m.s(t)} \quad 3.25$$

3.3.3.2.2. Mach-Zehnder (MZ) modulator

The Mach-Zehnder modulator is external optical modulator which uses electro-optic effect. It consists of two 3 dB couplers which are constructed by two waveguides of identical length.
The applied voltage in each arm can be used to vary the refractive index in each waveguide branch and hence speed of light in that branch.

The light traveling at different arm will be in phase and out of phase depending on applied voltage i.e. it will be added constructively or destructively at the output.

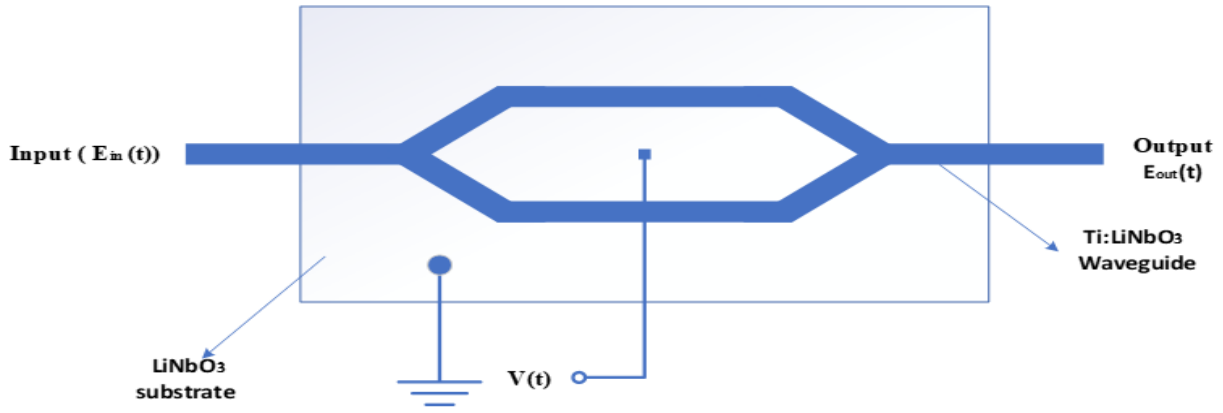

Figure 3. 17: MZ Modulator[65]

In Figure 3.17 above, the electric field of the light can be modulated changing applied external voltage which in turn alters the refractive index of the material LiNbO3 by electro-optic effect. If no voltage is applied, the optical fields in the two arms will have identical phase shift and interfere in a constructive manner. If an external voltage is applied, the phase shift in the two arms is no longer identical.

So, we can modulate output light using applied voltage as input for the modulator. By controlling one of the arms of the modulator by using the baseband signal we can modulate the incoming light to the MZ modulator.

Vπ is defined as a voltage that changes the refractive index of the lower arm of the MZ modulator in such a way that there is a 180° delay or phase shift compared to the unaffected path. This makes previously identical signals to be out of phase and their combination at the output will be destructive interference.

When the light propagates through MZM, the phase shift (Φ)can be approximated as [30]

$$\phi=\phi_0-\pi\frac{v(t)}{2V_\pi} \qquad 3.26$$

Where ϕ_0 *is unshifted phase*

$v(t)$ *is voltage on an arm*

V_π *is voltage tha cause π phase shift*

If $v_1(t)$ and $v_2(t)$ are applied in both arms of the MZ modulator the phase shift on each arm will be

$$\phi_1 = \phi_0 - \pi \frac{v_1(t)}{2V_\pi} \quad \text{and} \tag{3.27}$$

$$\phi_2 = \phi_0 - \pi \frac{v_2(t)}{2V_\pi} \tag{3.28}$$

If we assume that the input to the modulator is $E_{in}(t) = \sqrt{p}.e^{j\omega_0 t}$ and $\phi_0 = 2\pi$

Then $P = P_1 + P_2$ where $\sqrt{P_1}$ and $\sqrt{P_2}$ are amplitudes of optical fields in each arm of the Mach-Zehnder interferometer. ω_0 denotes the frequency of an optical signals.

We define the extinction ratio ξ_{ER} as the ratio between the maxima and minima output powers.

$$\varepsilon_{ER} = \left(\frac{\sqrt{P_1} + \sqrt{P_2}}{\sqrt{P_1} - \sqrt{P_2}}\right)^2 \tag{3.29}$$

If our system has $P_1 = P_2$ it is called infinite extinction ratio system and for this system we can calculate output electric field using the formula

$$E_{out}(t) = \sqrt{P}\cos\left(\pi \frac{v(t)}{2V_\pi}\right)e^{j\omega_0 t} \tag{3.30}$$

3.3.3.3. Optical Channel: Chromatic Dispersion

Chromatic dispersion can occur in any type of optical fiber and is caused by the optical source's finite spectral linewidth. There may be propagation delay differences between the different spectral components of the transmitted signal since optical sources emit a variety of frequencies. This creates chromatic dispersion by expanding each transmitted mode [31, 57]. The delay discrepancies could be due to the waveguide material's dispersive qualities (material dispersion) as well as guidance effects inside the fiber structure (waveguide dispersion).

3.3.3.3.1. Material Dispersion

The varying group velocities of the several spectrum components delivered into the fiber from the optical source cause pulse widening owing to material dispersion. Material dispersion occurs when the phase velocity of a plane wave moving through a dielectric medium fluctuates nonlinearly with wavelength, i.e. when the second differential of the refractive index with respect to wavelength is not zero ($\partial^2 n/\partial\lambda^2 \neq 0$). The group delay τ_g in the optical fiber, which is the reciprocal of the group velocity v_g. can be used to calculate the pulse spread owing to material dispersion. As a result, the group delay is given by [57]:

$$\tau_g = \frac{\partial\beta}{\partial\omega} = \frac{1}{c}\left(n - \lambda\frac{\partial n}{\partial\lambda}\right) \qquad 3.31$$

where n is the refractive index of the core material. In a fiber of length L, the pulse delay due to material dispersion is thus:

$$\tau_m = \frac{\partial\beta}{\partial\omega} = \frac{L}{c}\left(n_1 - \lambda\frac{\partial n_1}{\partial\lambda}\right) \qquad 3.32$$

The rms pulse broadening due to material dispersion σ_m may be determined by expanding Eq. (3.33) in a Taylor series around for a source with rms spectral width σ_λ and a mean wavelength of λ where:

$$\sigma_m = \sigma_\lambda \frac{\partial\tau_m}{\partial\lambda} + \sigma_\lambda \frac{2\partial^2\tau_m}{\partial\lambda^2} + \ldots \qquad 3.33$$

Because the first part in Eq. (3.33) frequently dominates, especially for sources operating in the 0.8 to 0.9 nm wavelength range, the equation can be written as follows:

$$\sigma_m \simeq \sigma_\lambda \frac{\partial\tau_m}{\partial\lambda} \qquad 3.34$$

Hence the pulse spread may be evaluated by considering the dependence of τ_m on λ, where from Eq. (3.31):

$$\frac{\partial \tau_m}{\partial \lambda} = \frac{L\lambda}{c}\left[\frac{\partial n_1}{\partial \lambda} - \frac{\partial^2 n_1}{\partial \lambda^2} - \frac{\partial n_1}{\partial \lambda}\right] = -\frac{L\lambda}{c}\frac{\partial^2 n_1}{\partial \lambda^2} \qquad 3.35$$

As a result, the rms pulse broadening owing to material dispersion may be calculated by replacing the expression derived in Eq. (3.34) into Eq. (3.33):

$$\sigma_m \simeq \sigma_\lambda \frac{\partial \tau_m}{\partial \lambda} \simeq \frac{\sigma_\lambda L}{c}\left|\lambda \frac{\partial^2 n}{\partial \lambda^2}\right| \qquad 3.36$$

Therefore, optical fiber material dispersion is sometimes expressed as:

$$D_m = \left|\frac{\partial^2 n}{\partial \lambda^2}\right| \qquad 3.37$$

3.3.3.3.2. Waveguide Dispersion

Chromatic dispersion can be caused by the fiber's wave guiding. The difference in group velocity with wavelength for a given mode causes this. When using the ray theory technique, it is comparable to the angle between the ray and the fiber axis changing with wavelength, resulting in a variation in the rays' transmission times, and hence dispersion. When the propagation constant of a single mode is $\partial^2\beta/\partial\lambda^2 \neq 0$, the fiber shows waveguide dispersion. Waveguide dispersion is almost non-existent in multimode fibers, as the bulk of modes propagate far from cutoff, and it is often minimal when compared to material dispersion. Waveguide dispersion can be significant in single-mode fibers because the effects of the various dispersion mechanisms are difficult to distinguish. It can be stated mathematically as follows [57]:

$$D_w = -\frac{n_1 \lambda \Delta}{c}\left|\lambda \frac{\partial^2 \beta}{\partial \lambda^2}\right| \simeq \left|\frac{\partial^2 \beta}{\partial \lambda^2}\right| \qquad 3.38$$

So chromatic dispersion of optical fiber is the combination of both material and waveguide dispersions.

$$D_c = D_m + D_w \qquad 3.39$$

3.3.3.4. Optical Detection

Depending on the detection mechanism utilized at the receiver, optical detection is divided into two types. Direct detection and coherent detection are the two kinds, each with its own set of advantages and limitations. Direct detection has shown to be more cost-effective than coherent detection since it requires fewer components at the transmitter and receiver. When compared to Direct detection, Coherent detection has a higher spectral efficiency and better receiver sensitivity, but it is negative when it comes to complexity and expense. Direct detection, on the other hand, is a good choice for applications that require low cost and complexity by avoiding the use of a local oscillator laser, but coherent detection is a good choice when high receiver sensitivity is required. The use of an in-phase, quadrature component, and local oscillator at the receiver for creating electrical signals is the fundamental distinction between a direct detection system and a coherent detection system.

3.3.3.4.1. Direct Detection

In optical fiber technology, direct detection is the earliest sort of detecting technique. Intensity modulation direct detection (IM/DD) is the most common name for this technique. After being produced at the transmitter, OFDM signals are transferred to the optical domain, i.e. electrical to optical conversion (E/O), via intensity modulation. Optical to electrical conversion (O/E) is conducted at the receiver after optical transmission through fiber using a photo diode for photo-detection. This uses the square law detection technique and is followed by OFDM reception[55].

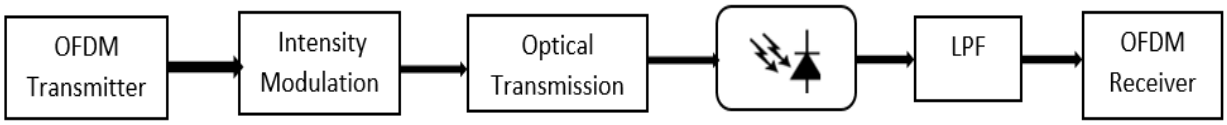

Figure 3.18: Intensity Modulation Direct Detection(IM/DD) [65]

Received signal with photo detection can be described mathematically as equation (3.41) [65],

$$\mathbf{E_{e1}(t)=|E_{01}(t)|^2 \otimes h_e(t)+w(t)} \quad 3.41$$

$$\mathbf{E_{01}(t)=e^{j(\omega_{L1}t+\phi_{L1})}s(t)} \quad 3.42$$

where $E_{e1}(t)$ represents output electrical signal, $E_{01}(t)$ represents input optical signal, $h_e(t)$ represents impulse response of fiber link and w(t) represents noise. The input optical signal $E_{01}(t)$

can be described as eq. (3.42), where ω_{L1} and $^{\Phi}_{L1}$ represent the frequency and phase of the transmitter laser, and s(t) represents the output OFDM signal.

3.3.3.4.2. Coherent Detection

Coherent detection is a sophisticated detection method in which the receiver calculates decision variables based on the retrieval of the total electric field, including amplitude and phase information. Because information can be encoded in amplitude and phase, or alternatively in both in phase (I) and quadrature (Q) components of a carrier, coherent detection gives us the most freedom in modulation forms[22, 55]. As shown in figure 3.19, the received signal is fed to one arm of the hybrid coupler, while the other input to the hybrid is the signal from the local oscillator.

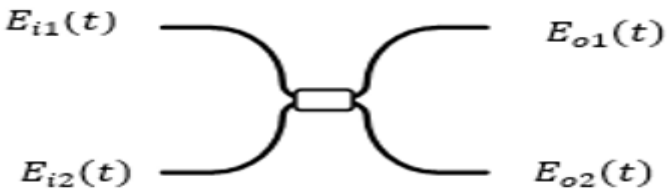

Figure 3. 19: Hybrid Coupler[65]

Based on the frequency generated by the local oscillator, coherent detection can be classed as either heterodyne or homodyne detection. When the local oscillator's frequency equals that of the incoming signal, homodyne detection occurs, but heterodyne detection happens when the local oscillator's frequency does not match that of the incoming signal. In the heterodyne approach, an optical hybrid is used to directly down convert the optical signal to the baseband for obtaining the I/Q components of the signal, whereas in the homodyne approach, an optical hybrid is used to directly down convert the optical signal to the baseband for obtaining the I/Q components of the signal using an electrical In-phase/Quadrature (I/Q) demodulator to retrieve the real and imaginary components.

Coherent detection reduces the effect of noise by recovering in-phase (I) and quadrature phase (Q) parts at the receiver [55, 58, 59]. For I/Q optical to electrical conversion, coherent detection employs balanced coherent detectors, an optical hybrid, and two sets of photo-detectors. The photodetector detects the hybrid's output, which is subsequently passed to the digital receiver, where the digital signal is recovered.

CHAPTER FOUR

System Model and Mathematical Formulation

Here there are two general system models, namely system model of high speed fiber optic communication with Co-O-OFDM and system model of high speed optical fiber communication using integration of Co-O-OFDM with FBG as dispersion compensation technique.

4.1. Coherent Optical OFDM (Co-O-OFDM) System

The general block diagram of high speed fiber optic communication with Optical OFDM is depicted in figure 4.1 below. For the purpose of simplification and detail description this model divided into parts as Co-O-OFDM transmitter model, transmission link model and optical Co-O-OFDM receiver model.

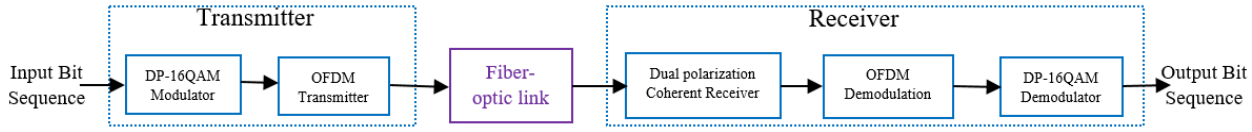

Figure 4. 1: General Block Diagram of high speed optical fiber communication with Co-O-OFDM

4.1.1. DP-16QAM Co-O-OFDM Transmitter

As shown in the following block diagram, the serial to parallel converter groups the incoming bits and buffer into two 16QAM modulators which each maps those bits into QAM signals to corresponding M-ary symbols as discussed in previous section.

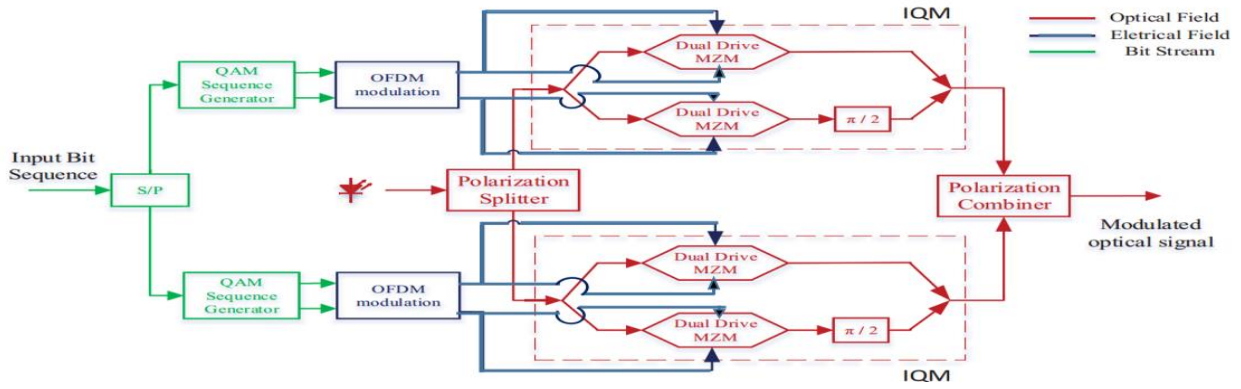

Figure 4. 2: DP-16-QAM Co-O-OFDM transmitter [61]

This QAM symbol can be represented as follow[63]:

$$X_n(t) = A_n g(t)\cos(2\tau f_c t + \theta_n) \quad 4.1$$

where $g(t)$ is a pulse-shaping function.

The OFDM modulation component performs numerous operations such as S/P conversion, inverse fast Fourier transform (IFFT), addition of cyclic prefix, P/S conversion, digital to analog conversion, and filtering, as explained in the previous section. As a result, the following is the representation of a base band OFDM signal[46]:

$$S_{BB}(t) = \sum_{i=-\infty}^{\infty} \sum_{\frac{N_{sc}}{2}}^{\frac{N_{sc}}{2}} a_n e^{j(\phi_n + n\Delta\omega t)} s_k(t - iT_s) \quad 4.2$$

In each in phase and quadrature modulator(IQM), the OFDM electrical signal modulates the optical signal. Before being applied to MZM, this signal is up converted into an intermediate frequency signal. To make computations easier, the remaining analysis is done for only one symbol period. As a result, the up converted signal can be expressed as follows for only one symbol period:

$$S_{up}(t) = \mathrm{Re}(S_{BB}(t)).\cos(\omega_{RF} t) - \mathrm{Im}(S_{BB}(t)).\sin(\omega_{RF} t) \quad 4.3$$

$$S_{up}(t) = \sum_{n=-\frac{N_c}{2}}^{\frac{N_c}{2}} [a_n \cos(n\Delta\omega t + f_n).\cos(\omega_{RF} t) - a_n \sin(n\Delta\omega t + f_n).\sin(\omega_{RF} t)] \quad 4.4$$

$$S_{up}(t) = \sum_{n=-\frac{N_c}{2}}^{\frac{N_c}{2}} [a_n \cos(n\Delta\omega t + \phi_n + \omega_{RF} t)] \quad 4.5$$

If the up-converted signal is optically modulated by a carrier utilizing dual drive MZM, the optical signal will be as shown in Equations 4.6 through 4.8 mathematically.

$$S_{op}(t) = (1 + S_{up}(t)).\cos(\omega_o t) \quad 4.6$$

$$S_{op}(t) = \left(\cos(\omega_o t) + \sum_{n=-\frac{N_{sc}}{2}}^{\frac{Ns_c}{2}} [a_n \cos(n\Delta\omega t + \phi_n + \omega_{RF} t).\cos(\omega_o t)] \right) \quad 4.7$$

$$S_{op}(t) = \cos(\omega_o t) + \sum_{n=-\frac{N_{sc}}{2}}^{\frac{N_{sc}}{2}} \frac{a_n}{2}[\cos((\omega_o + \omega_{RF})t + n\Delta\omega t + \phi_n) + \cos((\omega_o - \omega_{RF})t - n\Delta\omega t - \phi_n)] \quad 4.8$$

4.1.2. Fiber link Model: The Channel

Chromatic dispersion (CD), as stated in the earlier discussion, is a phase shift caused by a frequency and fiber length dependent distortion. CD can be viewed mathematically as a transfer function of the fiber media given by the following formula [57].

$$H(f) = e^{j\frac{1}{2}\beta_2 (2\pi)^2 (f - f_{REF})^2 L} \quad 4.9$$

Where, β_2 is the second derivative of β with respect to ω (see Equation 4.10), f refers to the optical carrier; f_{REF} is a reference frequency setting the time origin; and L is the fiber link length. The CD characteristic of the fiber, as seen in Equation 4.10, determines the parameter β_2 where c is the vacuum speed of light and D is the fiber dispersion parameter.

$$\beta_2 = \frac{d^2\beta}{d\omega^2} \quad 4.10$$

$$\beta_2 = -\frac{c}{2\pi f_{REF}^2} D \quad 4.11$$

By replacing β_2 in equation 4.9, a medium transfer function is generated (Equation 4.11 and 4.12).

$$H(f) = e^{-j\frac{c}{4\pi f_{REF}^2} D(2\pi)^2 (f - f_{REF})^2 L} \quad 4.12$$

$$H(f) = e^{-j\pi cD\left(\frac{f - f_{REF}}{f_{REF}}\right)^2 L} \quad 4.13$$

The reference frequency parameter must be handled with extreme caution. This is not a physical property of the fiber; it is critical to understand this at this time. This is a point of reference against which phase shifts are measured. It is intimately linked to the receiver's synchronization. The establishment of a symbol window at reception is done differently mathematically than in practice. Instead of employing training symbols, a frequency is specified that will be used as the start of relevant information receipt; this value is known as the reference frequency. The simulation environment is no different. The simulation's intelligent setup of this parameter will enable for accurate detection and a better understanding of how CD impacts the transmitted signal. As a result, a complete mathematical analysis of the sent signal at key stages of the link has been implemented.

When an optical modulated signal is transmitted across a fiber media, it is susceptible to chromatic dispersion (CD). As a result, the above-mentioned transfer function of fiber medium has an impact on it mathematically as follow:

$$S_{CD}(t) = S_{op}(t) * h(t) \quad 4.14$$

$$S_{CD}(\omega) = S_{op}(\omega).H(\omega) = S_{op}(\omega).e^{-j\frac{\beta_2}{2}(\omega-\omega_{REF})^2 L} \quad 4.15$$

The signal now depends on the mathematical parameter in question (reference frequency), as shown in Equation 4.15.

$$S_{CD}(t) = 1 + \sum_{n=-\frac{N_c}{2}}^{\frac{N_c}{2}} a_n e^{-j\frac{\beta_2}{2}(\omega_{REF}+n\Delta\omega)^2 L} [\cos((\omega_{RF}+n\Delta\omega)(t-\beta_2(\omega_o-\omega_{REF})L)+\phi_n)] \quad 4.16$$

$$S_{CD}(t) = 1 + \sum_{n=-\frac{N_c}{2}}^{\frac{N_c}{2}} a_n e^{-j\frac{\beta_2}{2}(\omega_{REF}+n\Delta\omega)^2 L} e^{j[(\omega_{RF}+n\Delta\omega)(t-\beta_2(\omega_o-\omega_{REF})L)]} \quad 4.17$$

4.1.3. DP-16QAM Co-O-OFDM Receiver

Coherent detection is an enhanced detection approach in which the receiver recovers the entire electric field, including amplitude and phase information. Because information can be encoded in amplitude and phase, polarization, or a combination of the above components of a carrier, coherent detection gives us the most flexibility in modulation forms. Because the received signal is demodulated by a local oscillator that serves as an absolute phase reference in coherent detection, the receiver will have prior knowledge of the carrier phase[33].

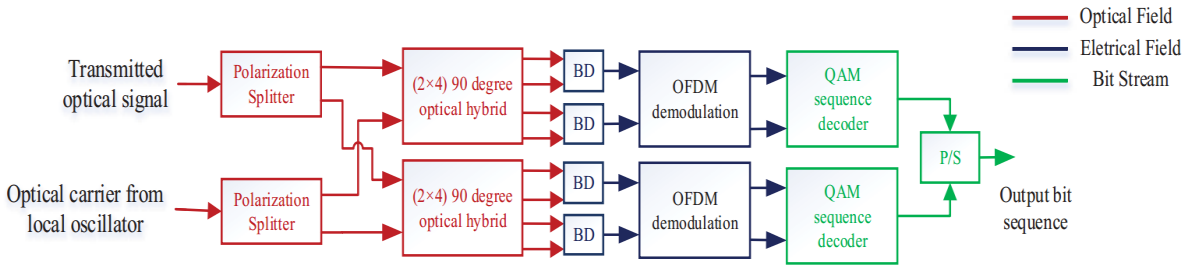

Figure 4. 3: DP-16QAM Co-O-OFDM receiver[61]

As shown in the figure above both transmitted optical signal and optical carrier from local oscillator are divided into X and Y polarizations using polarization splitter before mixed in optical hybrid. That is the received signal is fed to one arm of hybrid coupler where the other input to hybrid is local oscillator signal. The output of the hybrid is detected on the photodetector and then transferred to the digital receiver which is OFDM modulation and the digital signal is recovered. To understand coherent detection better let's have a look at the working principle of hybrid.

Let the transmitted optical signal $E_s(t)$ can be represented as[61]:

$$E_s(t) = \sqrt{p_s} * e^{j(\omega_s t + \phi_s)} \quad 4.17$$

Where P_s is Optical transmitted power

ω_s is the frequency of a transmitted optical wave

ϕ_s is phase of a transmitted optical wave

Similarly, Local oscillator is represented as

$$E_{Lo}(t) = \sqrt{p_{Lo}} * e^{j(\omega_{Lo}t+\phi_{Lo})} \quad 4.18$$

Where P_{LO} is Optical power of Local-oscillator

ω_{LO} is the frequency of Local-oscillator

ϕ_{LO} is phase of Local-oscillator

Both signals are combined in an optical hybrid, which then sends the outputs to the digital receiver. This hybrid is constructed by using four 180° hybrids and a 90° phase shifter as shown in figure below. Here we focus only on homodyne coherent receiver.

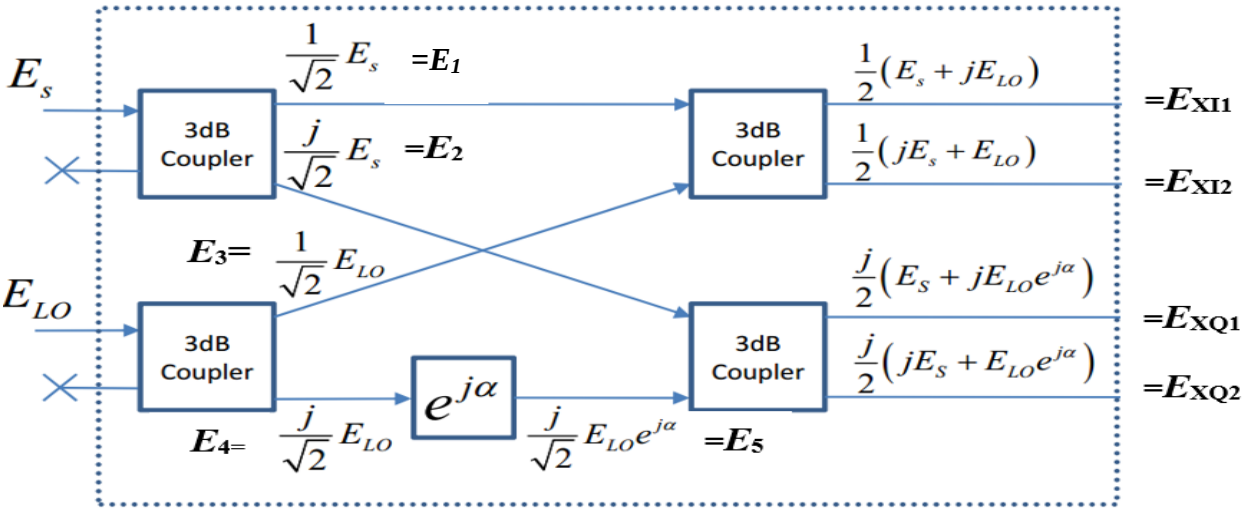

Figure 4. 4: Homodyne Optical hybrid where $\alpha=90^0$[66]

Setting the phase shift to α=90°, The transfer function of ideal or equally divided 3 dB coupler is given by [66]:

$$\begin{pmatrix} E_{output1}(t) \\ E_{output2}(t) \end{pmatrix} = \frac{1}{\sqrt{2}} \begin{pmatrix} 1 & j \\ j & 1 \end{pmatrix} \begin{pmatrix} E_{input1}(t) \\ E_{input2}(t) \end{pmatrix} \quad 4.19$$

Using ideal hybrid equation

$$\begin{bmatrix} E_1 \\ E_2 \end{bmatrix} = \frac{1}{\sqrt{2}} \begin{pmatrix} 1 & j \\ j & 1 \end{pmatrix} \begin{bmatrix} E_s(t) \\ 0 \end{bmatrix} \quad 4.20$$

$$E_1 = \frac{1}{\sqrt{2}} E_s(t) \quad 4.21$$

$$E_2 = j\frac{1}{\sqrt{2}} E_s(t) \quad 4.22$$

Similarly,

$$\begin{bmatrix} E_3 \\ E_4 \end{bmatrix} = \frac{1}{\sqrt{2}} \begin{pmatrix} 1 & j \\ j & 1 \end{pmatrix} \begin{bmatrix} E_{Lo}(t) \\ 0 \end{bmatrix} \quad 4.23$$

$$E_3 = \frac{1}{\sqrt{2}} E_{LO}(t) \quad 4.24$$

$$E_4 = j\frac{1}{\sqrt{2}} E_{LO}(t) \quad 4.25$$

$$E_5 = -jE_4 = -\frac{1}{\sqrt{2}} E_{LO}(t) \quad 4.26$$

E_4 goes through a 90 ˚ phase delay to get $E_5 = -jE_4 = -\frac{1}{\sqrt{2}} E_{LO}(t)$

$$\begin{bmatrix} E_{X11} \\ E_{X12} \end{bmatrix} = \frac{1}{\sqrt{2}} \begin{pmatrix} 1 & j \\ j & 1 \end{pmatrix} \begin{bmatrix} E_1 \\ E_3 \end{bmatrix} = \frac{1}{\sqrt{2}} \begin{pmatrix} 1 & j \\ j & 1 \end{pmatrix} \begin{bmatrix} \frac{1}{\sqrt{2}} E_s(t) \\ \frac{1}{\sqrt{2}} E_{LO}(t) \end{bmatrix} \quad 4.27$$

$$E_{XI1} = \frac{1}{2}(E_s(t) + jE_{LO}(t)) \quad 4.28$$

$$E_{XI2} = \frac{1}{2}(jE_s(t) + E_{LO}(t)) \quad 4.29$$

$$\begin{bmatrix} E_{XQ1} \\ E_{XQ2} \end{bmatrix} = \frac{1}{\sqrt{2}}\begin{pmatrix} 1 & j \\ j & 1 \end{pmatrix}\begin{bmatrix} E_2 \\ E_5 \end{bmatrix} = \frac{1}{\sqrt{2}}\begin{pmatrix} 1 & j \\ j & 1 \end{pmatrix}\begin{bmatrix} j\frac{1}{\sqrt{2}}E_s(t) \\ -\frac{1}{\sqrt{2}}E_{Lo}(t) \end{bmatrix} \quad 4.30$$

$$E_{XQ1} = \frac{1}{2}(jE_s(t) - jE_{Lo}(t)) \quad 4.31$$

$$E_{XQ2} = \frac{j}{2}(jE_s(t) + jE_{Lo}(t)) \quad 4.32$$

Using square law detection, the current generated by the photodiode corresponding to the balanced receiver is as follows, where R is the photodiode's responsivity [61, 66].

$$\mathrm{I}_{XI1} = R\,|\,E_{XI1}(t)\,|^2 = R\,|\,\frac{1}{2}(E_s(t) + jE_{LO}(t)\,|^2 \quad 4.33$$

$$\mathrm{I}_{XI2} = R\,|\,E_{XI2}(t)\,|^2 = R\,|\,\frac{1}{2}(jE_s(t) + E_{LO}(t)\,|^2 \quad 4.34$$

$$\mathrm{I}_{XQ1} = R\,|\,E_{XQ1}(t)\,|^2 = R\,|\,\frac{1}{2}(jE_s(t) - jE_{LO}(t)\,|^2 \quad 4.35$$

$$\mathrm{I}_{XQ2} = R\,|\,E_{XQ2}(t)\,|^2 = R\,|\,\frac{j}{2}(jE_s(t) + jE_{LO}(t)\,|^2 \quad 4.36$$

Then by substituting the values of $E_s(t)$ and $E_{LO}(t)$ in above equations:

$$\mathrm{I}_{XI1} = \frac{1}{4}RP_s + \frac{1}{4}RP_{XLO} - \frac{1}{2}R\sqrt{P_sP_{XLO}}\cos[(\omega_s - \phi_{XLO})t + (\omega_s - \phi_{XLO})] \quad 4.37$$

$$I_{XI2} = \frac{1}{4}RP_s + \frac{1}{4}RP_{XLO} + \frac{1}{2}R\sqrt{P_s P_{XLO}}\cos[(\omega_s - \phi_{XLO})t + (\omega_s - \phi_{XLO})] \quad 4.38$$

$$I_{XQ1} = \frac{1}{4}RP_s + \frac{1}{4}RP_{XLO} - \frac{1}{2}R\sqrt{P_s P_{XLO}}\sin[(\omega_s - \phi_{XLO})t + (\omega_s - \phi_{XLO})] \quad 4.39$$

$$I_{XQ2} = \frac{1}{4}RP_s + \frac{1}{4}RP_{XLO} + \frac{1}{2}R\sqrt{P_s P_{XLO}}\sin[(\omega_s - \phi_{XLO})t + (\omega_s - \phi_{XLO})] \quad 4.40$$

The ratio of the photocurrent I_P to the incident light power P at a certain wavelength is the responsivity of a silicon photodiode, which is defined as the ratio of the photocurrent I_P to the incoming light power P at that wavelength.

Bringing the above equations into $I_{XI}=I_{XI2}-I_{XI1}$ and $I_{XQ}=I_{XQ2}-I_{XQ1}$ to get the current output by the X polarization balanced receiver as:

$$I_{XI} = R\sqrt{P_s P_{XLO}}\cos[(\omega_s - \phi_{XLO})t + (\omega_s - \phi_{XLO})] \quad 4.41$$

$$I_{XQ} = R\sqrt{P_s P_{XLO}}\sin[(\omega_s - \phi_{XLO})t + (\omega_s - \phi_{XLO})] \quad 4.42$$

Similarly, the current output by the Y polarization balanced receiver is:

$$I_{YI} = R\sqrt{P_s P_{XLO}}\cos[(\omega_s - \phi_{XLO})t + (\omega_s - \phi_{XLO})] \quad 4.43$$

$$I_{YQ} = R\sqrt{P_s P_{XLO}}\sin[(\omega_s - \phi_{XLO})t + (\omega_s - \phi_{XLO})] \quad 4.44$$

The electrical signal in the form of electrical current is obtained after coherent detection comprises the amplitude, frequency, and phase information of the received optical signal, as shown in the theoretical derivation above. The electrical signal becomes a digital signal after sampling by the ADC, and it enters the digital domain for processing. That means these output electrical signals are transferred to dual OFDM demodulation block for digitization process.

Signal detected from OFDM demodulation process can be represented as follow for one OFDM symbol.

$$S_d(t) = \sum_{n=-\frac{N_c}{2}}^{\frac{N_c}{2}} a_n \cos(\omega_{RF} + n\Delta\omega)(t - \beta_2(\omega_0 - \omega_{REF})L - \frac{\beta_2}{2}(\omega_{RF} + n\Delta\omega)L)) \quad 4.45$$

This detected signal is down converted and filtered.

$$S_R(t) = S_d(t).(\cos(\omega_{RF}t) - j\sin(\omega_{RF}t)) \quad 4.46$$

After down conversion and filtering the above signal can have the following form for one OFDM symbol.

$$S_{Rx}(t) = \sum_{n=-\frac{N_c}{2}}^{\frac{N_c}{2}} a_n e^{\{jn\Delta\omega[t-\beta_2(\omega_0-\omega_{REF})-\beta_2-\frac{\beta_2}{2}n\Delta\omega]-j\beta_2\omega_{REF}(\omega_0-\omega_{RF}-\frac{\omega_{RF}}{2})\}} \quad 4.47$$

The disappearance of a fading component, such as the cosine factor, which was reliant on the RF up conversion frequency, and the appearance of a delay that is variable for each subcarrier are highlighted in the preceding expression. To avoid leakage to nearby symbols, this would require the usage of a CP.

The reference frequency in this example is in the center of the OFDM band, which means that the reception window will begin in the middle of the interval in which the subcarriers arrive. For correct insertion and extraction of the CP in simulations, this must be taken into account.

As discussed in the previous chapter, the output of the I-channel mixer in the DP-16QAM demodulator can be represented with the following wave form.

$$s_I(t) = \frac{1}{2}[d_I + d_I\cos(4\tau f_c t) + d_I d_Q \sin(4\tau f_c t)] \quad 4.48$$

The output of the I-channel mixer, as shown in the above equation, is an analog signal with four level data pulses d_I and high-frequency components $d_I\cos(4\pi f_c t)$ and $d_I d_Q \sin(4\pi f_c t)$. The four-level data pulses d_Q and high frequency components are also included in the Q-channel

mixer's output. The high-frequency components are removed by the LPF, leaving only the data pulses.

The detection circuit must sample these signals once per symbol period and then decide which state each sample represents because the integrated signal in each channel is a time-varying analog signal. To determine what levels each sampled level represents, the decision circuit compares it to three thresholds. This circuit produces a stream of bipolar data pulses with fixed amplitudes. This signal is converted to a digital signal via the 4 to 2 level Converter circuit. Each channel's dibits are combined into a serial stream of data bits via the Parallel to Serial Converter. This data is identical if no errors occur during the modulation, transmission, and demodulation processes.

4.2. Coherent Optical OFDM System with FBG

As it can be seen from figure below, the FBG sub-block is added to the previous general block of Co-O-OFDM to integrate Co-O-OFDM system with FBG as dispersion compensation technique. Here we discuss how FBG compensate dispersion since other blocks are discussed in the previous section.

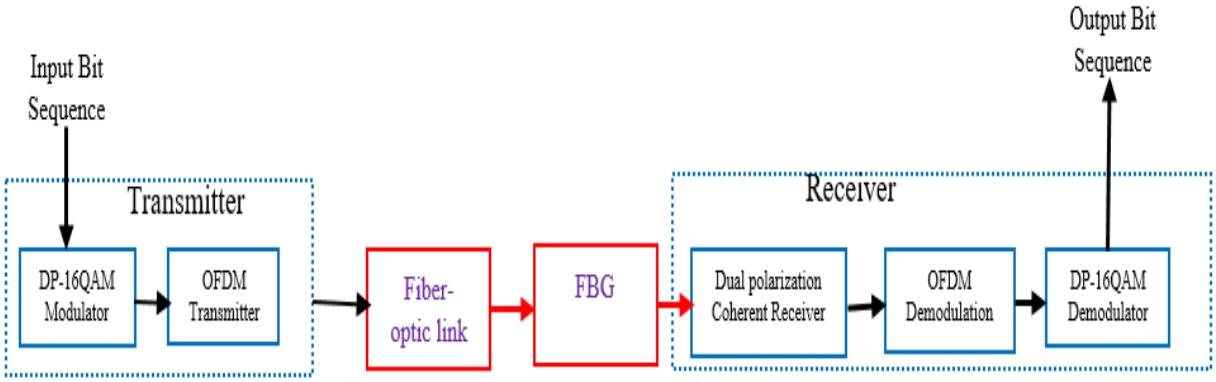

Figure 4. 5: General Block Diagram of high speed optical fiber communication with Co-O-OFDM with FBG

4.2.1. Fiber Braggs Gratings (FBG)

Nowadays, chromatic dispersion adjustment is achieved by recompressing the dispersed optical signal using entirely optical components such as FBG [7, 41]. It consists of a direct intelligent device with an intelligent record profile that changes in direct proportion to the fiber length. As indicated in the diagram below, the grinding reflects light based on the wavelength of the light that enters the grinding. Light with a longer wavelength travels a greater distance inside the grinding before being considered, whereas light with a shorter wavelength travels a shorter distance inside the grinding before being reflected. Thus, a Fiber Bragg Grating(FBG) is used to compress the pulse that is expanded by chromatic passing in order to scat in an SMF.

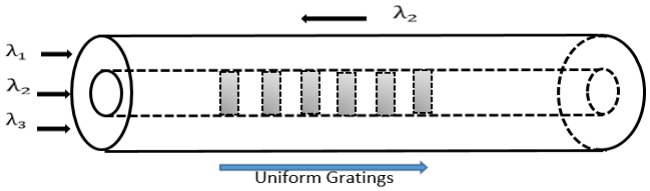

Figure 4. 6: Principles of Fiber Bragg Gratings[67]

FBG is a reflecting device in an optical fiber that causes core refractive index modification at a specific wavelength. When the wavelength of the signal traveling through the optical fiber matches the modulation periodicity of FBG, reflection occurs in gratings. The Bragg wavelength (b) is the reflected wavelength that is expressed by the following equation[41]:

$$\lambda_b = 2\Lambda n_{eff} \tag{4.49}$$

Where n_{eff} is the grating's effective refractive index in the fiber core, and Λ represents the grating. The operation of a fiber Bragg grating is determined by factors such as light reflection from grating fringes and mode coupling. Between the forward and backward propagating fields, there is a coupling. The two fields have strong coupling if they follow the stated Bragg criterion, according to the coupling process:

$$\beta_1 - \beta_2 = \frac{2m\pi}{\Lambda} \tag{4.50}$$

Where, β_1 and β_2 are the phase constants of two coupling modes, m is the order of diffraction, and Λ displays the grating time based on refractive index fluctuation (assuming sinusoidal variation). For first order, m =1.

Using two inverse propagating modes that are equal

$$\beta_1 = -\beta_2 \tag{4.51}$$

The Bragg diffraction condition is obtained from equation (4.50).

$$\beta_1 = \frac{m\pi}{\Lambda} \tag{4.52}$$

We can get: by substituting the value of grating period from equation (4.49) to equation (4.52) and m=1. [12]

$$\beta_1 = \frac{2n_{eff}}{\lambda_b} \tag{4.53}$$

When m=1, the Bragg wavelength significantly reflected by the grating may be calculated by putting equation 4.52 into equation 4.53. For momentum conservation requirement of Bragg grating condition π can be ignored.

$$\lambda_b = 2n_{eff}\Lambda \tag{4.54}$$

This is the last wave condition that a Fiber Bragg Grating will reflect. Only wavelengths that satisfy the Bragg criterion are affected, and they are strongly reflected back.

4.3. Analytical Tool

The optical signal-to-noise ratio (OSNR) is a measurement of how much optical noise interferes with optical signals. Within a proper bandwidth, it is the ratio of service signal power to noise power. The optical signal to noise ratio (OSNR) is reduced when a signal is amplified by an optical amplifier (OA), such as an EDFA, and this is the major rationale for having a small number of OAs in a network. The receiver's OSNR values are the most important, because a low OSNR value

indicates that the receiver will most likely not detect or recover the signal. One of the key criteria that determines how far a wavelength can travel before regeneration is the OSNR limit.

The optical signal to noise ratio (OSNR) is used to evaluate the performance of optical transmission systems. The bit error rate(BER) is defined as the number of bits in error divided by the total number of transmitted bits. The minimal signal-to-noise ratio (SNR) necessary to get a specified BER for a given signal is indicated by the quality factor (Q-factor).

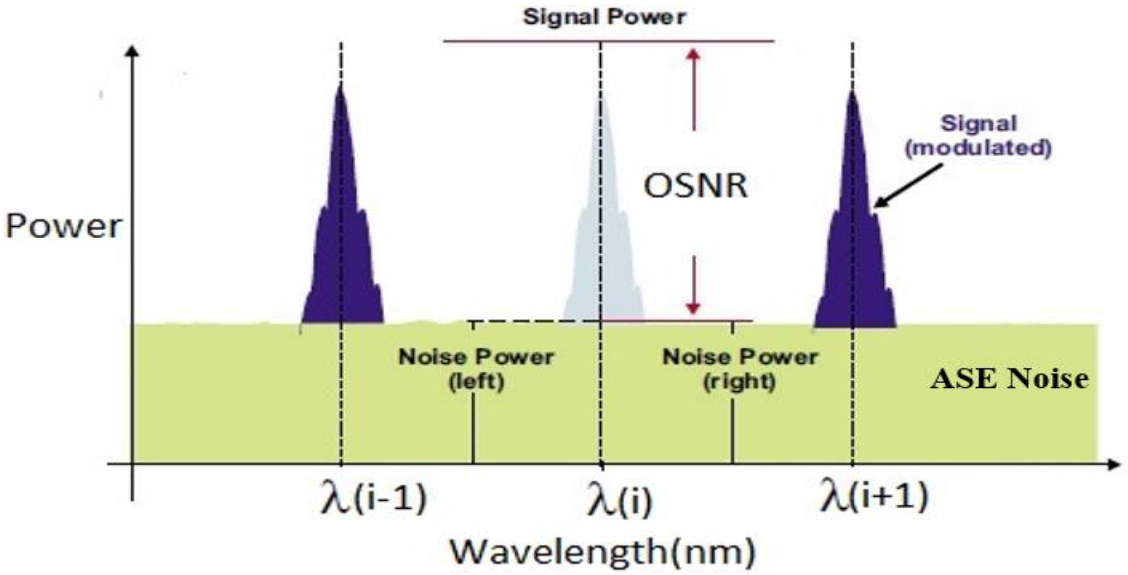

Figure 5. 1: OSNR measurement

. The bit error rate (BER), which is the final value for measuring the quality of a transmission, has a direct relationship with OSNR.

They are stated mathematically as follows [68]:

$$\text{OSNR}=\frac{P_s}{P_n}=\frac{E_b R_b}{N_o B_N} \tag{4.55}$$

$$\text{BER}=\frac{1}{2}\text{erfc}\left(\sqrt{\frac{E_b}{N_o}}\right)=\frac{1}{2}\text{erfc}\left(\sqrt{OSNR.\frac{B_N}{R_b}}\right) \tag{4.56}$$

$$Q=10\log_{10}\left(2*OSNR*\frac{B_N}{R_b}\right) \tag{4.57}$$

Where P_s is transmitted signal power, P_n is noise power, E_b is the average energy per bit, R_b is the bit rate, N_o is the noise power spectral density, and B_N is the noise bandwidth.

CHAPTER FIVE

Simulation Results and Discussion

In this chapter, simulation setup, simulation parameters and simulation results were discussed. The simulation software used in this thesis are OptiSystem version 17 and MATLAB 17a.

5.1. DP-16QAM Co-O-OFDM Simulation Setup

DP-16QAM Co-O-OFDM without FBG system consists five components, namely, DP-16QAM OFDM transmitter, RF to optical converter, a fiber link, optical to RF down converter and a DP-16QAM Co-OFDM receiver.

5.1.1. DP-16QAM OFDM Transmitter Simulation Setup and its Parameters

Pseudo Random Binary Sequence (PRBS) generator was used to generate a bit sequence that will approximate the random data characteristics, and these generated bits fed into serial to parallel converter. Serial to parallel converter converts those serial bits into parallel bits and deliver to X and Y components of DP-16QAM (8 bit per symbol) encoder. From both respective 16-QAM signal is connected to respective an OFDM modulators with a 128 subcarrier.

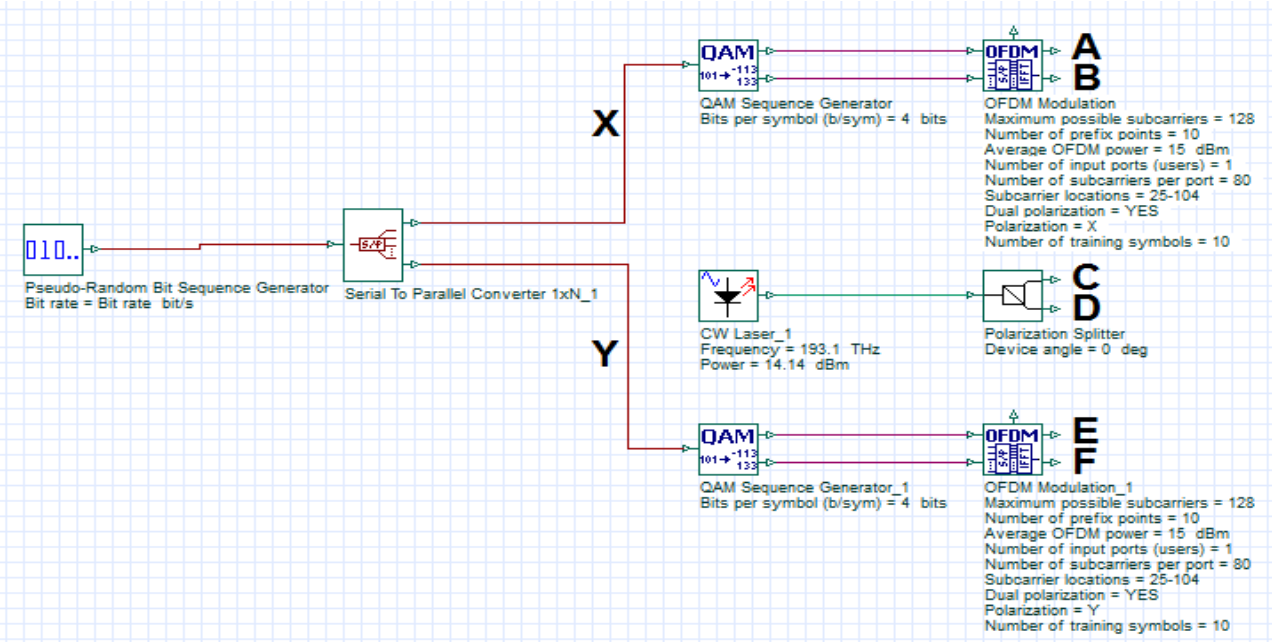

Figure 5. 2: DP-16QAM Co-O-OFDM Transmitter Simulation setup

After filtered and amplified the in-phase (I) and quadrature (Q) components of both OFDM modulators are transmitted via ports A, B, E and F to respective ports of the direct I/Q optical modulator which consists of two lithium Niobate (LiNb) Mach-Zehnder modulators (MZM) as shown in figure below. MZM will modulate the electrical signal from the OFDM modulator to the optical carrier with a laser source of 193.1 THz which are connected through C and D. The power of the laser source is 14.14 dBm

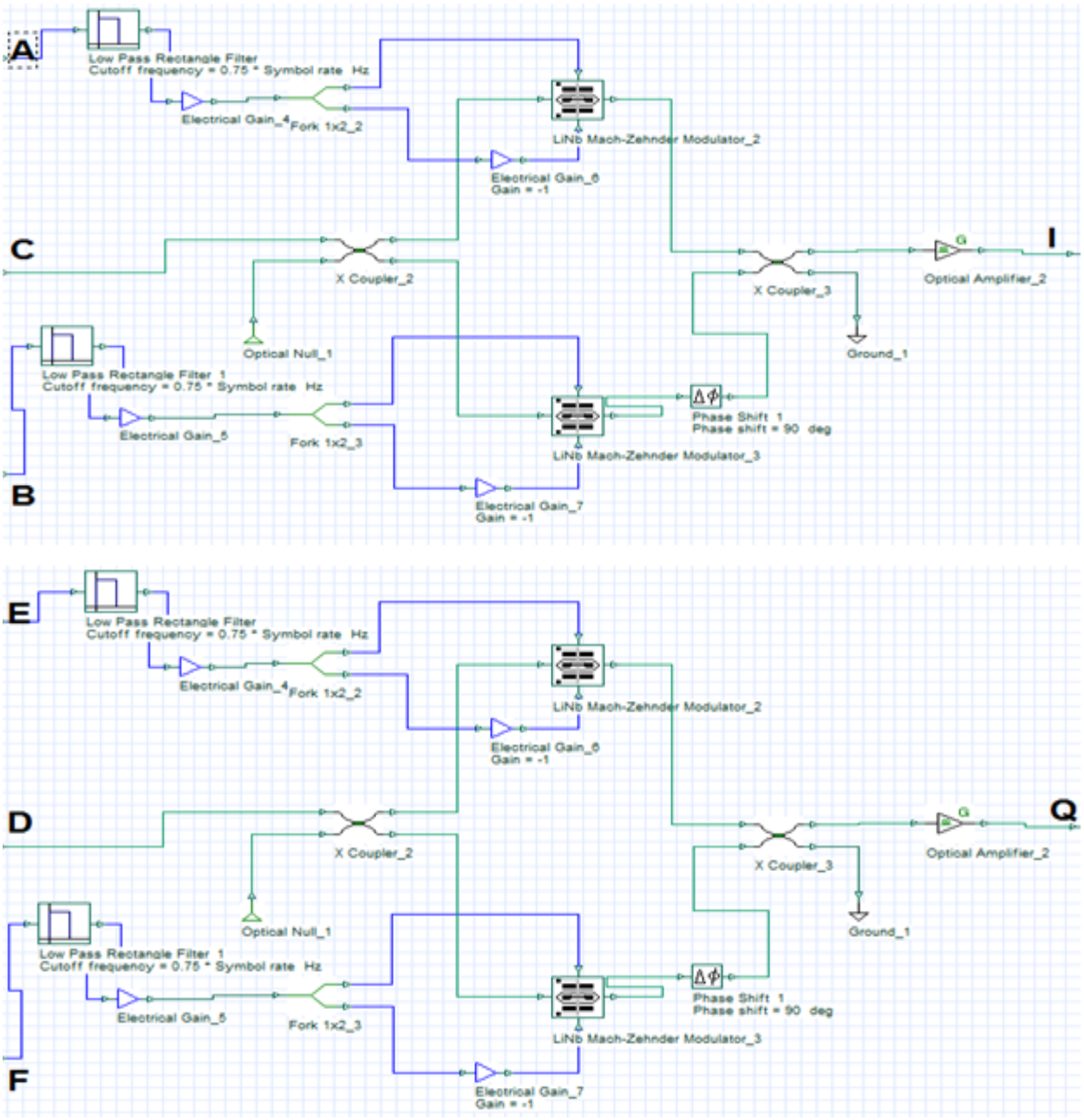

Figure 5. 3: Filter and RF to Optical up converter Simulation Setup

As shown in the above figure signal through ports A, B, E and F passed is given to low pass filter with cutoff frequency of o.75*symbol rate.

General Parameters	
Bit Rate	100E+9, 200E+9, 400E+9 and 1.00E+12
Sequence length	32768
Symbol Rate	12.5E+9, 25E+9, 50E+9 and 125E+9 baud/s
Power	0 dBm
Resolution	0.1nm

Table 5.1: General Parameters

OFDM Parameters	
Maximum Possible subcarriers	128
Number of prefix points	10
Average OFDM Power	15 dBm
Number of input ports(users)	1
Number of subcarriers per port	80
Subcarriers locations	25-104
Dual polarization	Yes
Number of training symbols	10

Table 5.2: OFDM Parameters

How simulation parameters listed above are chosen are discussed here. Four bit rates i.e. 100G, 200G, 400G and 1T were analyzed. The symbol rate is derived from the following equation for all three bit rates using bit per symbol of DP-16QAM.

$$bit\ rate = symbol\ rate * bit/symbol$$

Since DP-16QAM has 8 bit per symbol so the resulting Baud rate or symbol rates are 12.5G, 25G, 50G and 125G for 100G, 200G, 400G and 1T bit rates respectively. Most optical LASER modules in the market operate in the output power range -4 dBm to +4 dBm. In this simulation average, 0 dBm is chosen [19] [35]. The total optical noises of a transmission system are normally measured over a standard noise resolution bandwidth of 0.1 nm. So, resolution bandwidth of 0.1nm is chosen

[53]. The EDFA Gain is calculated by considering the total length of the fiber and the attenuation per km.

$EDFA\ Gain = 80k(length) \times 2dB\ km = 16\ dB$

5.1.2. Fiber link Simulation setup and its Parameters

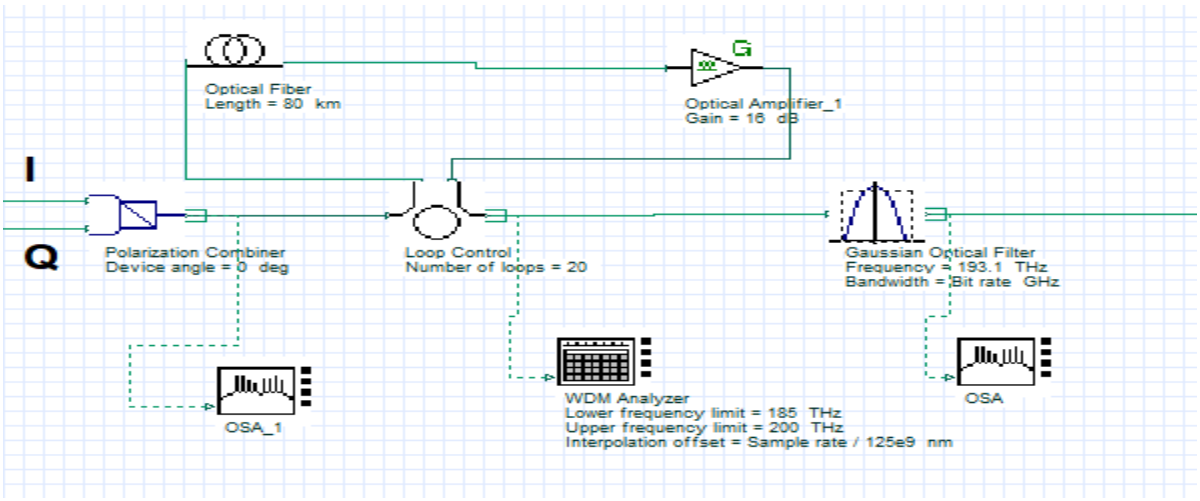

Figure 5. 4: Polarization combiner and Fiber Link Simulation Setup

The fiber parameters are characteristics of standard single mode fiber that conforms with Recommendation ITU-T G.652 [54]. The fiber length/reach is set to be 80km.

Fiber Parameters	
Reference Wavelength	1550 nm
Length	80km
Attenuation Effect	Enabled
Attenuation	0.2 dB/km
Dispersion	16.75 ps/nm/km
n_2	2.60E-20m^2/w
Beta 2	-20 ps^2/km
Beta 3	0 ps^2/km
Differential Group delay	0.2 ps/km
Effective area	80μm^2

Table 5.3: Fiber Parameters

The reason for the selection of 80 km is also to fit the typical distance of repeater housing in early optical transmission systems of the 1980s for single-mode fiber without optical amplifiers. At that time, the repeater distance was determined at 40 km for IM/DD and bitrate was normally at 155 or 622 Gb/s. There were many repeater sites built for such housing, and hence it is more economical to design the span length of 80 km to take advantage of these housing infrastructures [20].

EDFA Parameters	
Operation Mode	Gain control
Gain	16 dBm
Noise figure	4

Table 5.4: EDFA parameters

5.1.3. Co-O-OFDM Receiver Simulation setup

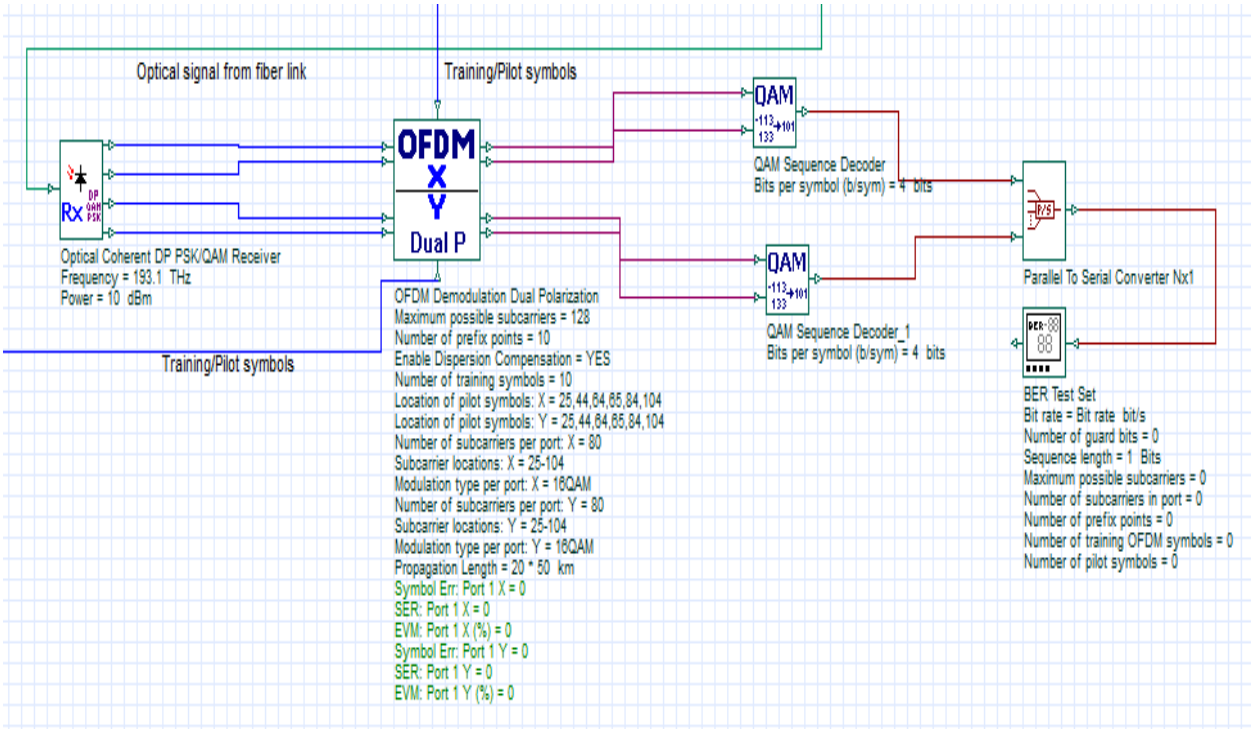

Figure 5. 5: Co-O-OFDM Receiver

As shown from Above Co-O-OFDM receiver simulation set up consists of DP-16QAM Optical coherent reciever, OFDM Demodulation Dual polarization, two QAM sequence decoder and

parellel to serial converter. As discussed in the previous chapter, dual polarization coherent receiver consists of eghit 3-dB couplers which are used to mix optical siganl transmitted with locally generated signal of CW-laser. Corresponding APD(avalanche photo diode) will do balanced detection.

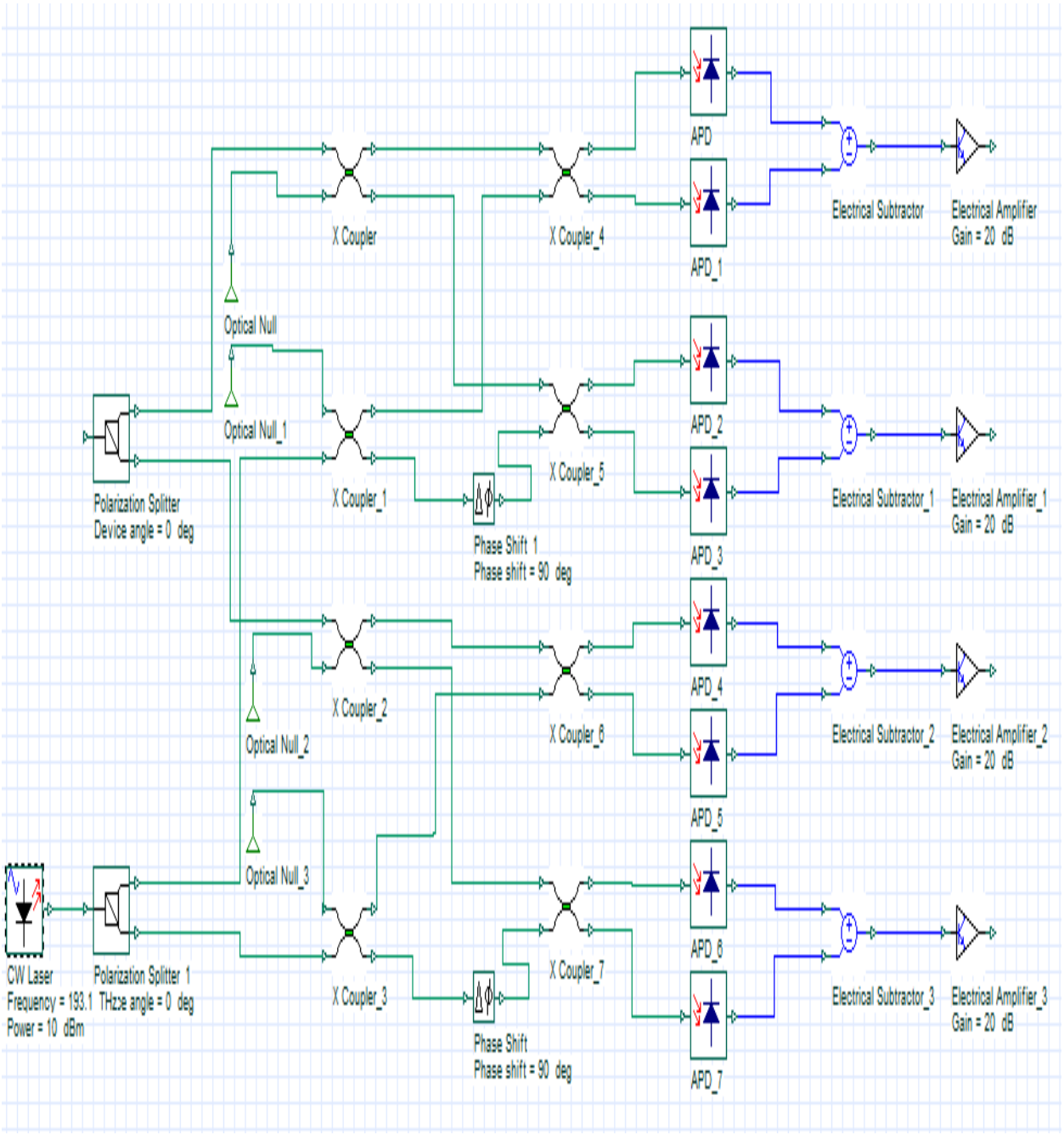

Figure 5. 6: Coherent Receiver Structure Simulation Setup

Finally, after combining all parts discussed above final simulation setup of DP-16QAM Co-O-OFDM without FBG system is shown with figure xxx below.

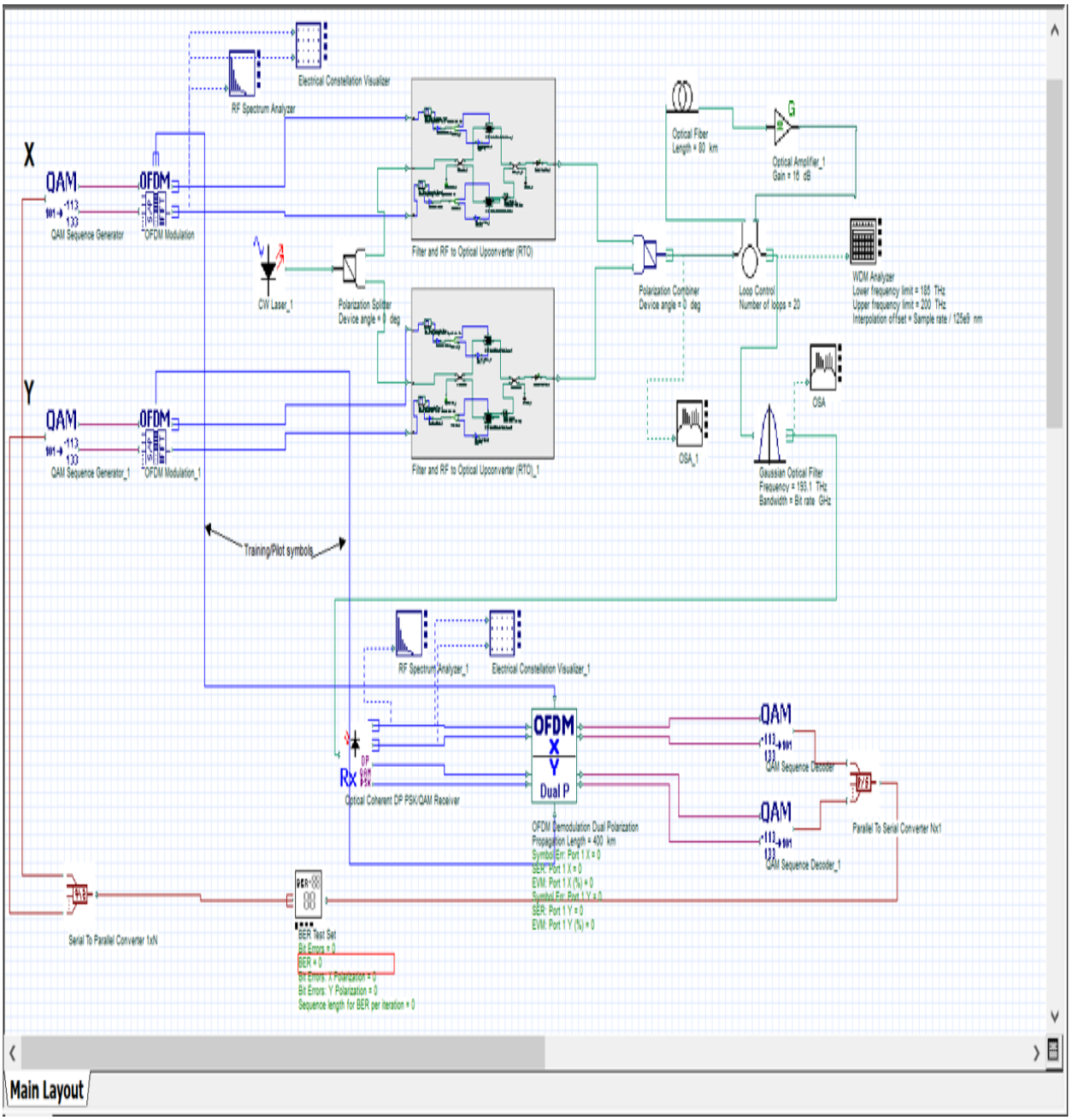

Figure 5. 7: Overall DP-16QAM Co-O-OFDM System Simulation Setup

5.2. FBG Integrated DP-16QAM Co-O-OFDM Simulation Setup

Like system without FBG, DP-16QAM Co-O-OFDM with FBG system consists five components with the same parameters except addition of FBG in the link. So here only FBG parameters and final simulation setup are shown.

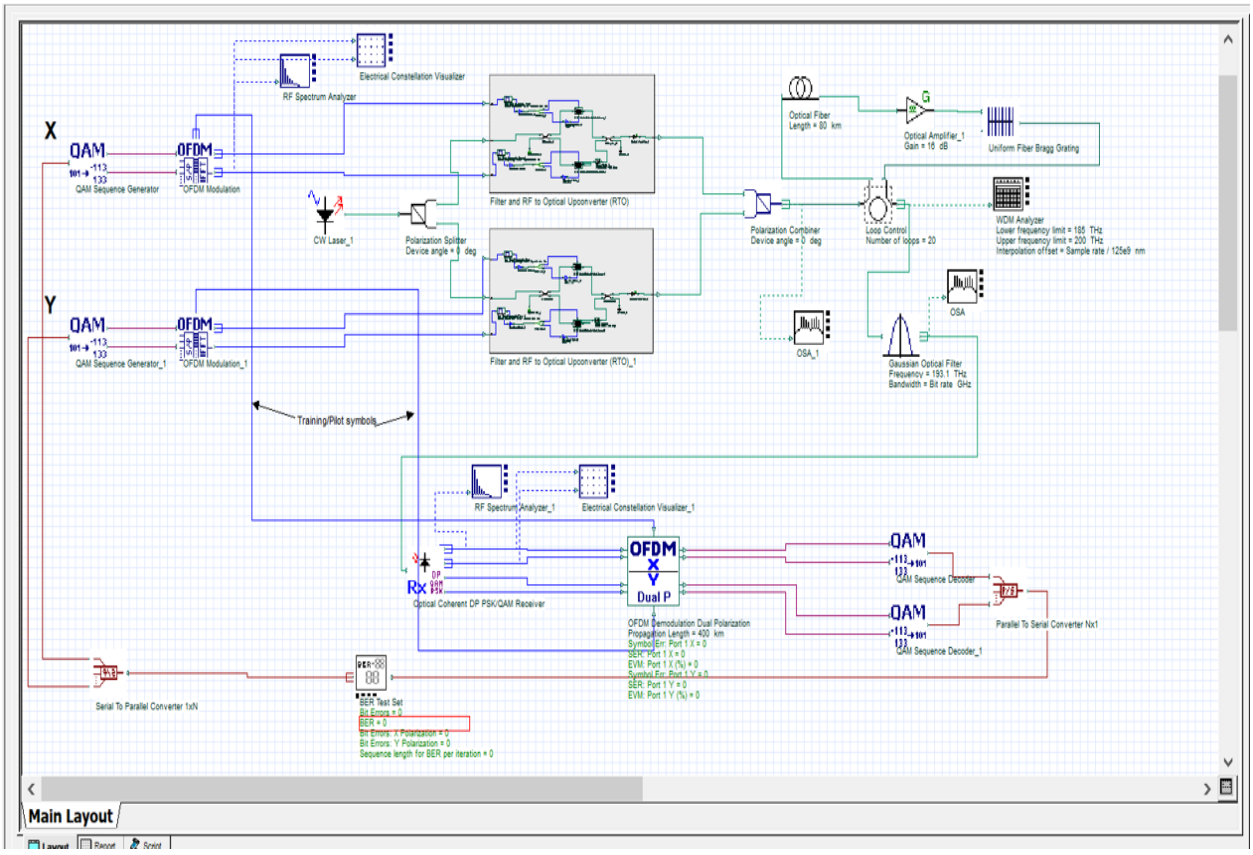

Figure 5. 8: Overall DP-16QAM Co-O-OFDM System with FBG Simulation Setup

FBG Parameters	
Frequenc(Hz)	193.1T
Effective Index	1.45
Length	2
Apodization Function	Uniform
Number of segments	100

Table 5.5: FBG parameters

5.3. Results and Discussions

The simulation results of DP-16QAM Co-OOFDM system with and without FBG at different stages and different transmission length are explained as such a way. It consists plots of RF spectrums, optical spectrums and constellation diagrams at different propagation distances for both systems (with and without FBG) and for four different rates (100G, 200G, 400G and 1T). In addition to these plots, BER vs propagation distances, BER vs OSNR, OSNR vs propagation distances and Q factor vs propagation distances are plotted using MATLAB for both systems (DP-16QAM Co-O-OFDM system with and without FBG) for four different rates.

Figures 5.9 to 5.12 show RF spectrums of DP-16QAM Co-O-OFDM system without FBG at 0km, 80 km, 320km and 1600km distances for 100G, 200G, 400G and 1T rates respectively. As can be seen from respective figures below amplitude or power of the signal is decreased as propagation distance increased. In other words, OSNR values of the system is decreased as the signal propagates longer distances due impairments like chromatic dispersion.

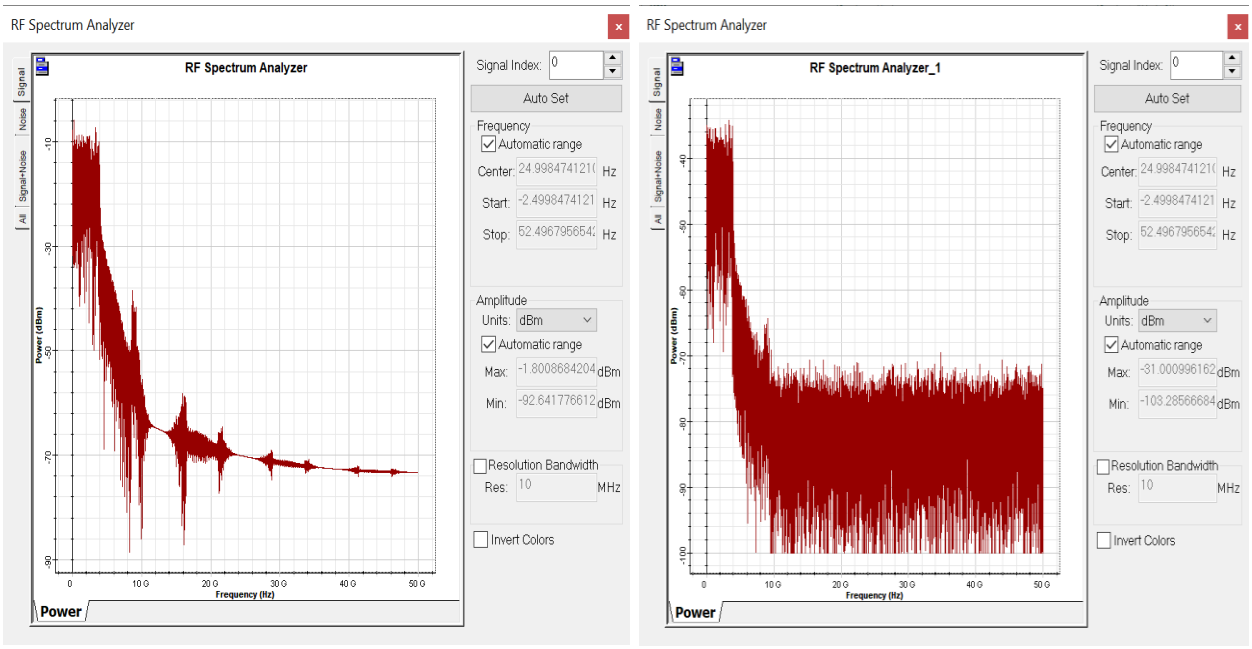

a) b)

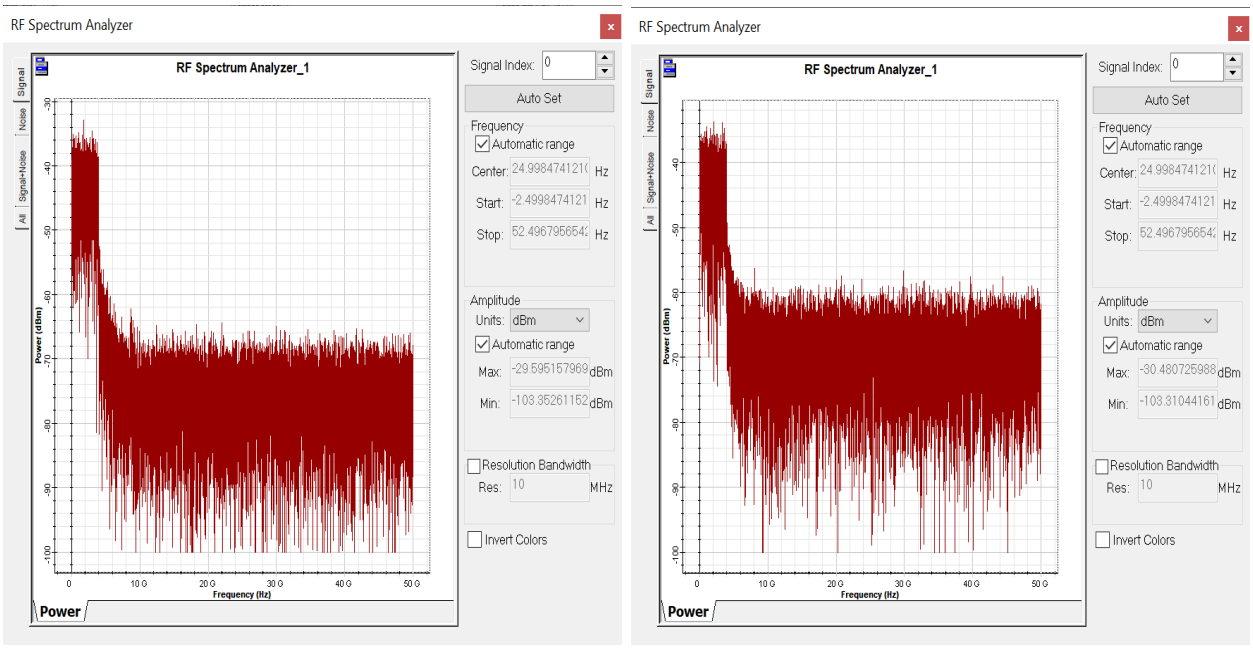

c) d)

Figure 5. 9: RF Spectrum of 100G without FBG a) at 0km b) at 80km c) at 320km d) at 1600km

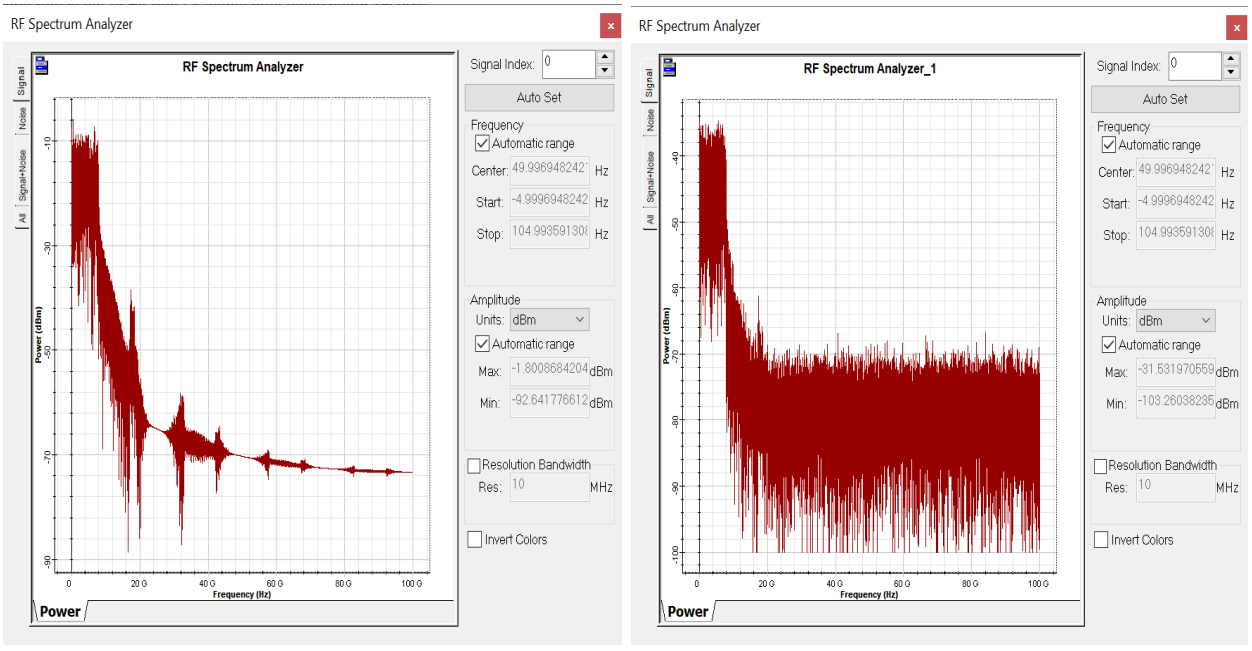

a) b)

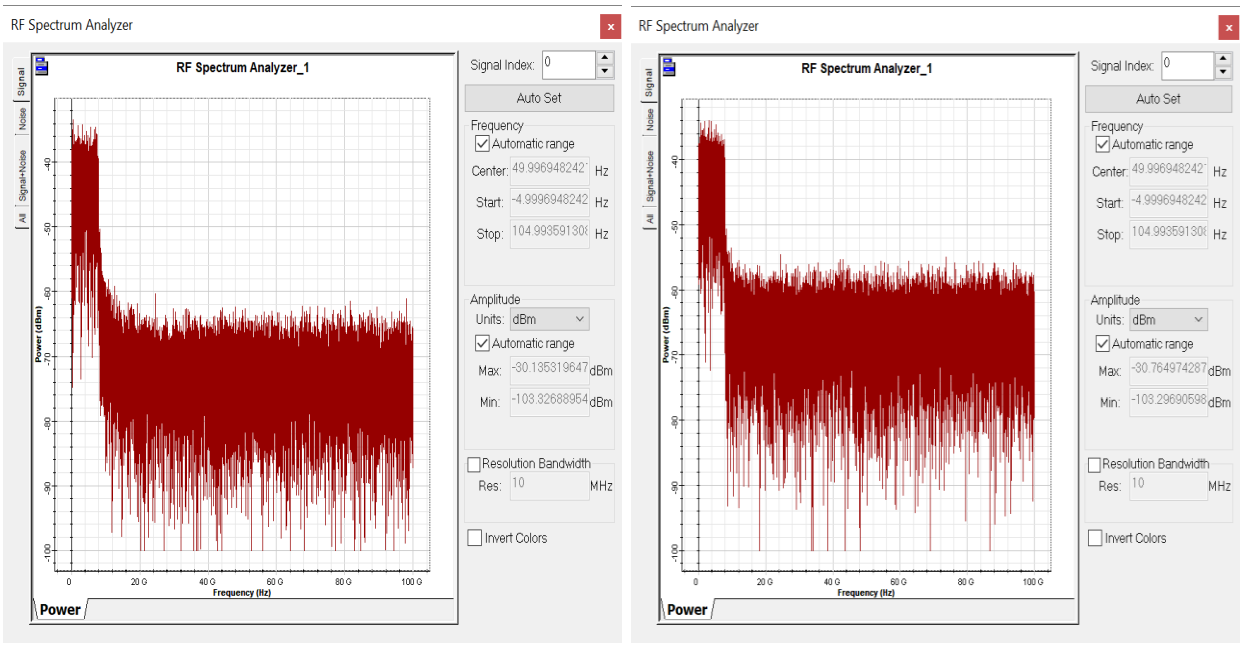

c) d)

Figure 5. 10: RF Spectrum of 200G without FBG a) at 0km b) at 80km c) at 320km d) at 1600km

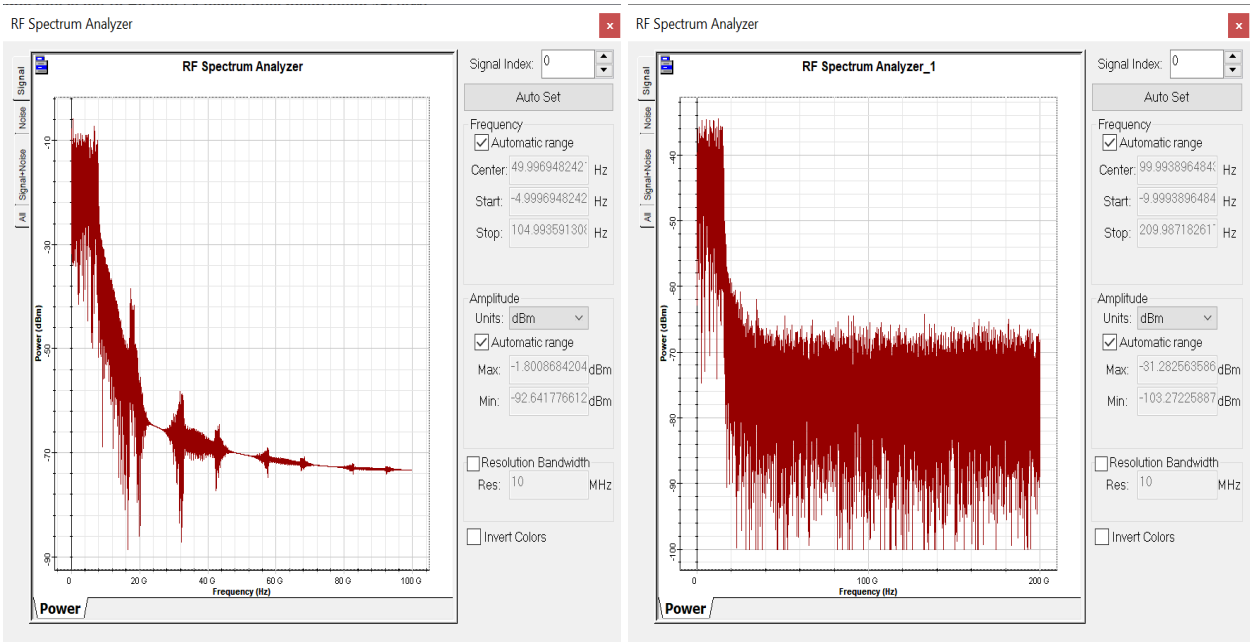

a) b)

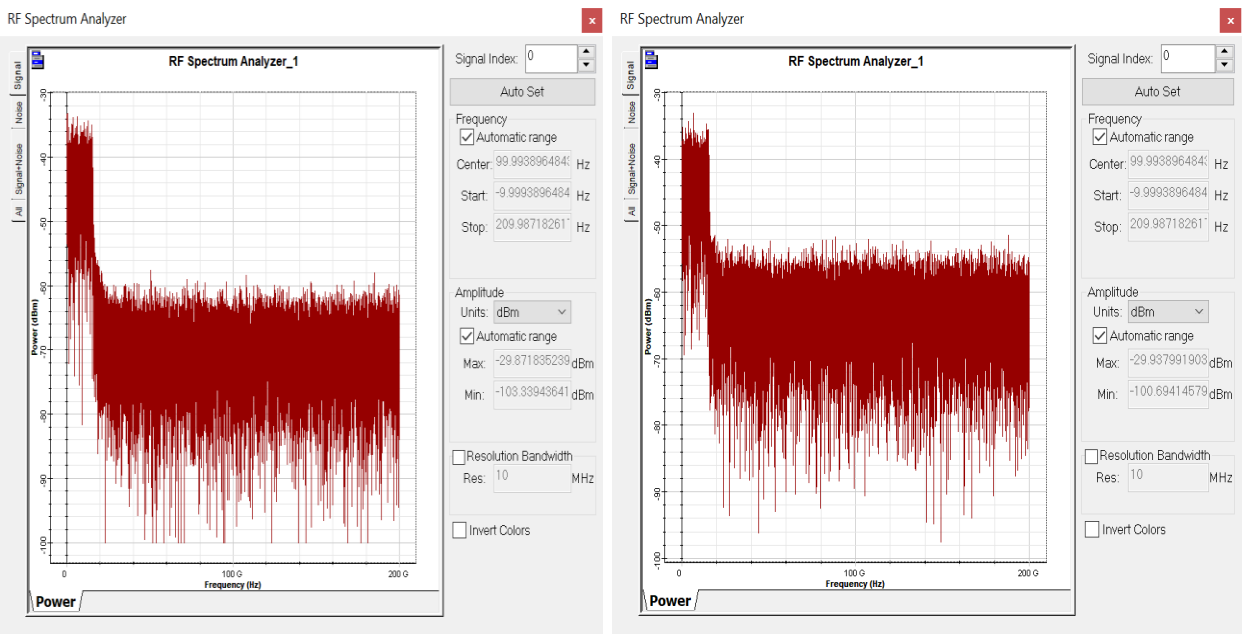

c) d)

Figure 5. 11: RF Spectrum of 400G without FBG a) at 0km b) at 80km c) at 320km d) at 1600km

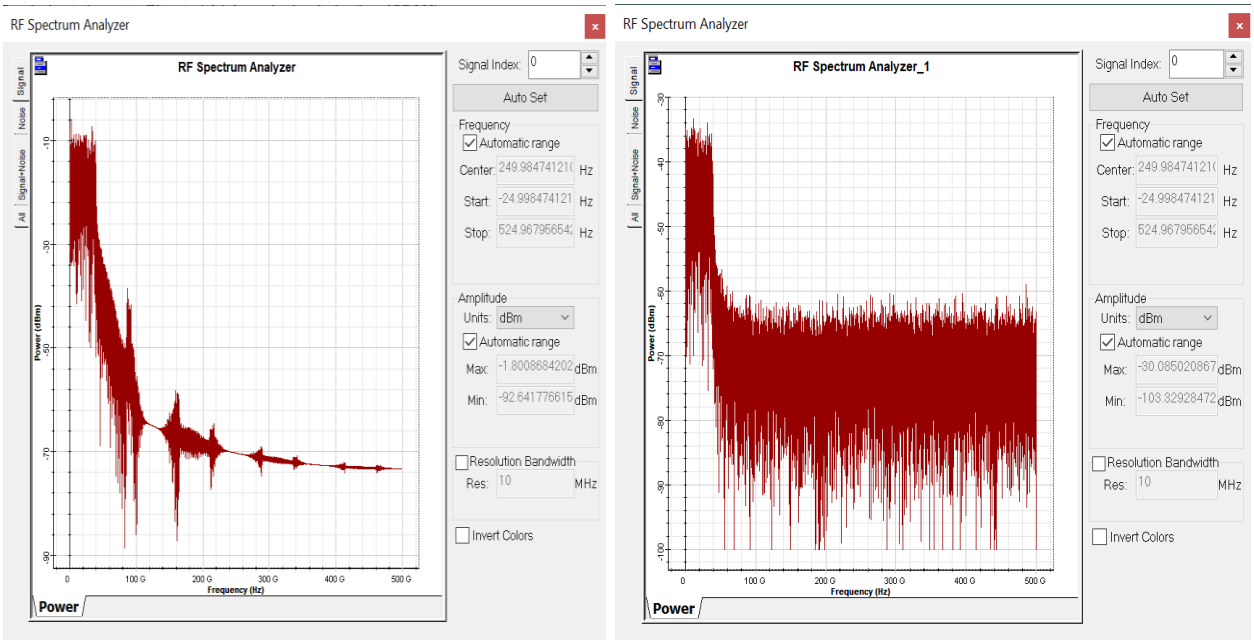

a) b)

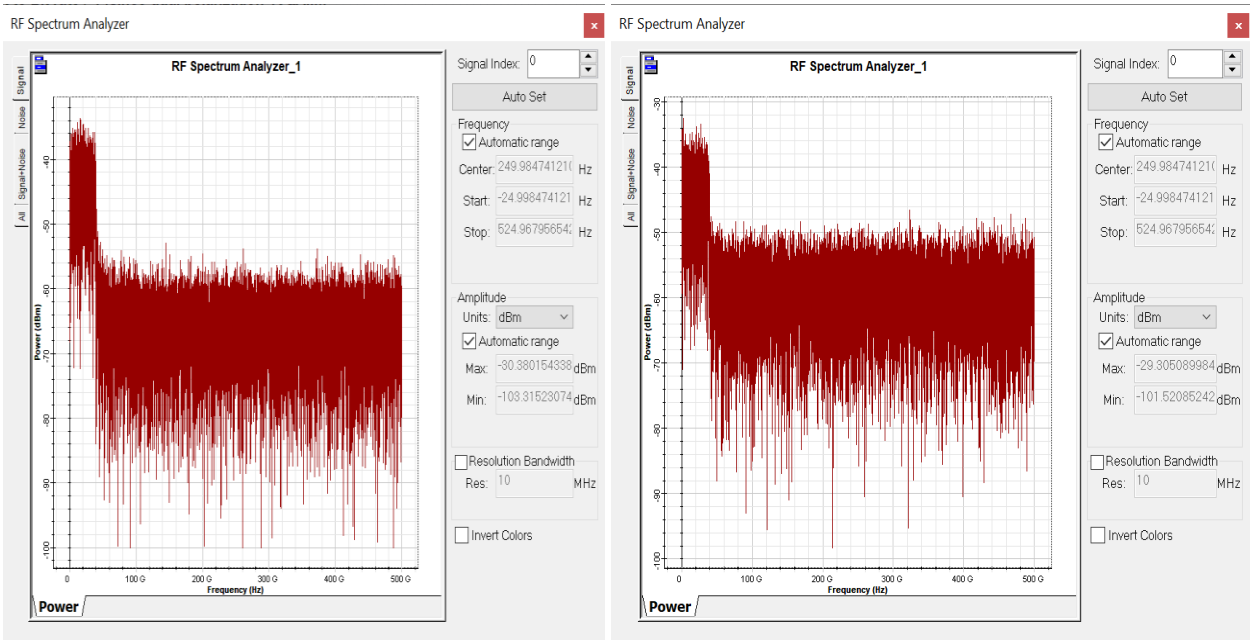

c) d)

Figure 5. 12: RF Spectrum of 1T without FBG a) at 0km b) at 80km c) at 320km d) at 1600km

Similarly, figures 5.13 to 5.16 below show RF spectrums of DP-16QAM Co-OOFDM system with FBG at 0km, 80 km, 320km and 1600km distances for 100G, 200G, 400G and 1T rates respectively. As can be seen from respective figures below amplitude or power of the signal is decreased as propagation distance increased. In other words, OSNR values of the system is decreased as the signal propagates longer distances due impairments like chromatic dispersion. It also shows side lobes, that are due to chromatic dispersion, are decreased using FBG.

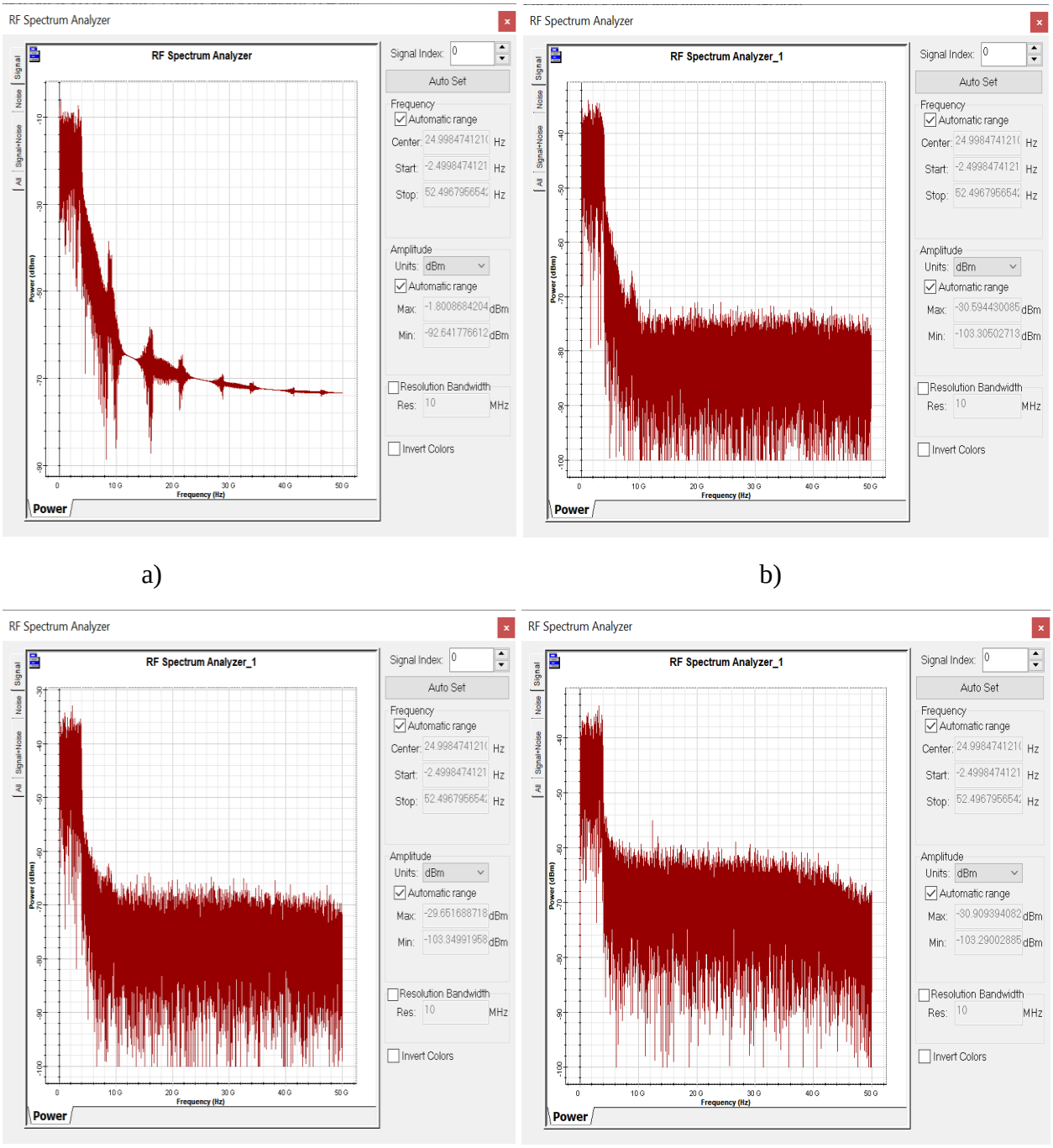

a) b)

c) d)

Figure 5. 13: RF Spectrum of 100G with FBG a) at 0km b) at 80km c) at 320km d) at 1600km

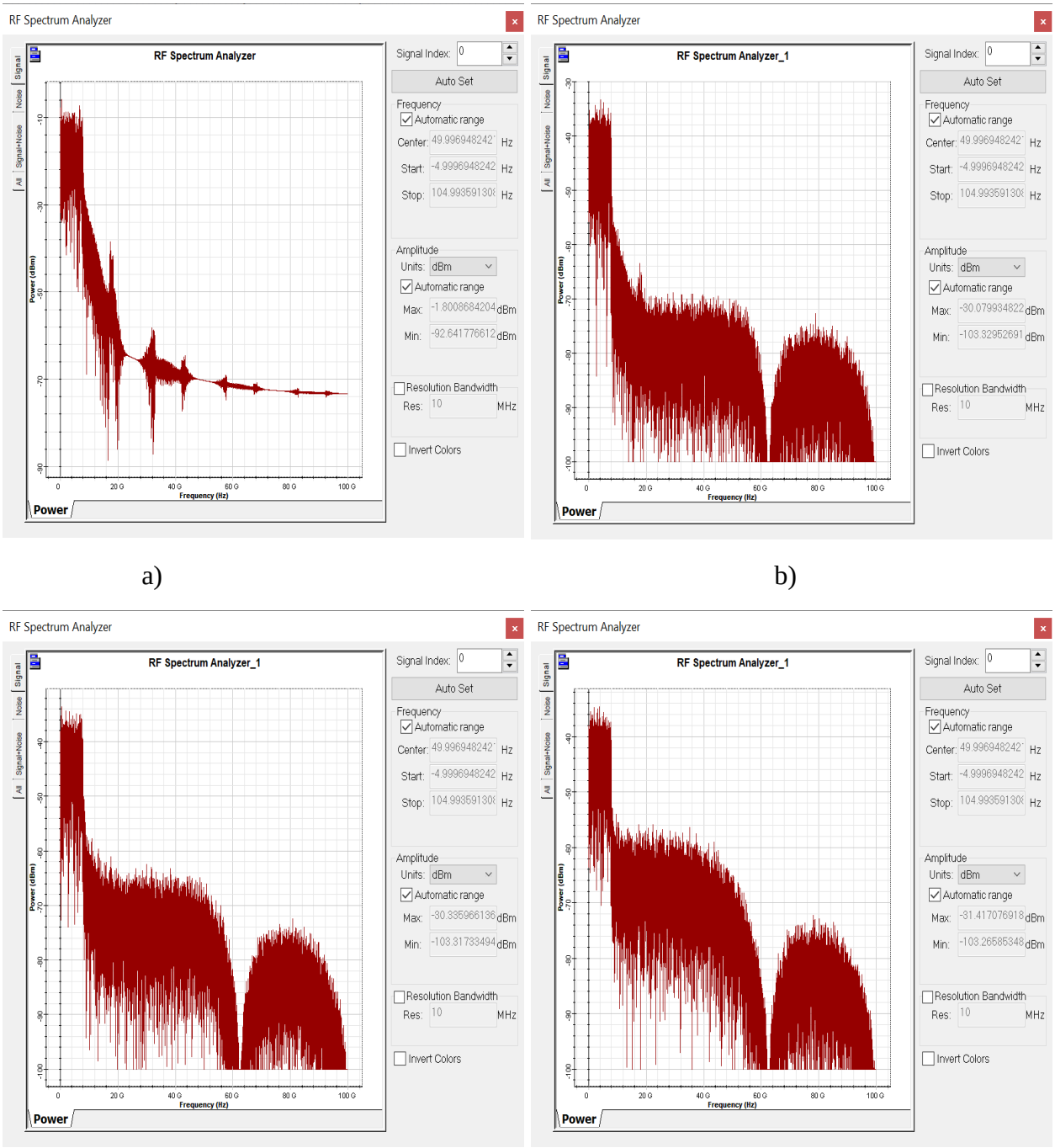

Figure 5. 14: RF Spectrum of 200G with FBG a) at 0km b) at 80km c) at 320km d) at 1600km

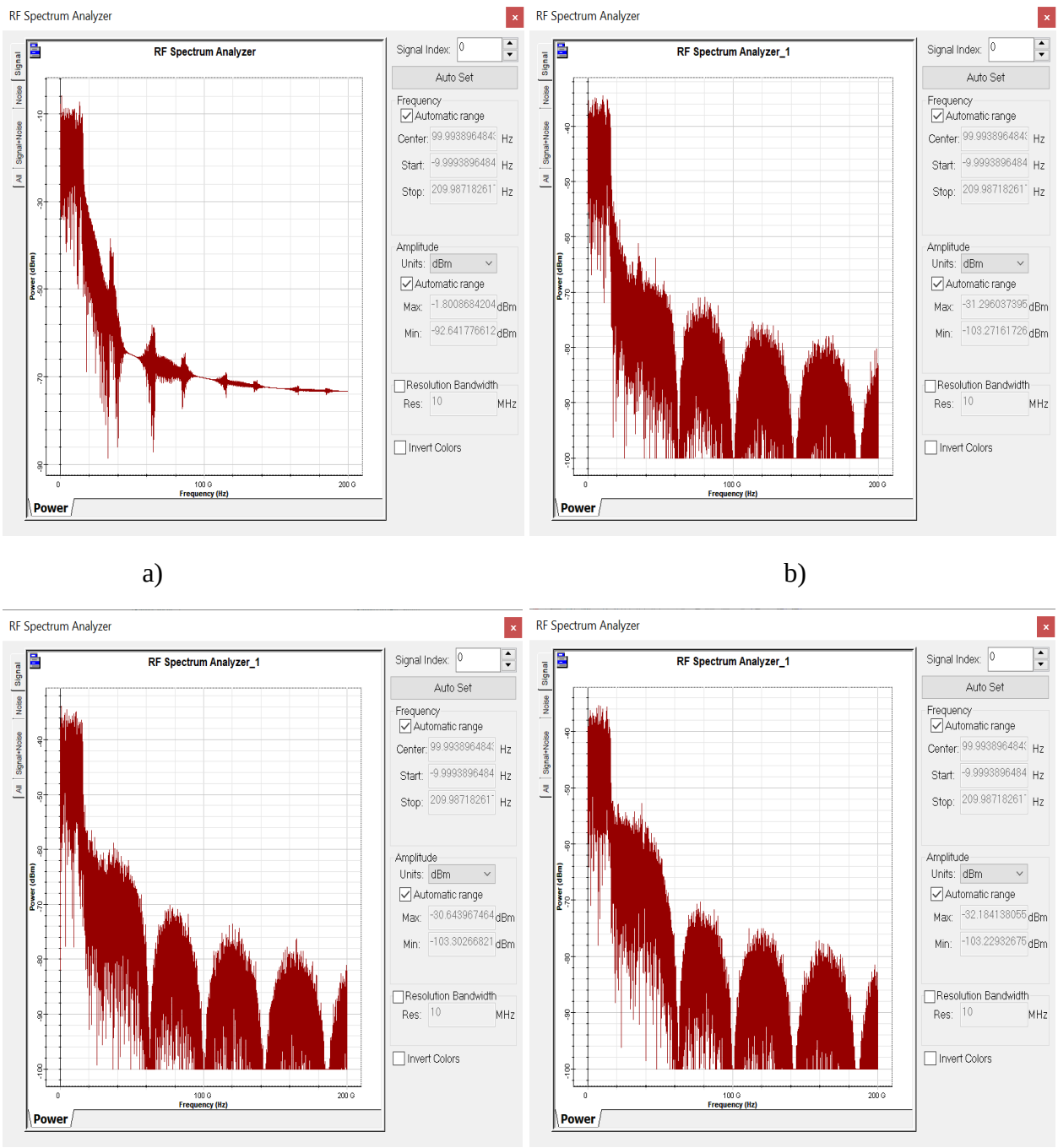

Figure 5. 15: RF Spectrum of 400G with FBG a) at 0km b) at 80km c) at 320km d) at 1600km

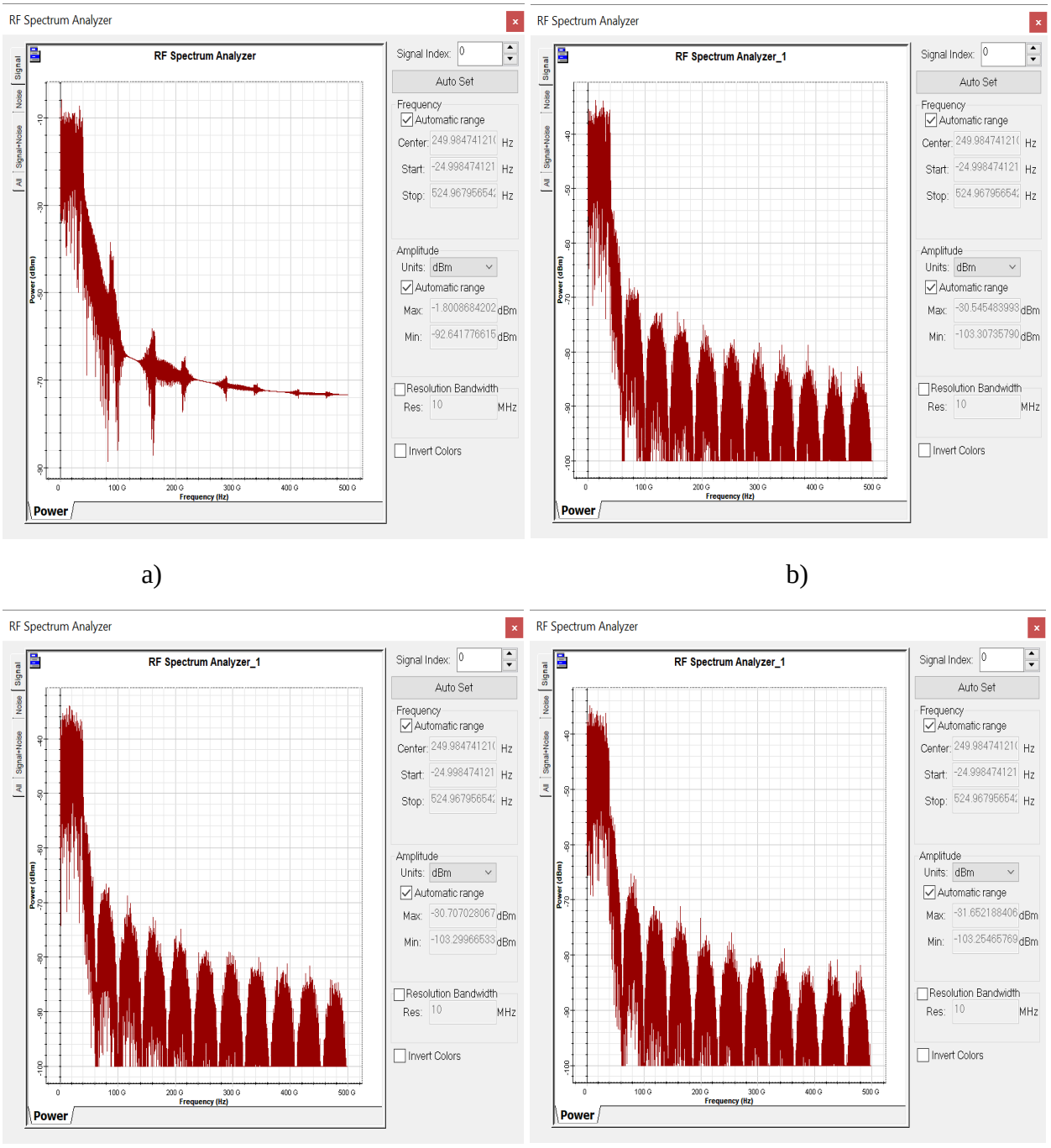

Figure 5. 16: RF Spectrum of 1T with FBG a) at 0km b) at 80km c) at 320km d) at 1600km

Figures 5.17 to 5.20 show optical spectrums of DP-16QAM Co-OOFDM system without FBG at 0km, 80 km, 320km and 1600km distances for 100G, 200G, 400G and 1T rates respectively. As can be seen from respective figures below due impairments like chromatic dispersion in the transmission medium amplitude or power of the signal is decreased as propagation distance

increased but amplitude of the noise is increased. In other words, OSNR values of the system is decreased as the signal propagates longer distances.

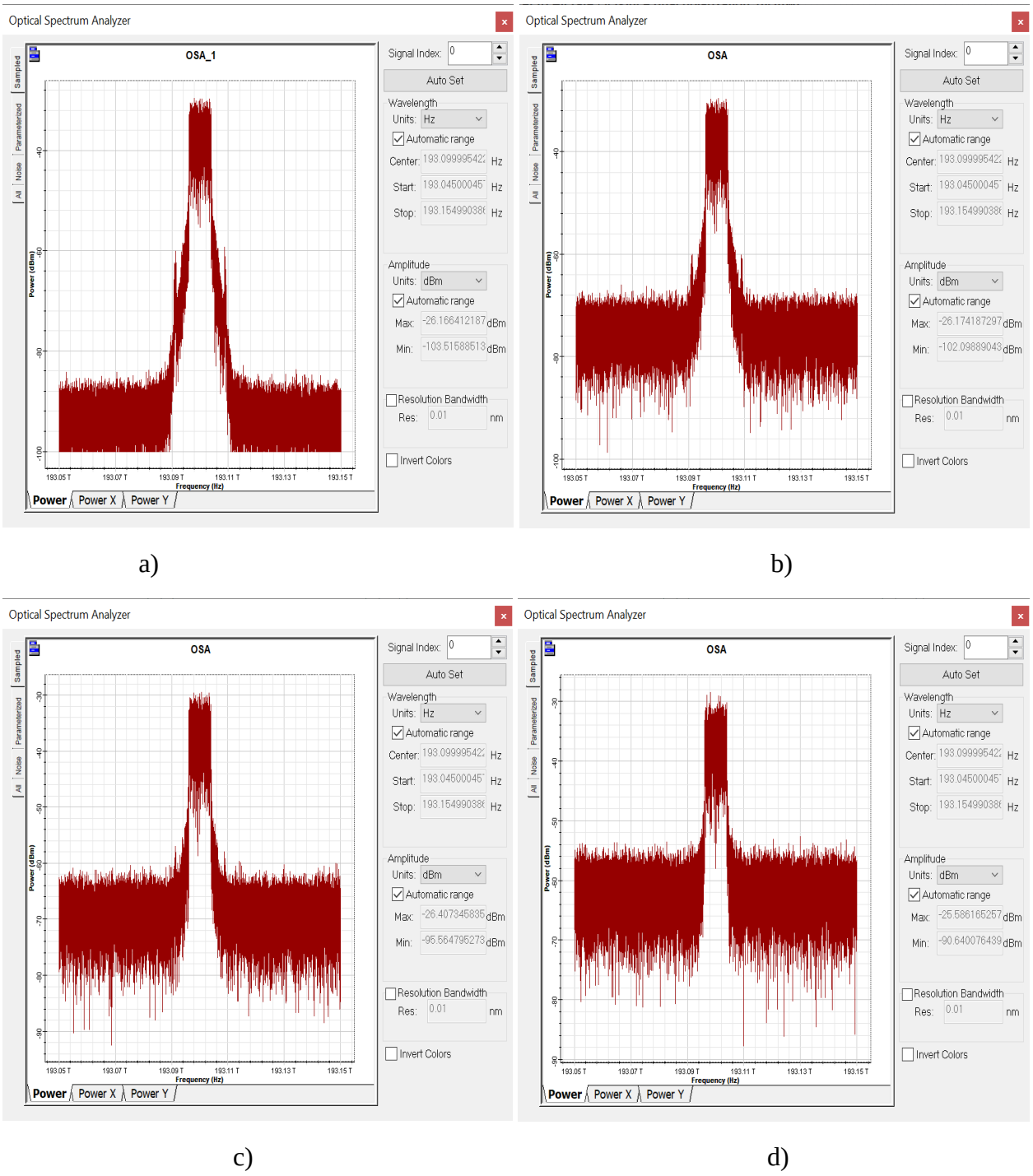

Figure 5. 17: Optical Spectrum of 100G without FBG a) at 0km b) at 80km c) at 320km d) at 1600km

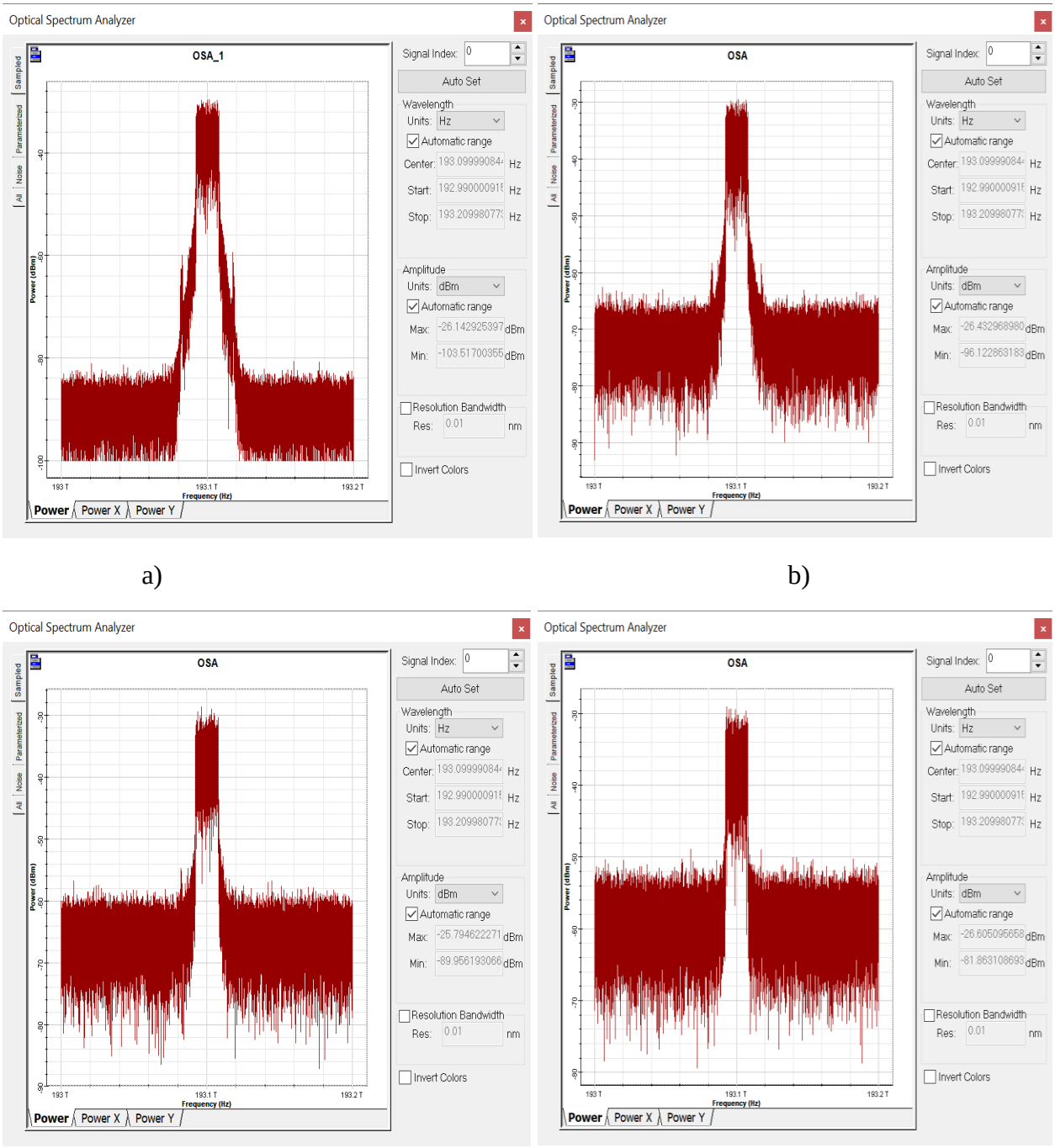

Figure 5. 18: Optical Spectrum of 200G without FBG a) at 0km b) at 80km c) at 320km d) at 1600km

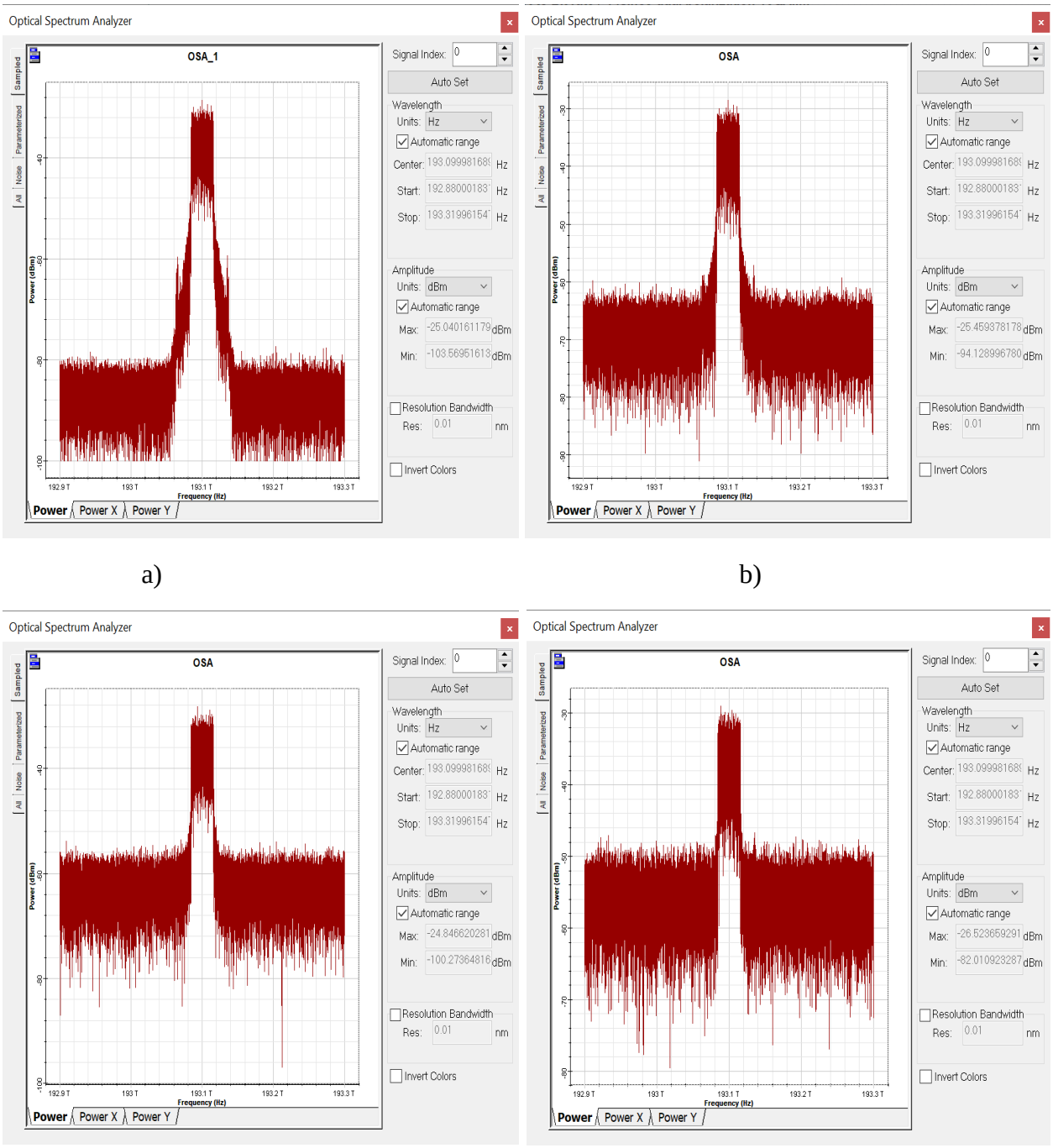

Figure 5. 19: Optical Spectrum of 400G without FBG a) at 0km b) at 80km c) at 320km d) at 1600km

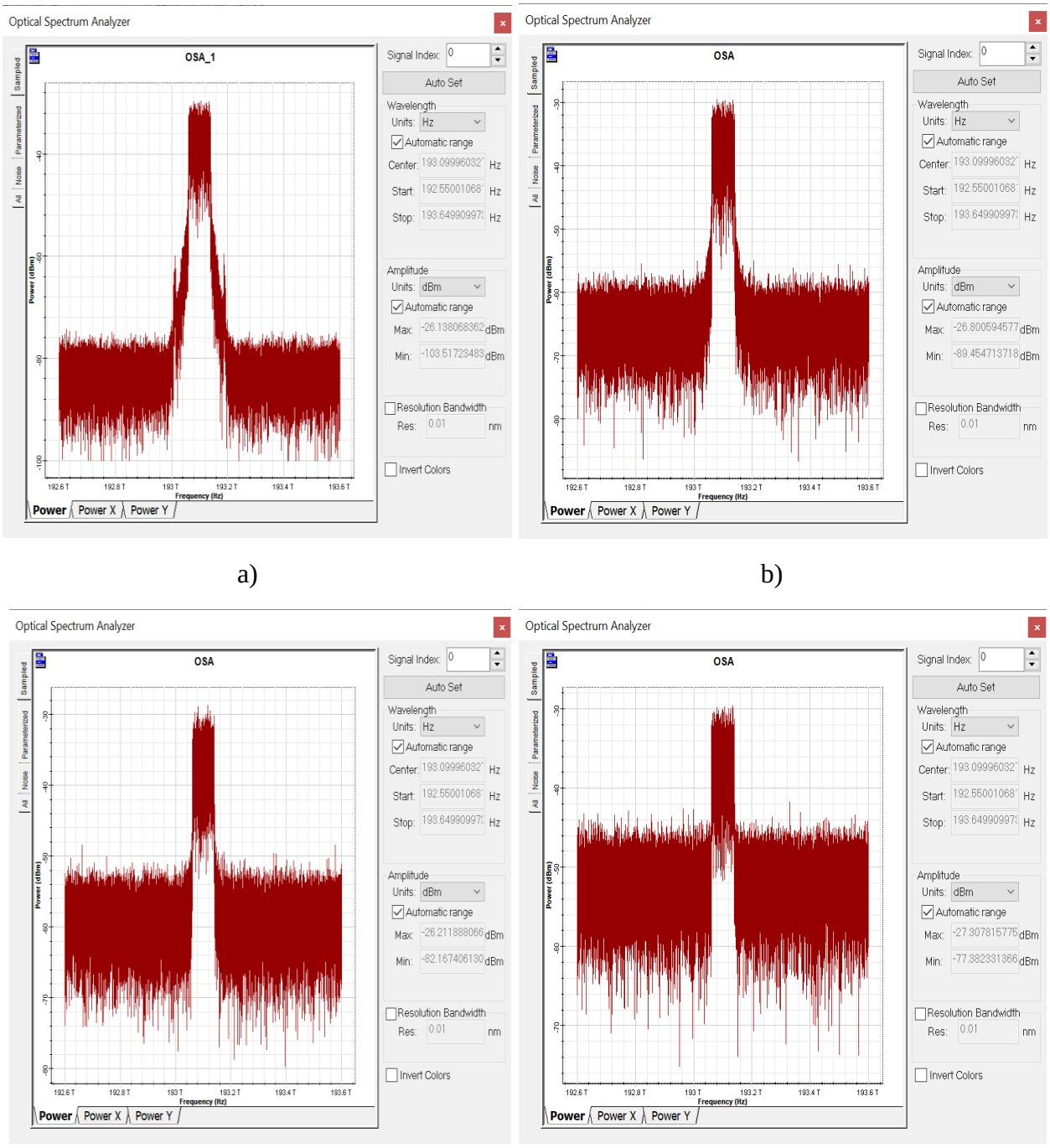

Figure 5. 20: Optical Spectrum of 1T without FBG a) at 0km b) at 80km c) at 320km d) at 1600km

Likewise, figures 5.21 to 5.24 show optical spectrums of DP-16QAM Co-OOFDM system with FBG at 0km, 80 km, 320km and 1600km distances for 100G, 200G, 400G and 1T rates respectively. As can be seen from respective figures below due impairments like chromatic

dispersion in the transmission medium, amplitude or power of the signal is decreased as propagation distance increased. In other words, OSNR values of the system is decreased as the signal propagates longer distances

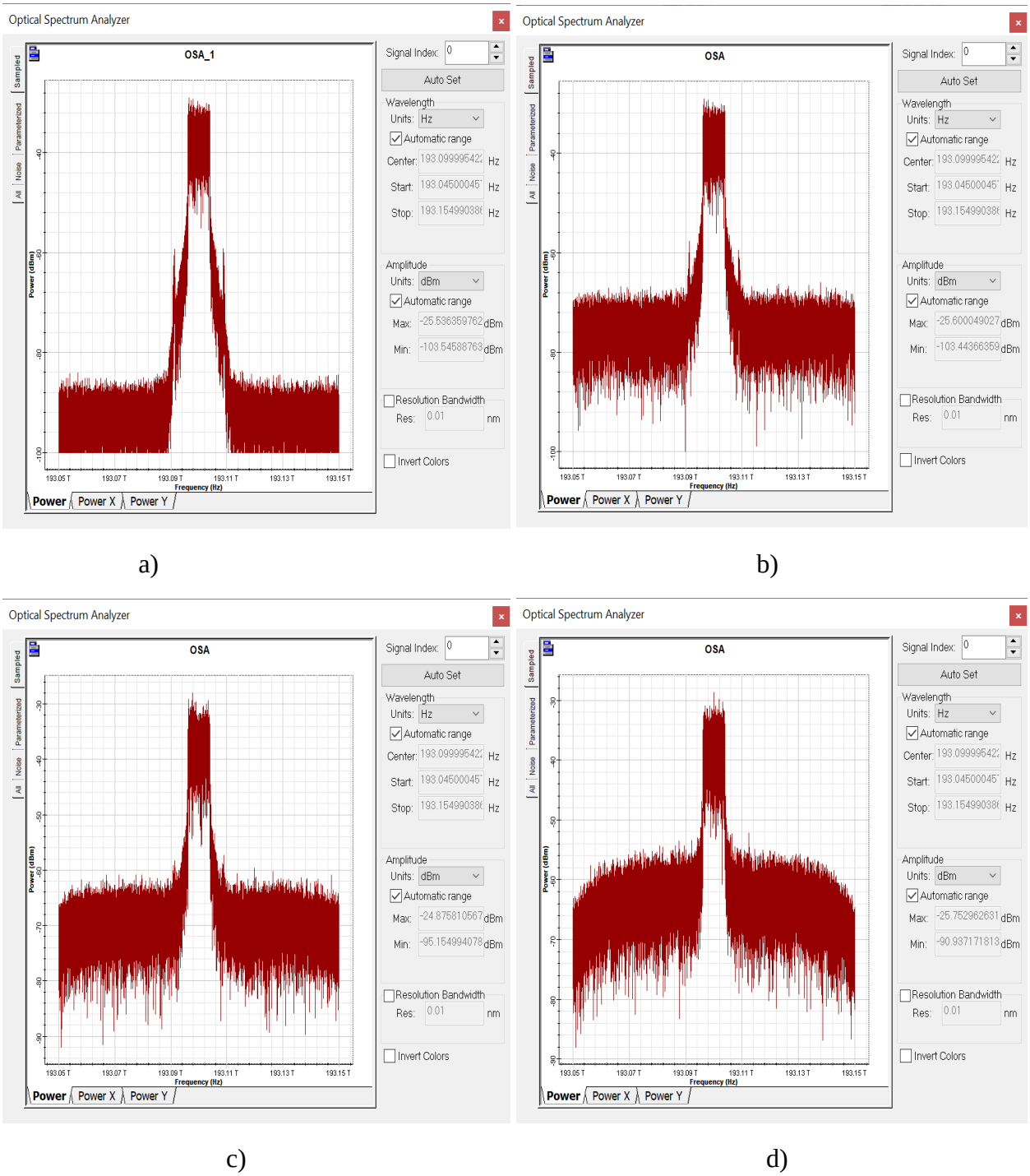

Figure 5. 21: Optical Spectrum of 100G with FBG a) at 0km b) at 80km c) at 320km d) at 1600km

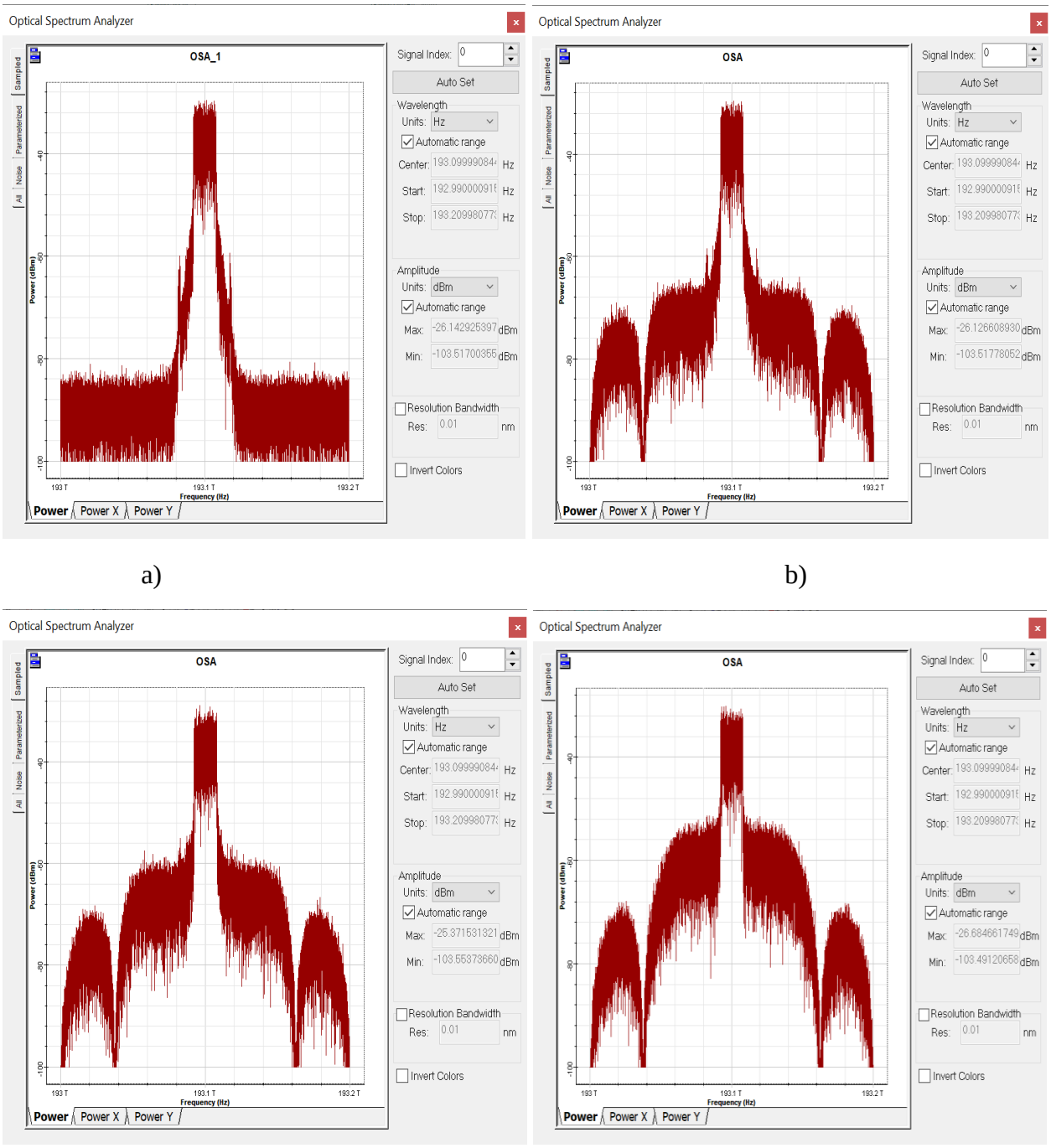

Figure 5. 22: Optical Spectrum of 200G with FBG a) at 0km b) at 80km c) at 320km d) at 1600km

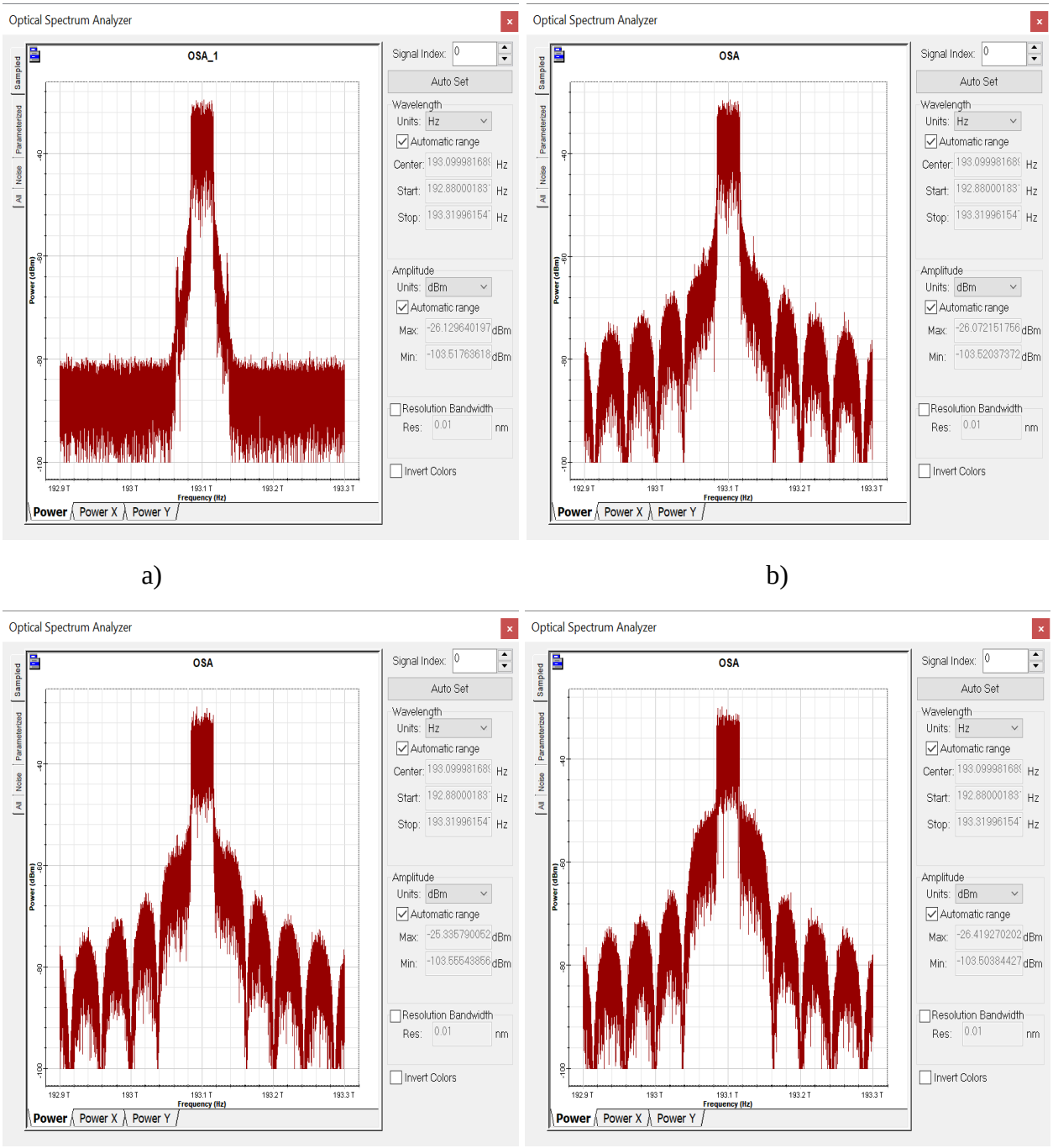

Figure 5. 23: Optical Spectrum of 400G with FBG a) at 0km b) at 80km c) at 320km d) at 1600km

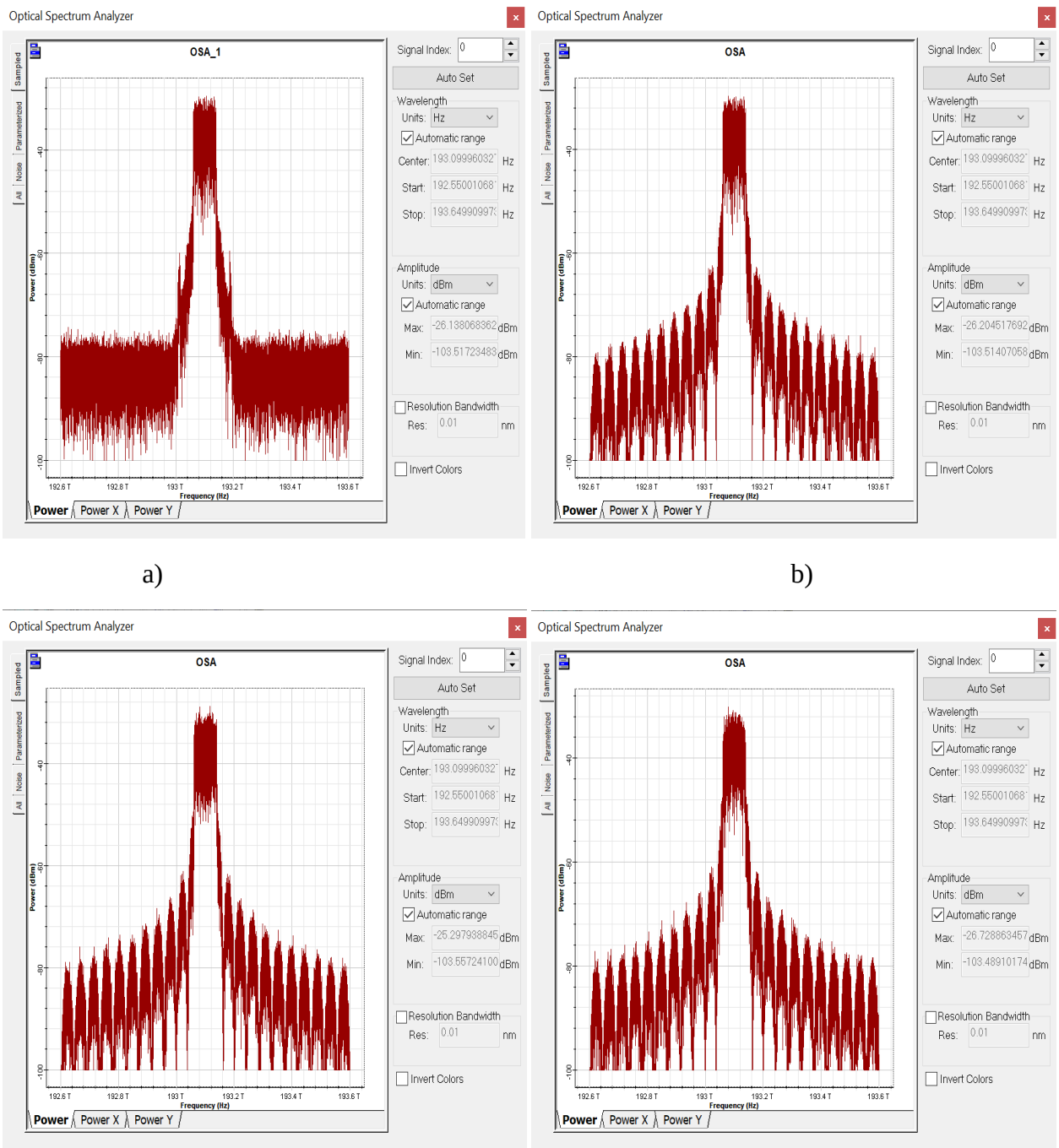

Figure 5. 24: Optical Spectrum of 1T with FBG a) at 0km b) at 80km c) at 320km d) at 1600km

Figures 5.25 a, b, c and d to 5.28 a, b, c and d show constellation diagrams of DP-16QAM Co-OOFDM system without FBG at 0km, 80 km, 320km and 1600km distances for 100G, 200G, 400G and 1T rates respectively. Constellation diagram displays the signal as a two-dimensional xy-plane scatter diagram in the complex plane at symbol sampling instants. The radius or the

distance of a point from the origin represents a measure of amplitude. The angle of a point, measured counterclockwise from the horizontal axis, represents the phase shift of the carrier wave from a reference phase. Accordingly, as can be seen from figures there is some phase shift and radius size reduction of each symbol and concentrating around the origin. This implies that there is dispersion and distortion of the signal as it propagates long distances in the fiber.

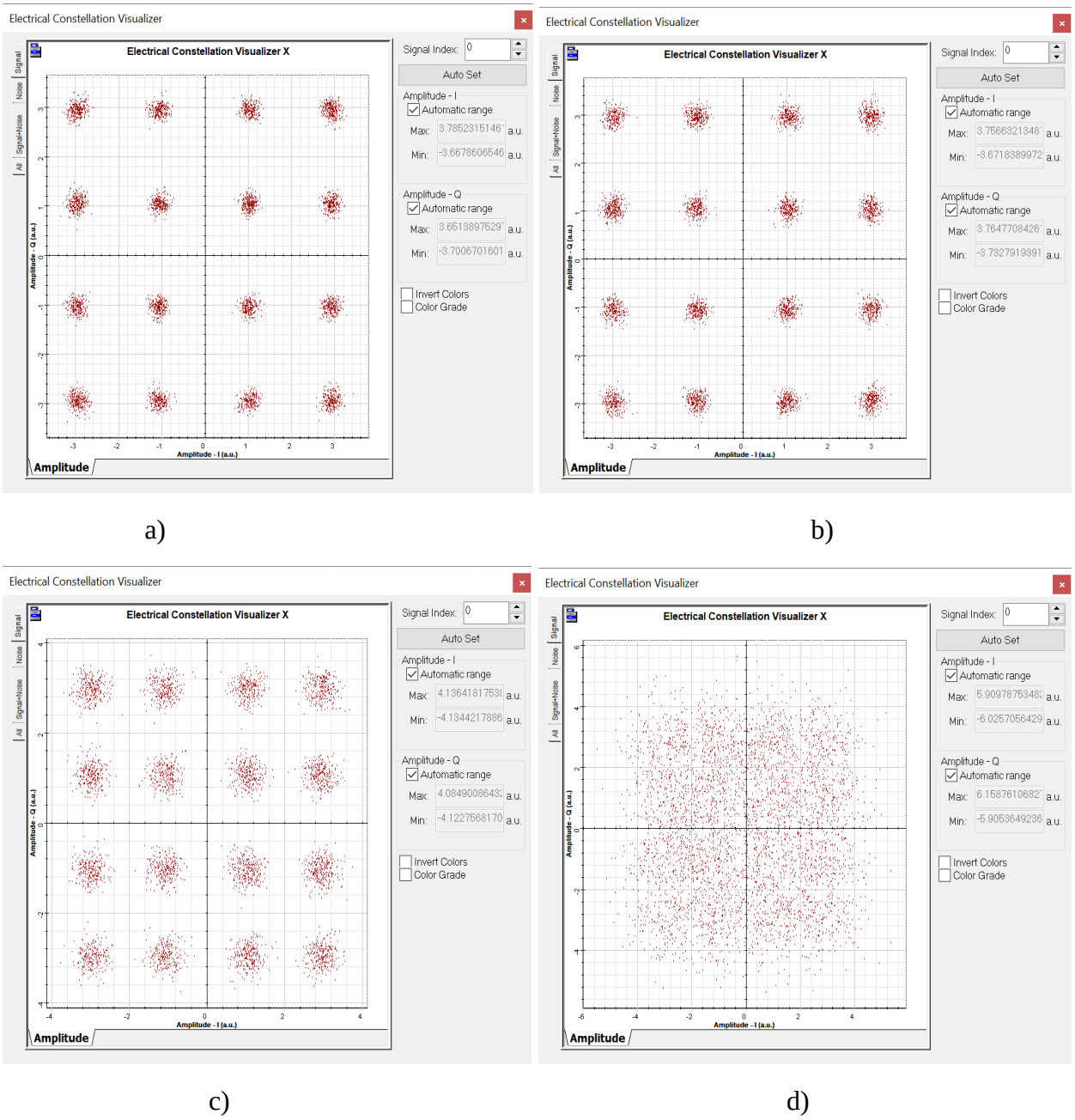

Figure 5. 25: Constellation diagram of 100G without FBG a) at 0km b) at 80km c) at 320km d) at 1600km

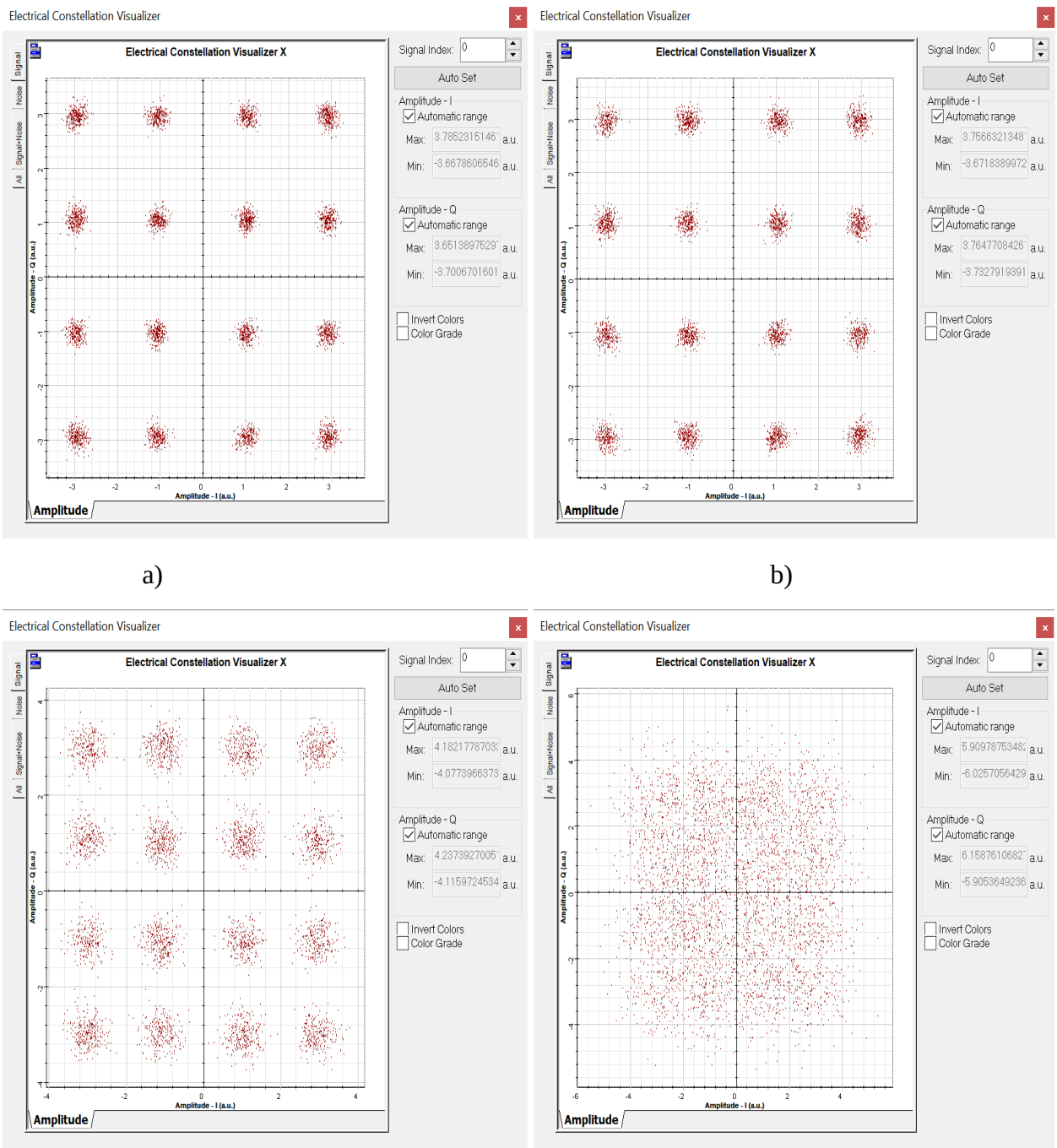

a) b)

c) d)

Figure 5. 26: Constellation diagram of 200G without FBG a) at 0km b) at 80km c) at 320km d) at 1600km

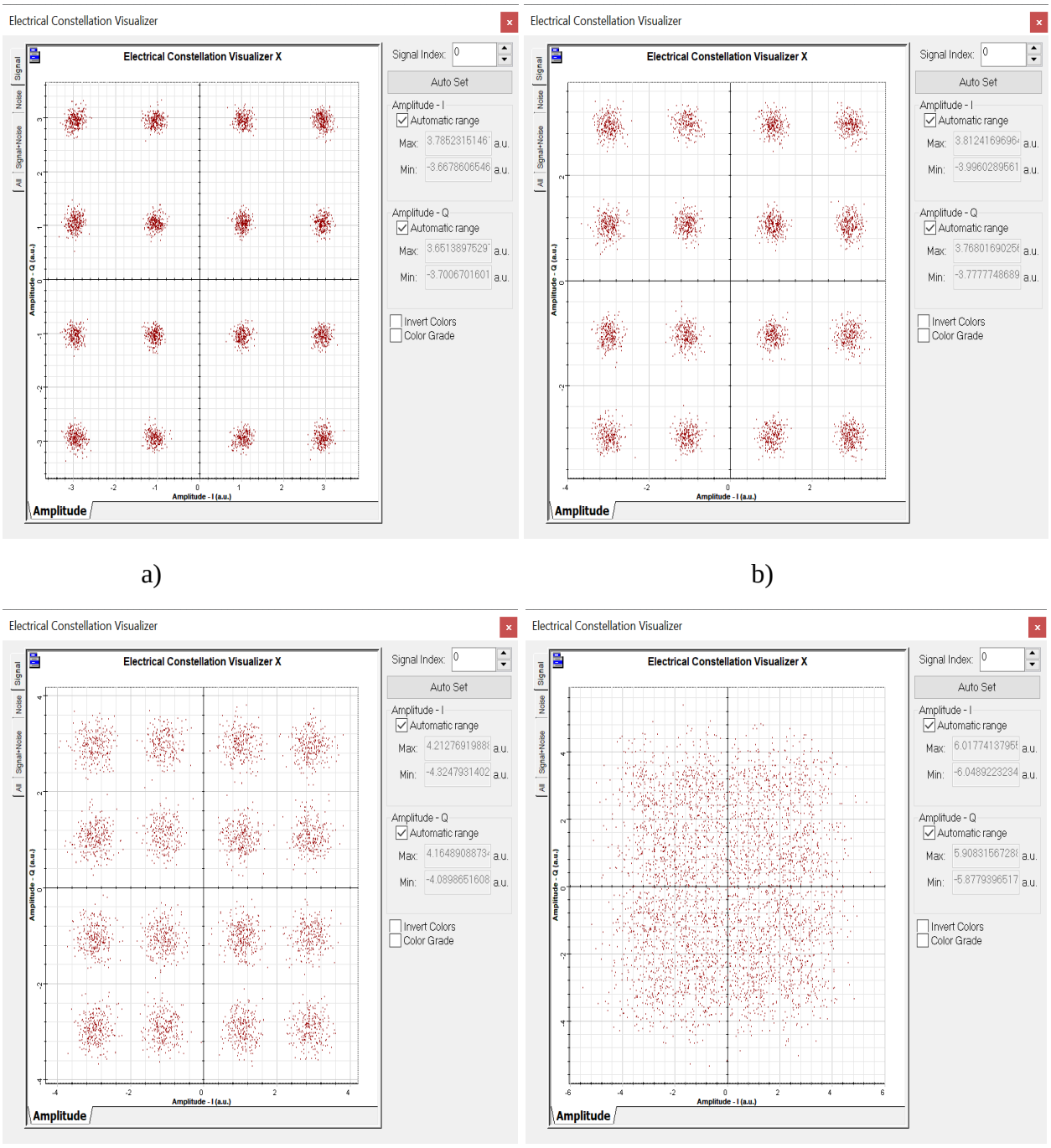

Figure 5. 27: Constellation diagram of 400G without FBG a) at 0km b) at 80km c) at 320km d) at 1600km

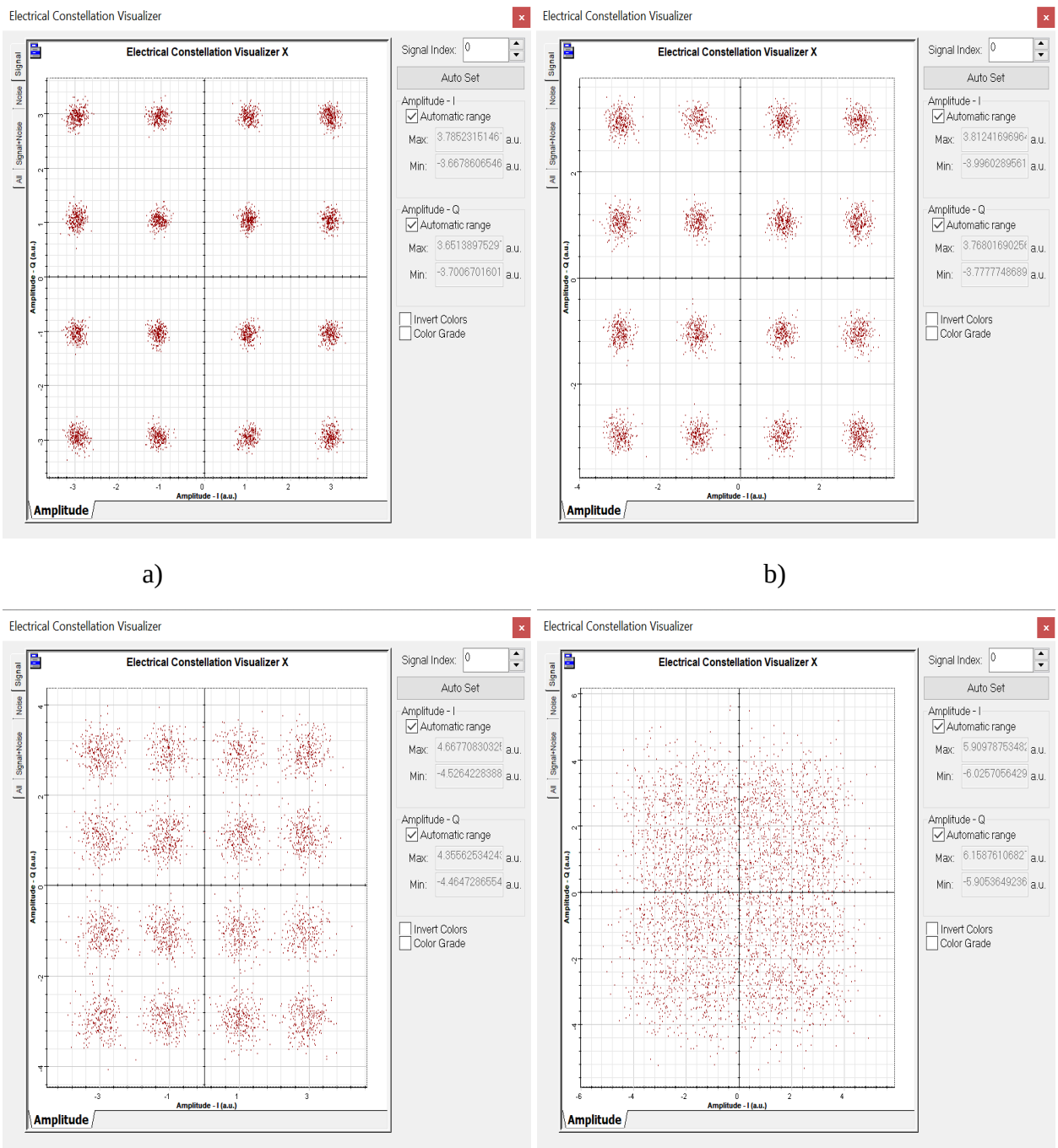

Figure 5. 28: Constellation diagram of 1T without FBG a) at 0km b) at 80km c) at 320km d) at 1600km

Similarly, figures 5.29 a, b, c and d to 5.32 a, b, c and d show constellation diagrams of DP-16QAM Co-OOFDM system with FBG at 0km, 80 km, 320km and 1600km distances for 100G, 200G, 400G and 1T rates respectively. Some phase shift and radius size reduction of each symbol and

concentrating around the origin is observed for this system also. This implies that there is dispersion and distortion of the signal as it propagates long distances in the fiber.

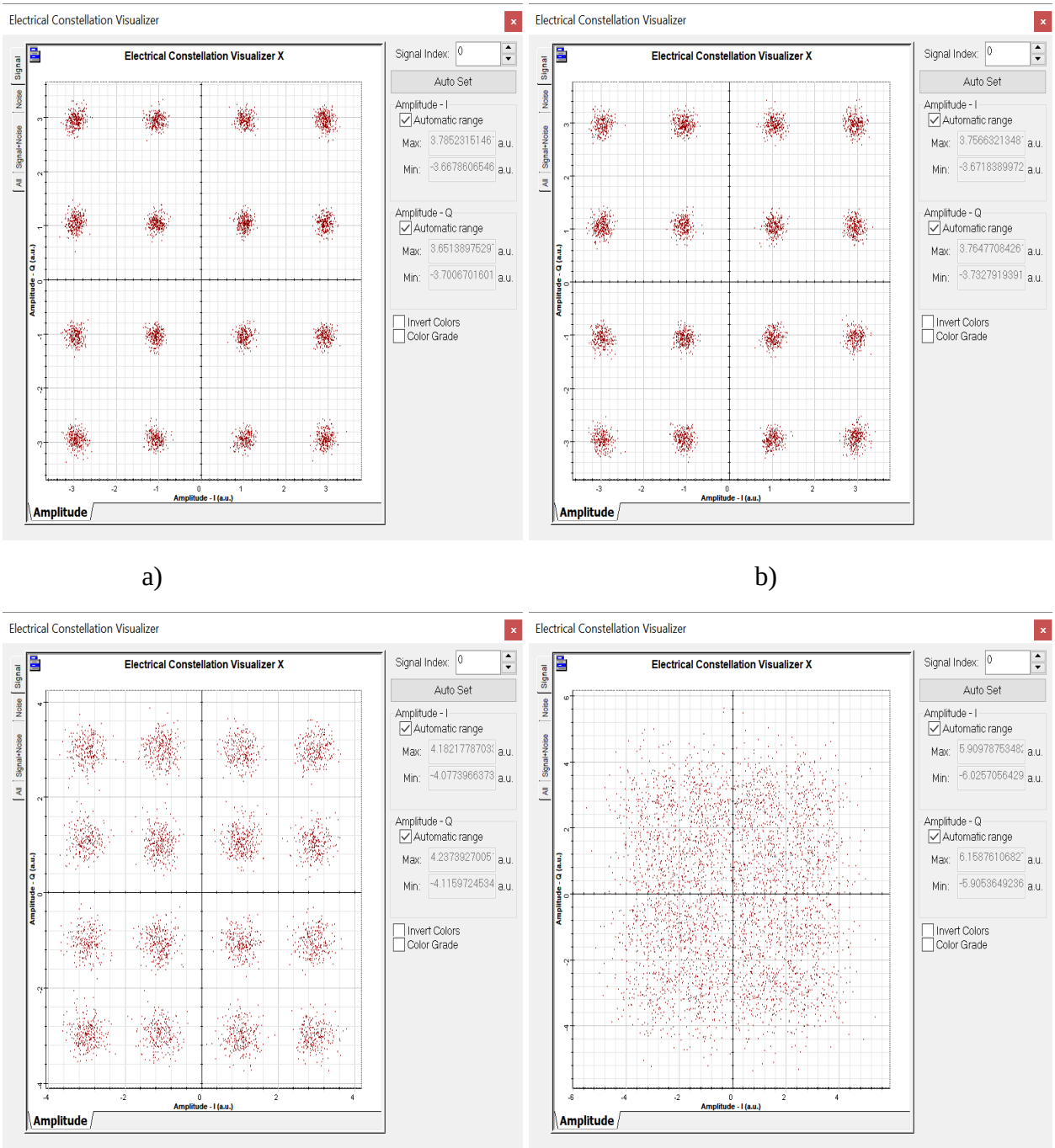

Figure 5. 29: Constellation diagram of 100G with FBG a) at 0km b) at 80km c) at 320km d) at 1600km

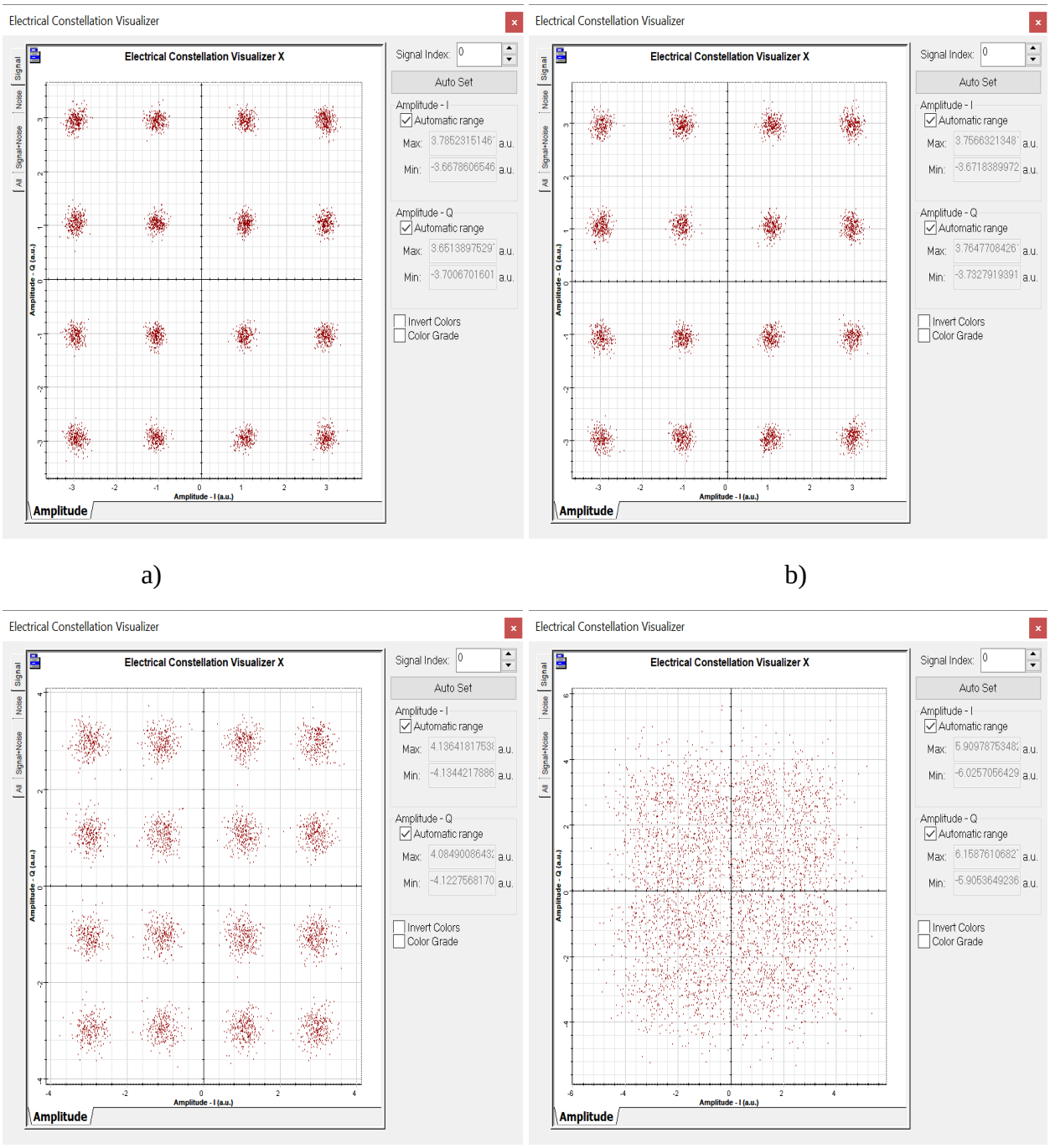

Figure 5. 30: Constellation diagram of 200G with FBG a) at 0km b) at 80km c) at 320km d) at 1600km

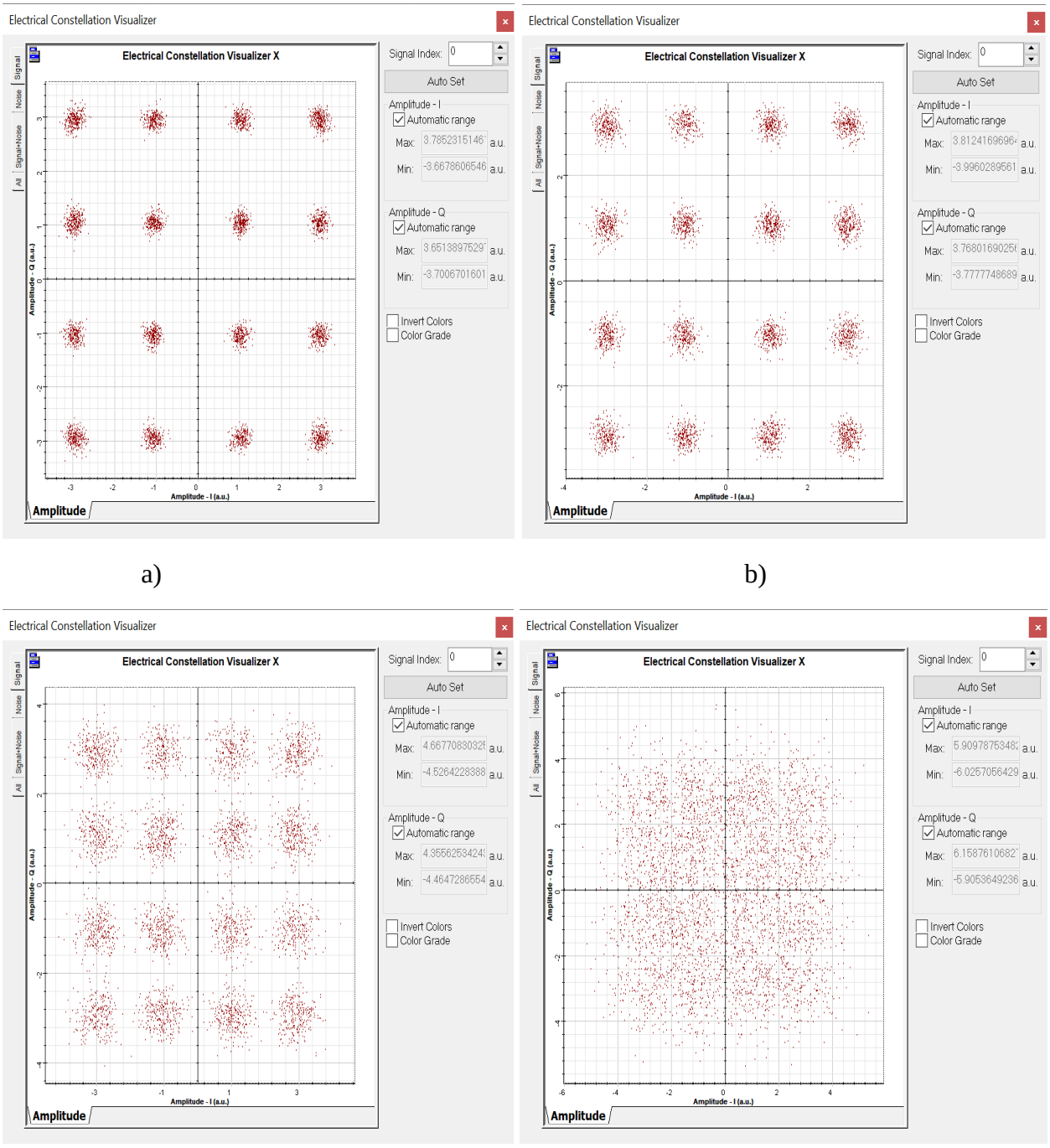

a) b)

c) d)

Figure 5. 31: Constellation diagram of 400G with FBG a) at 0km b) at 80km c) at 320km d) at 1600km

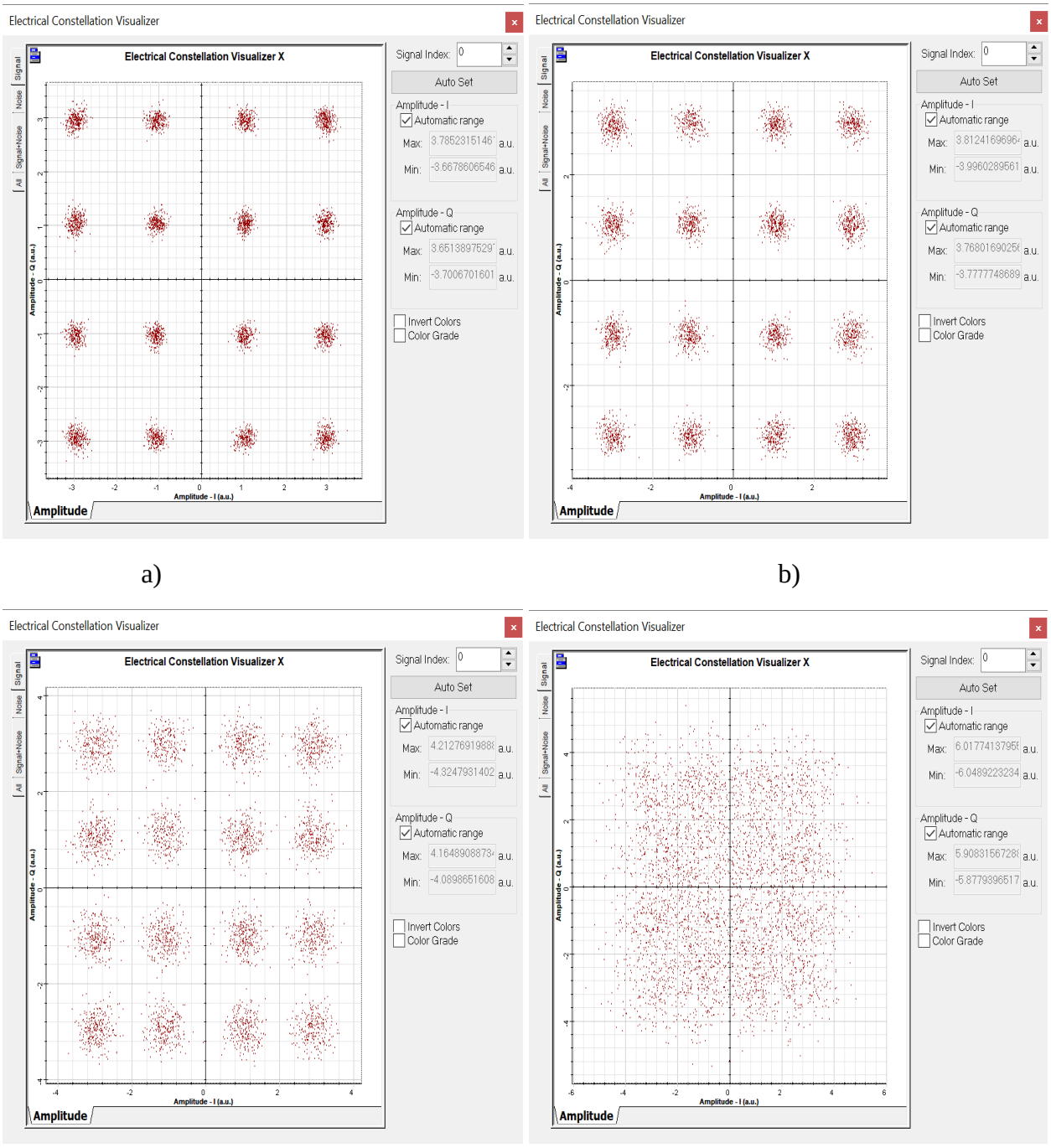

Figure 5. 32: Constellation diagram of 1T with FBG a) at 0km b) at 80km c) at 320km d) at 1600km

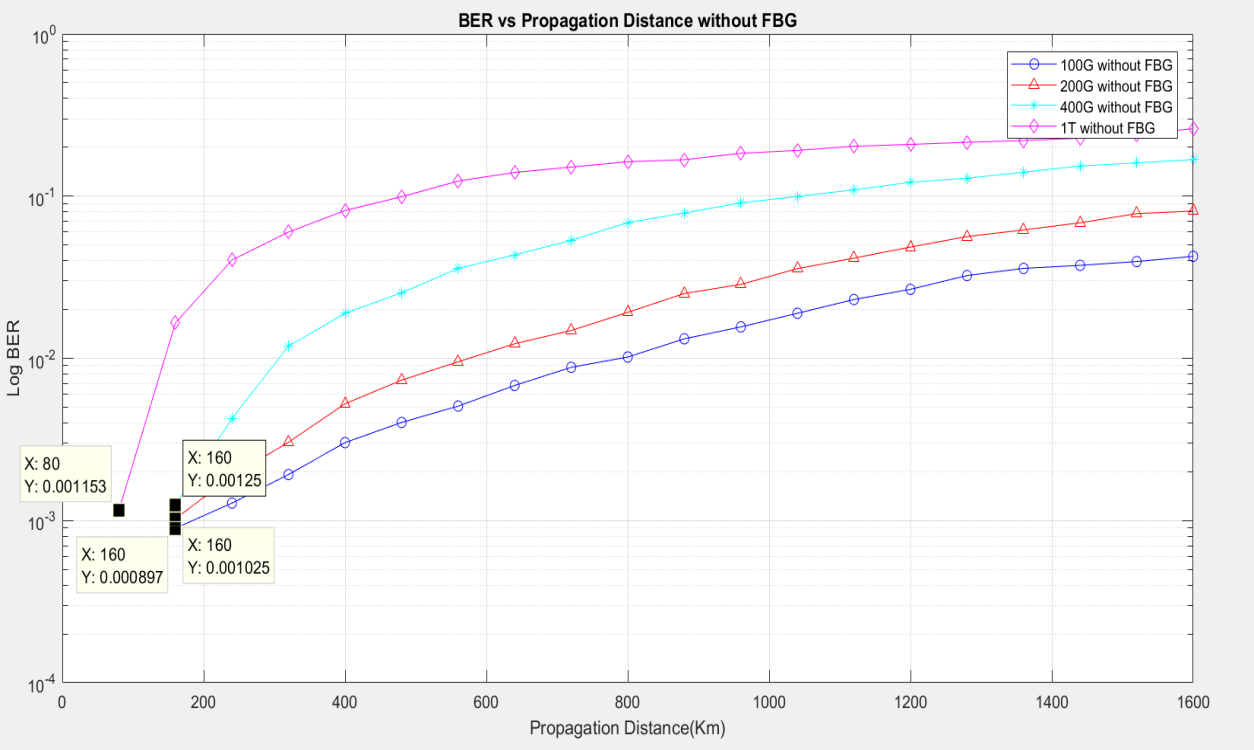

a)

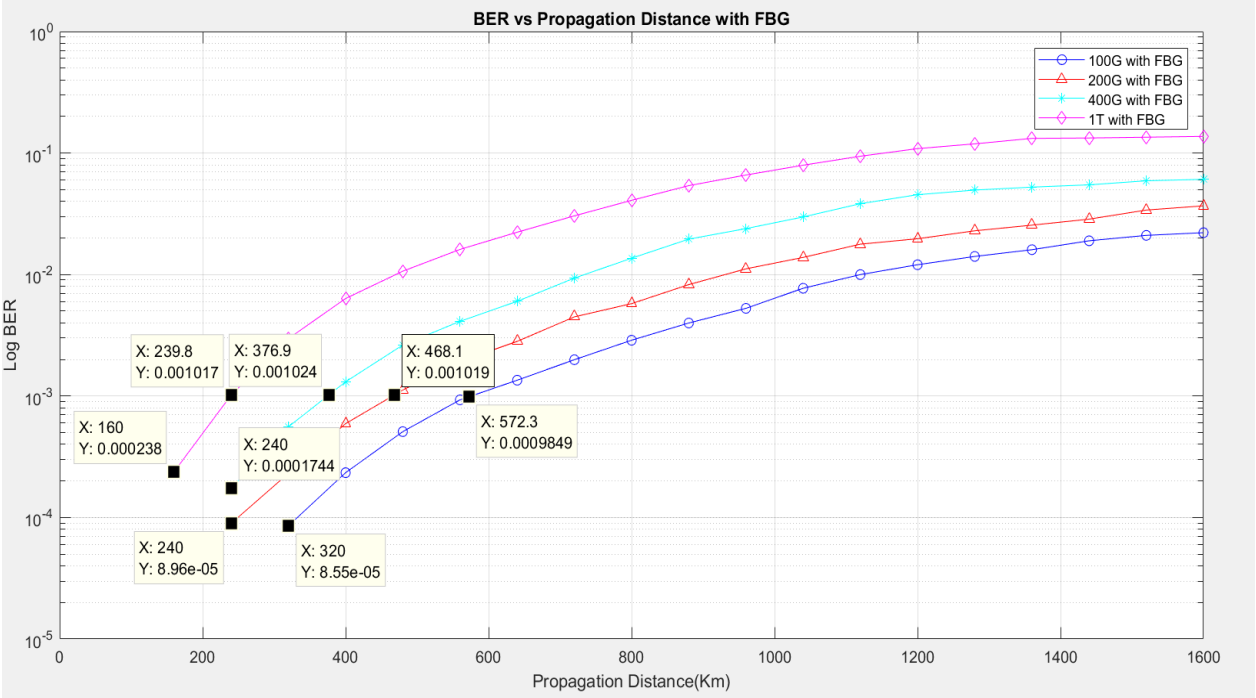

b)

Figure 5. 33: BER vs Propagation distance a) Without FBG b) With FBG

As can be seen from figure 5.33 a and b above, BER value of each transmission capacity is increased with propagation distance for both systems. When FBG not used, transmission of 100G, 200G, 400G encountered first error after propagation of 160 km even though number of error they made is different and transmission of 1T encountered first error after propagation of 80 km. When FBG used, transmission of 100G encountered the first error after propagation of 320 km, transmission of 200G and 400G encountered first error after propagation of 240 km and transmission of 1T encountered first error after propagation of 160 km. If no error correction method is used this is the highest distance, we can achieve with the given configuration. If an error correction algorithm that can recover a BER as low as 10^{-3} used, propagation distances can be extended to 572.3 km, 468.1 km, 376.9 km and 239.8 km for transmission of 100G, 200G, 400G and 1T capacities respectively when Co-OOFDM system integrated with FBG.

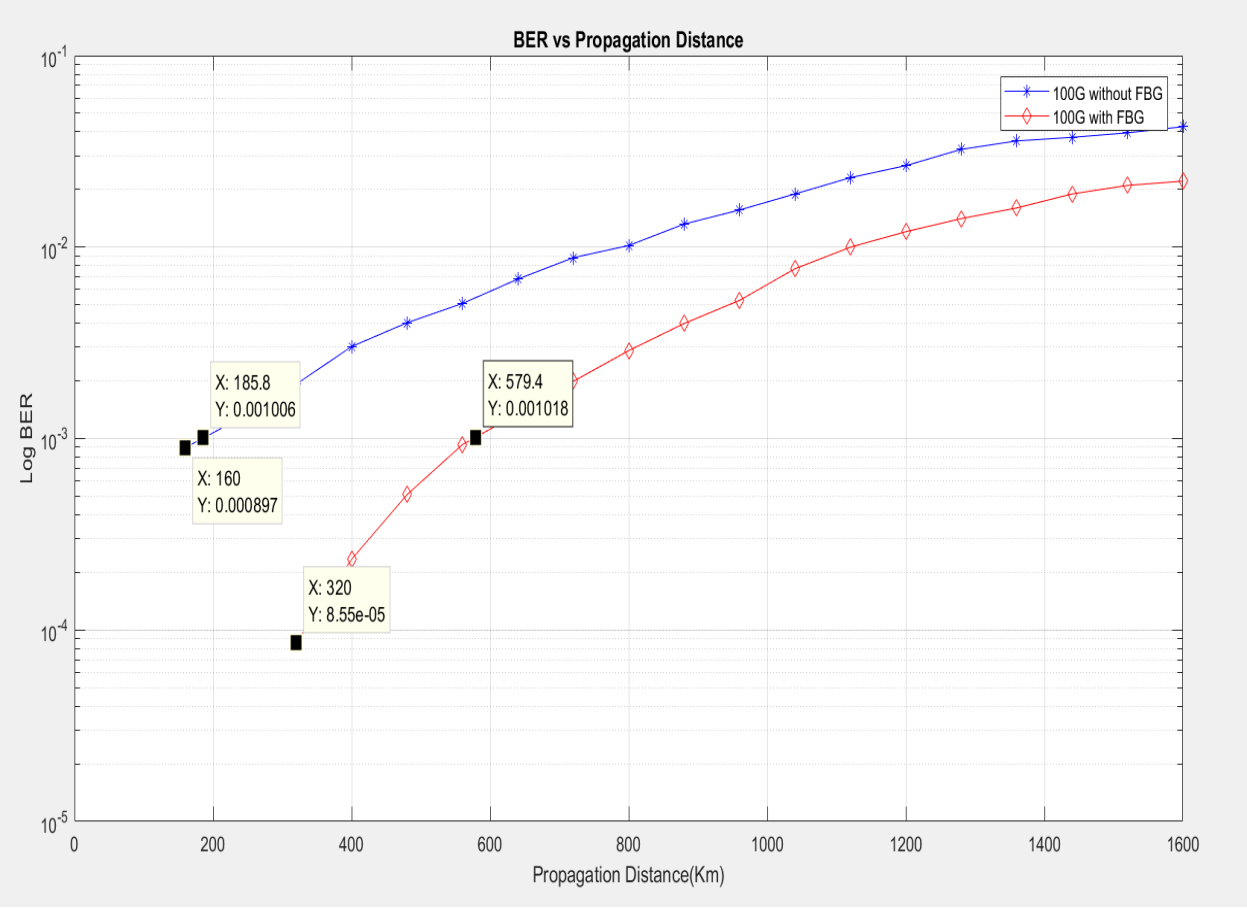

a)

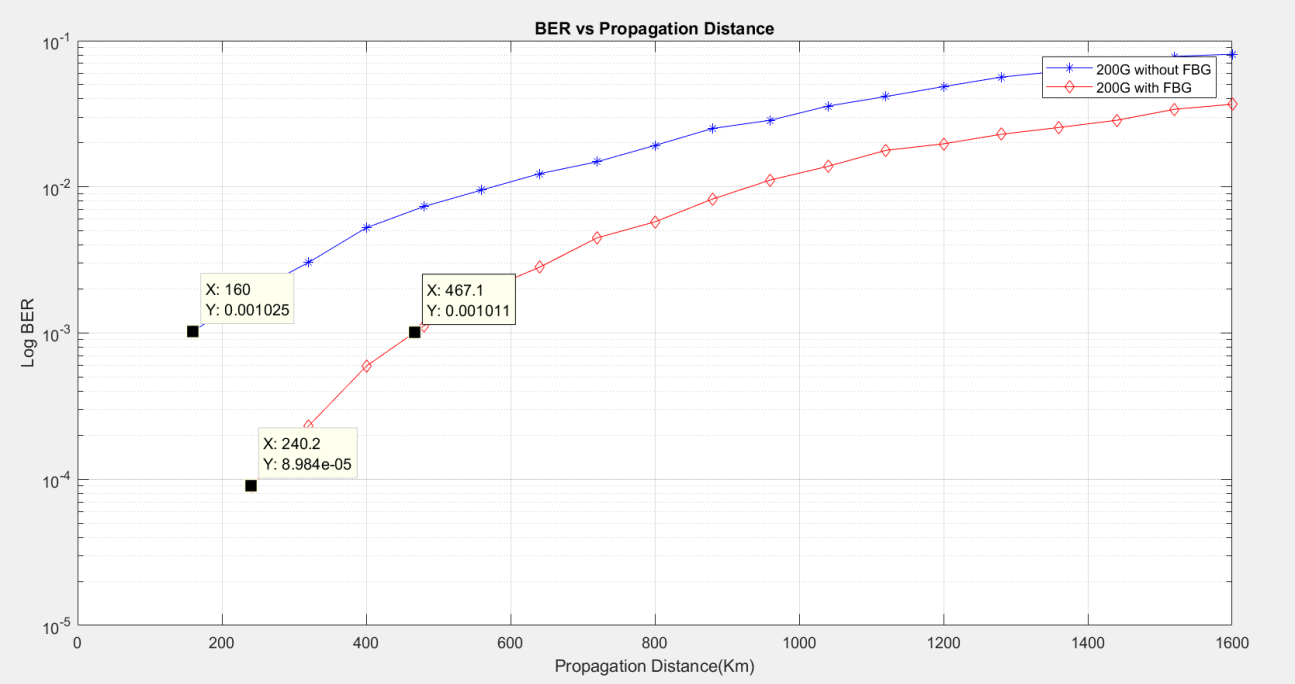
BER vs Propagation Distance
200G without FBG
200G with FBG
X: 160
Y: 0.001025
X: 467.1
Y: 0.001011
X: 240.2
Y: 8.984e-05
Log BER
Propagation Distance(Km)

b)

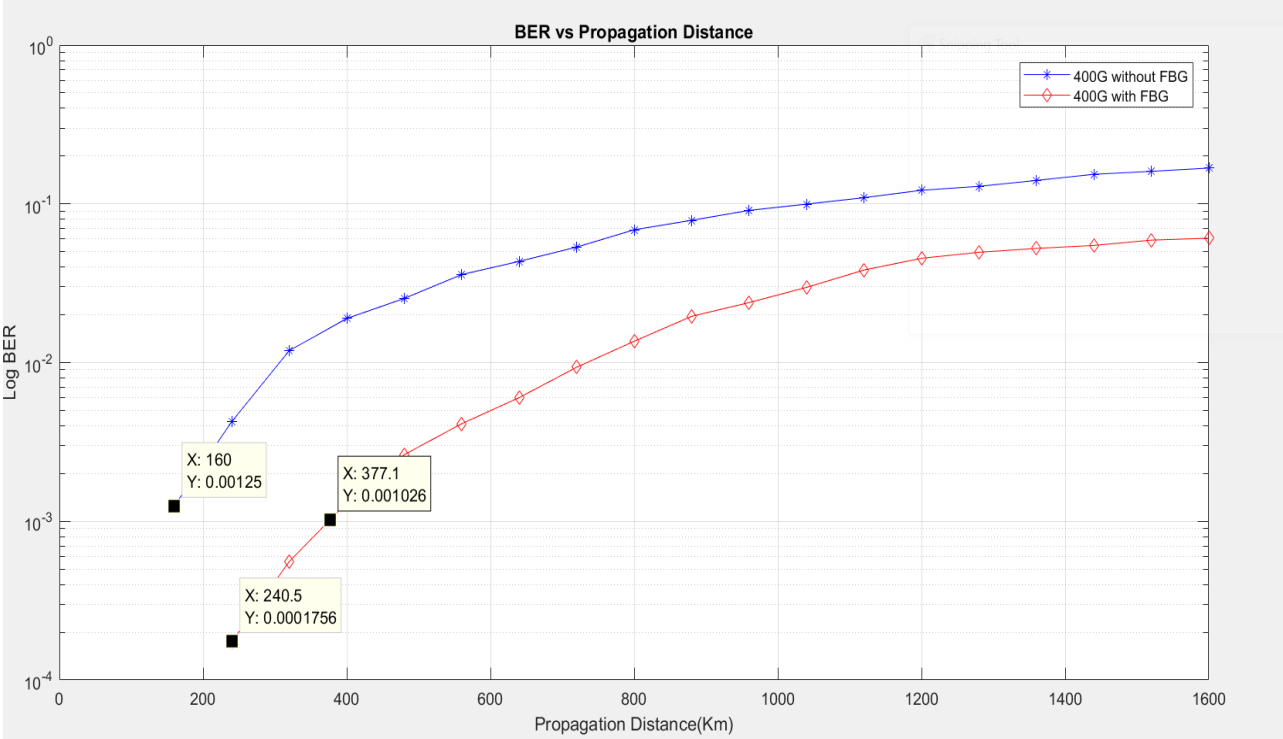
BER vs Propagation Distance
400G without FBG
400G with FBG
X: 160
Y: 0.00125
X: 377.1
Y: 0.001026
X: 240.5
Y: 0.0001756
Log BER
Propagation Distance(Km)

c)

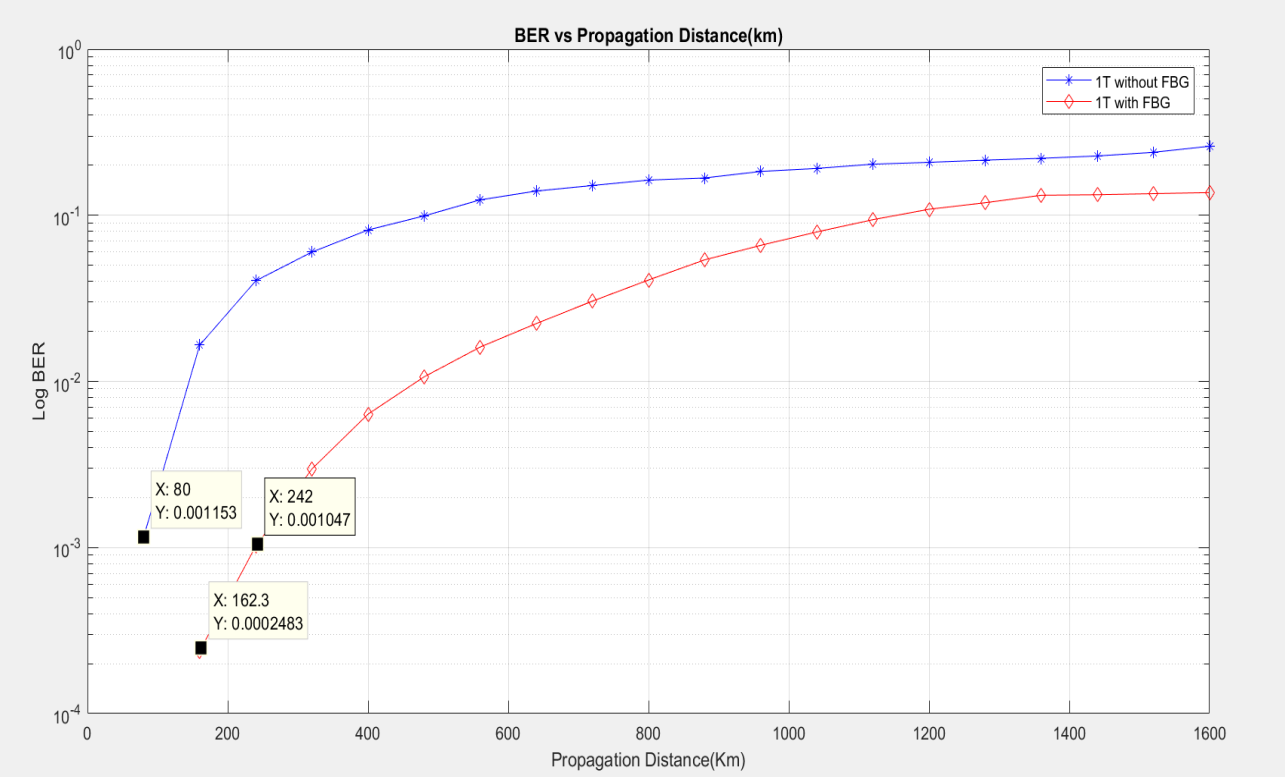

d)

Figure 5. 34: BER vs Propagation distance for the same rate but using different systems a) 100G b) 200G c) 400G d) 1T

As shown in Figure 5.34 a, b, c, and d, when FBG was combined with a Co-O-OFDM system, the error-free transmission or propagation distance improved from 160 km to 320 km for 100G, from 160 km to 240 km for both 200G and 400G, and from 80 km to 162 km for 1T. Similarly, when FBG was combined with a Co-O-OFDM system, the maximum transmission or propagation distance was increased from 160 km to 579 km for 100G, 160 km to 467 km for 200G, 160 km to 377 km for 400G, and 80 km to 242 km for 1T to reach target BER value of as low as 10^{-3}.

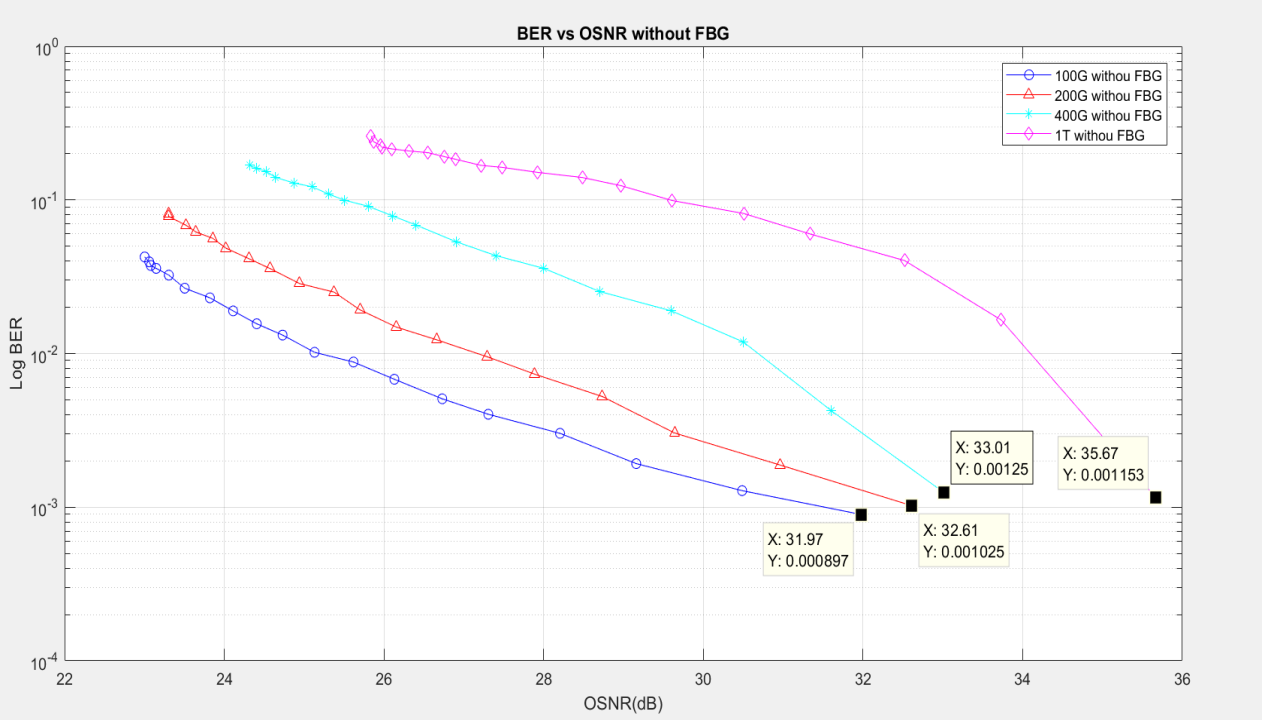

a)

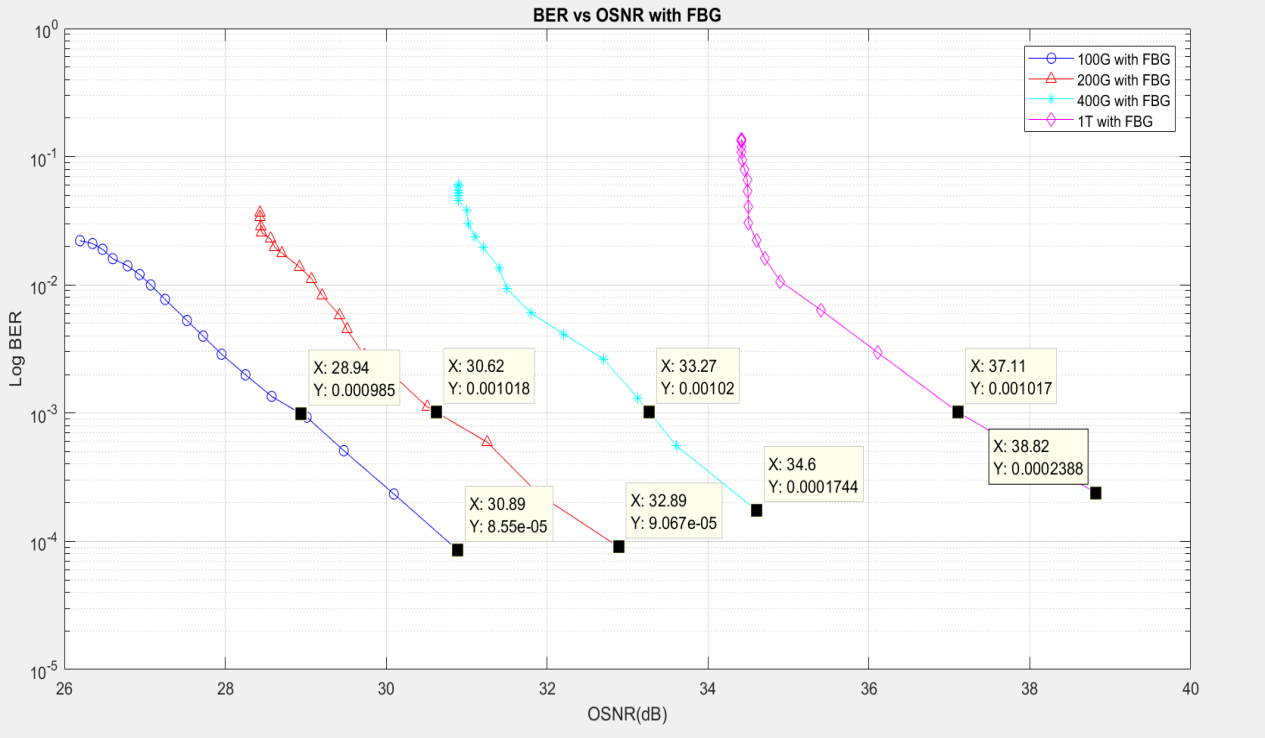

b)

Figure 5. 35: BER vs OSNR a) Without FBG b) With FBG

When FBG was not used, as shown in the figures 5.35 a and b above, the minimum BER values of 10^{-4} for 100G and 10^{-3} for 200G, 400G, and 1T were registered at 31.97dB, 32.61dB, 33.01dB, and 35.67dB OSNR values, respectively. However, when FBG was integrated, the minimum BER values of 10^{-5} for 100G and 200G and 10^{-4} for 400G and 1T were registered at 30.89 dB to have error free propagation distance.

When FBG was not used, Co-O-OFDM systems of 100G, 200G, 400G, and 1T reached the target BER value of 10^{-3} at 31.97 dB, 32.61 dB, 33.01 dB, and 35.67 dB OSNR values, respectively. When FBG was used, 100G, 200G, 400G, and 1T Co-O-OFDM systems achieved the target BER value of 10^{-3} at OSNR values of 28.94 dB, 30.62 dB, 33.27 dB and 37.11 dB respectively. Because the target BER value of 10^{-3} is reached at these points, these OSNR values can be used as a cutting point for both systems.

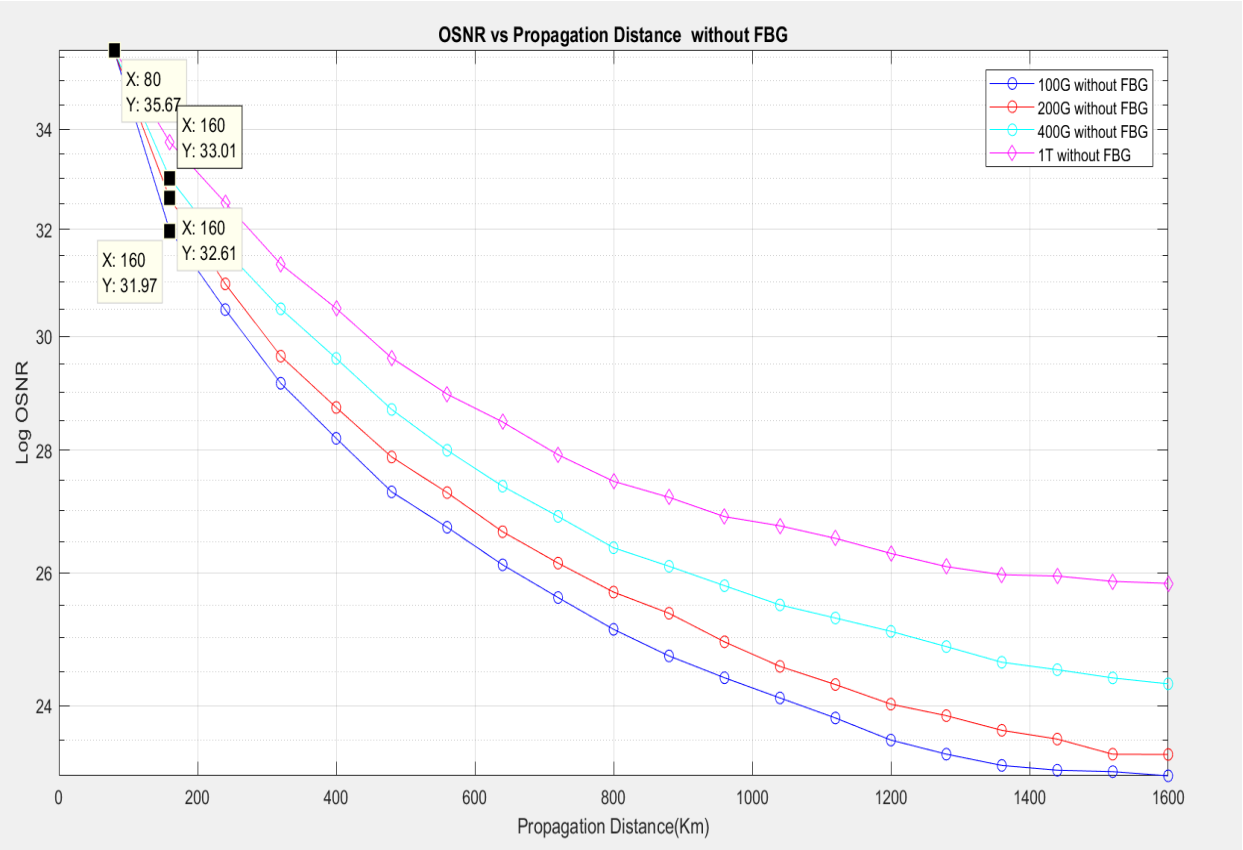

a)

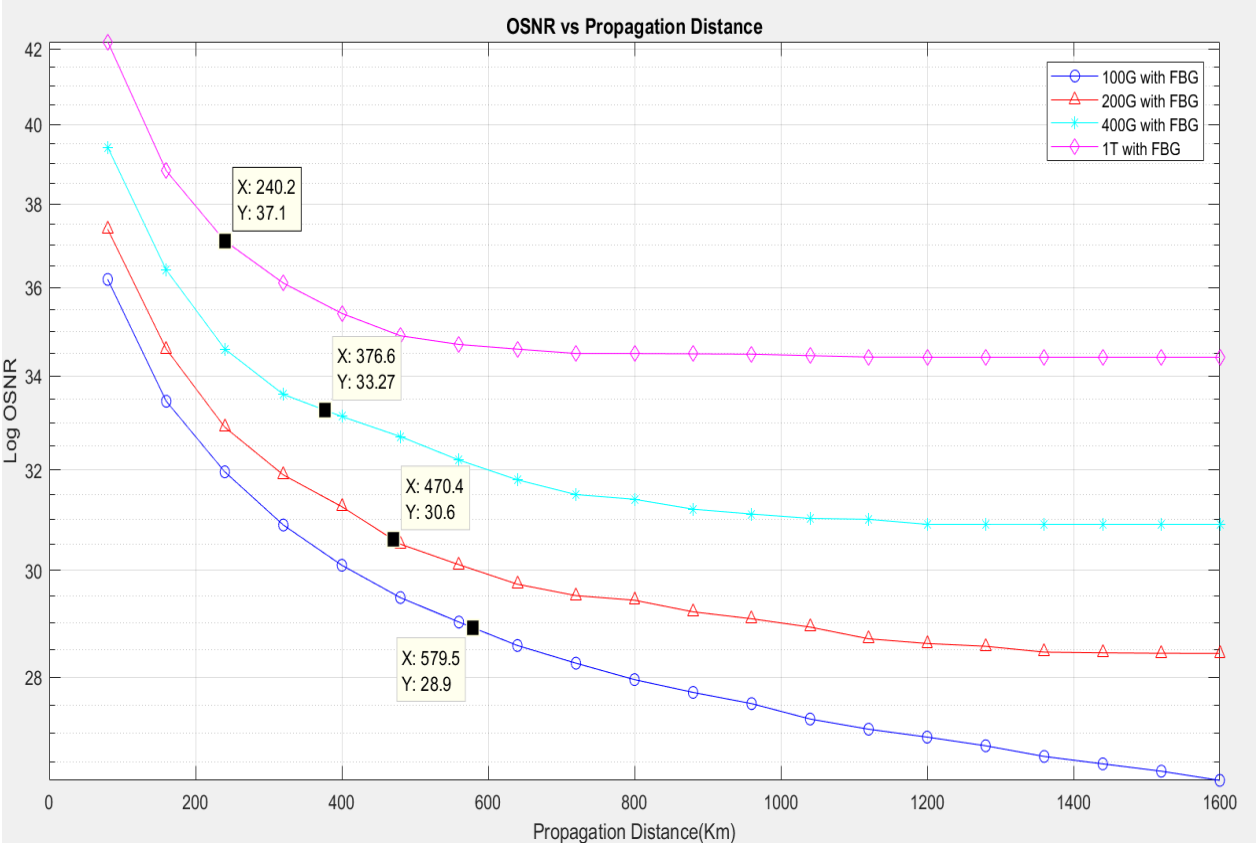

b)

Figure 5. 36: OSNR vs Propagation distance a) Without FBG b) With FBG

The OSNR values of each transmission capacity decrease as propagation distance increases for both systems, as shown in figures 5.36 a and b above. When FBG was not used in the system, transmission of 100G scored threshold 31.97 dB OSNR value at a distance of 160km, transmission of 200G scored threshold 32.61 dB OSNR value at a distance of 160km, transmission of 400G scored threshold 33.01 dB OSNR value at a distance of 160km, and transmission of 1T scored threshold 35.67 dB at a distance of 80km, according to the OSNR vs Propagation distance plot Transmission of 100G scored threshold 28.9dB OSNR value at a distance of 579.5km, transmission of 200G scored threshold 30.6 dB OSNR value at a distance of 470.4km, transmission of 400G scored threshold 33.27dB OSNR value at a distance of 376.6km, and transmission of 1T scored threshold 37.1dB at a distance of 240.2km when FBG was integrated in the system.

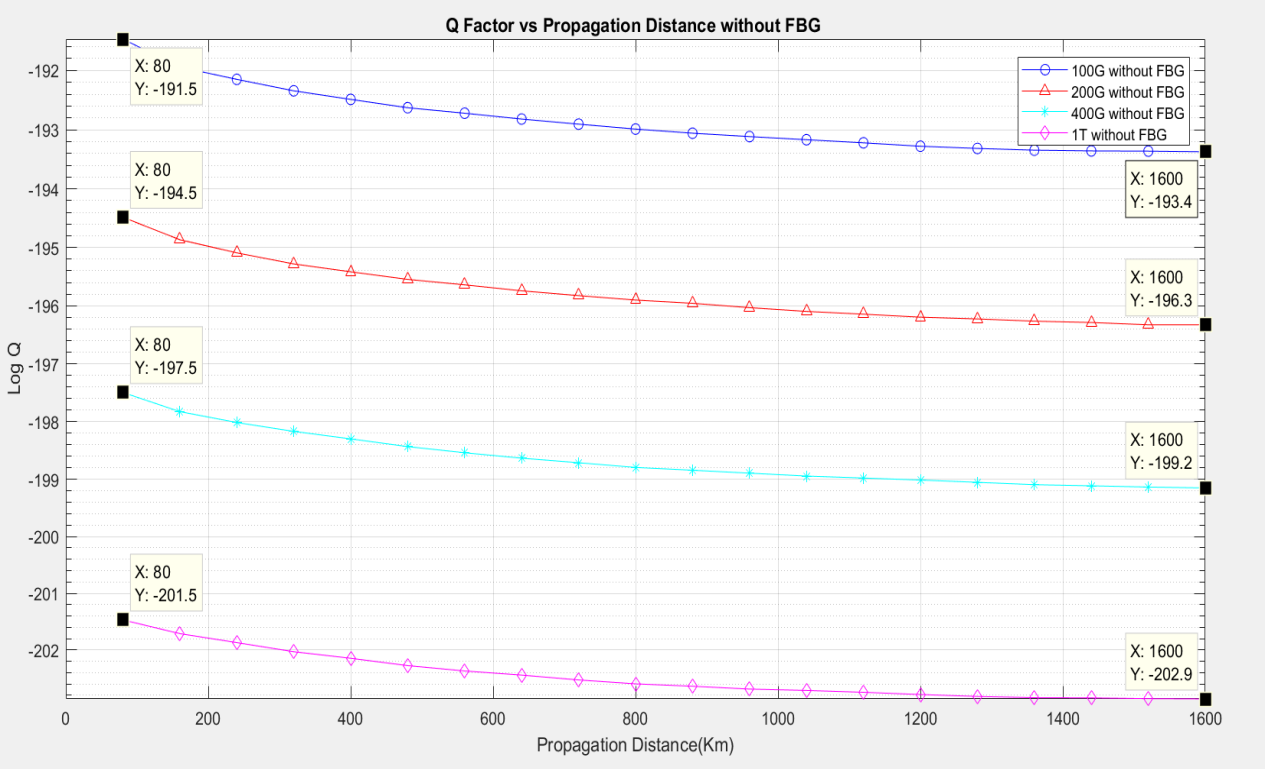

a)

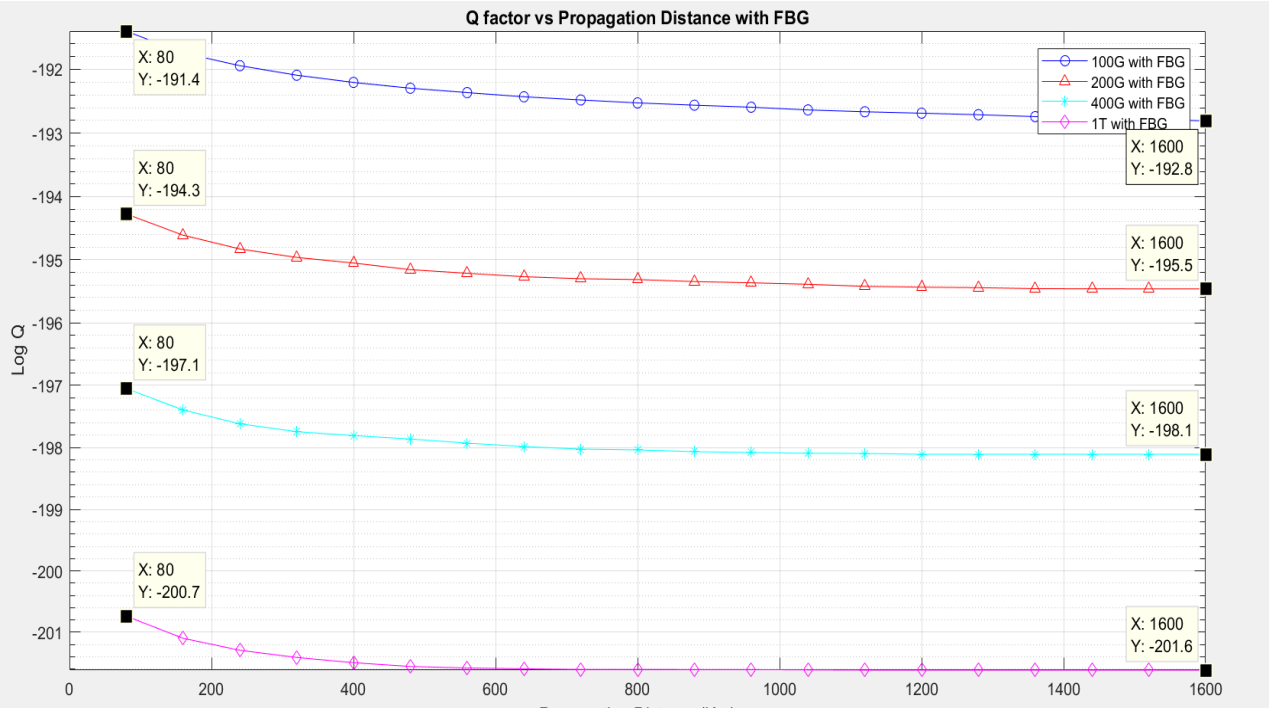

a) b)

Figure 5. 37: Q factor vs Propagation distance a) Without FBG b) With FBG

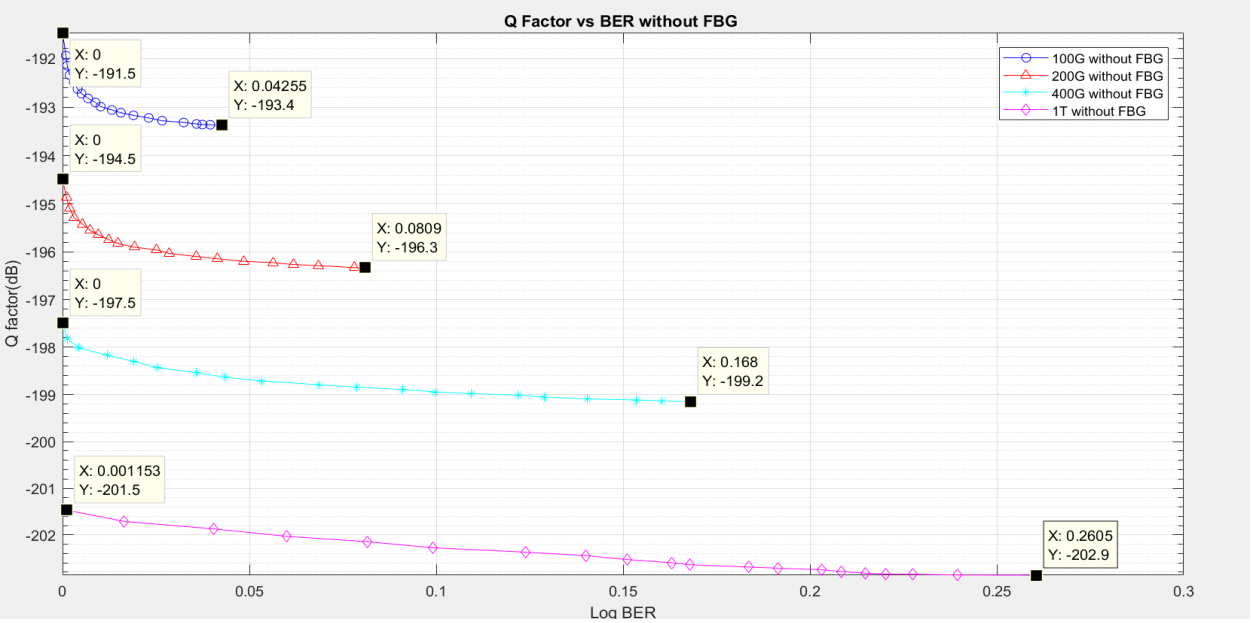

a)

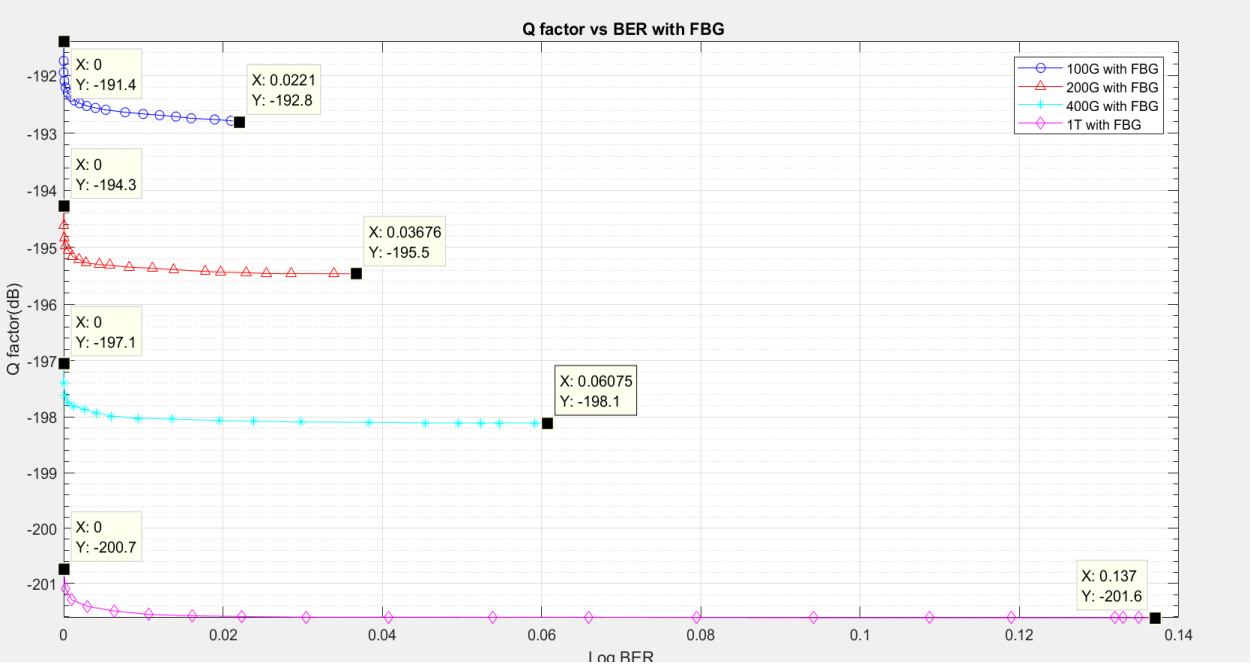

b)

Figure 5. 38: Q factor vs BER a) Without FBG b) With FBG

For both DP-16QAM Co-O-OFDM systems with and without FBG, as shown in figures 5.38 a and b, Q factor decreases as distance and BER increase. As BER and distance increase, the minimum optical signal-to-noise ratio (OSNR) required to get a specified BER value for a given signal decreases.

CHAPTER SIX

Conclusion and Recommendation

6.1. Conclusion

Finally, the purpose of this thesis was to investigate the impact of dispersion, such as chromatic dispersion (CD), on signal transmission across optical channels. As the transmission distance increases in optical communication, the signal overlaps with surrounding pulses, causing the signal to spread. The coherent detection OFDM system, as well as the integration of coherent detection with fiber Bragg grating (FBG) as dispersion compensation technique, have been used to mitigate this problem. Coherent optical OFDM is the future of optical communication since it combines the benefits of both the coherent detection system and OFDM technology, and it has been hailed as a potential solution for the next generation of high-capacity optical networks. Fiber Bragg Grating (FBG) is a conventional dispersion compensation technology that lowers the effect of dispersion by reflecting short wavelength signals back through its grating. In this thesis, two fiber optic communication systems, namely Co-O-OFDM and integration of Co-O-OFDM with FBG, were analyzed for four different high speeds i.e. for 100Gbps, 200Gbps, 400Gbps and 1Tbps at different propagation distances of single mode fiber. For both systems DP-16QAM advanced modulation technique was used for mapping and de-mapping as single carrier modulation technique in the RF OFDM transmitter and receiver. OSNR, BER and Q-factor, are metrics used to analyze the outputs of both systems and RF spectrum, optical spectrum and constellation diagrams were used to demonstrate the spectrum property of the signal for both systems.

Based on results of simulations we can conclude that for both systems distortion of the signal due to chromatic dispersion increased as transmission distance increased i.e. OSNR value decreased as transmission distance increased for both systems. Propagation distance required to get BER value of 10^{-3} (which represents the limit beyond which the FEC function becomes inefficient) is decreased for both systems with transmission capacity. That is Q-factor, which indicates the minimum signal-to-noise ratio (SNR) required to obtain a specific BER value of 10^{-3} for a given signal, is decreased with transmission distance. When we compare both systems namely Co-O-OFDM systems and FBG integrated Co-O-OFDM system, for specific transmission capacity, FBG

integrated Co-O-OFDM system has shown better performances in terms of BER, OSNR and Q-factor values obtained.

6.2. Recommendation

The focus of this thesis was to analyze performance of high speed fiber optic communication system using coherent optical OFDM and its integration with Fiber Bragg Grating(FBG) with DP-16QAM as single carrier modulation technique to minimize chromatic dispersion. This thesis can be further extended to the following areas, so that better performance can be obtained in different dimensions. It can be extended using higher order advanced modulation techniques like DP-64QAM, DP-128QAM and DP-256QAM instead of DP-16QAM so that spectral efficiency of the system can be increased. Other type of advanced modulation techniques like DP-16QPSK can be used as single modulation technique in the RF-OFDM stages and can be compared so that systems with better performance based on maximum propagation distance can be achieved to get BER value of 10^{-3}. Further this system can be integrated with WDM system to get better performance. This study can be extended using multimode fiber and multiple user. In the channel environment other linear and non-linear impairments can be considered in the future study.

References

[1] P. J. Winzer, D. T. Neilson, and A. R. Chraplyvy, "Fiber-optic transmission and networking: the previous 20 and the next 20 years," Optics express, vol. 26, pp. 24190-24239, 2018.

[2] N. Muchhal and A. Bhatt, "High Speed and Spectrally Efficient Optical Communication System-Review of the Recent Advances and Emerging Trends."

[3] W. shieh and I. Djordjevic, OFDM for Optical Communications, 2009.

[4] P. Sharma, S. Pardeshi, R. K. Arora, and M. Singh, "A review of the development in the field of fiber optic communication systems," International Journal of Emerging Technology and Advanced Engineering, vol. 3, pp. 113-119, 2013.

[5] G. P. Agrawal, Fiber-optic communication systems vol. 222: John Wiley & Sons, 2012.

[6] P. K. Dubey and V. Shukla, "Dispersion in optical fiber communication," International Journal of Science and Research, vol. 3, pp. 236-239, 2014.

[7] M. Chakkour, O. Aghzout, B. Ait Ahmed, F. Chaoui, and M. El Yakhloufi, "Chromatic Dispersion Compensation Effect Performance Enhancements Using FBG and EDFA-Wavelength Division Multiplexing Optical Transmission System," International Journal of Optics, vol. 2017, p. 6428972, 2017/12/14 2017.

[8] I. I. Jude, Y. Adamu, O. D. Onoja, and B. Andrew, "Efficient Chromatic and Residual Dispersion Postcompensation for Coherent Optical OFDM."

[9] K. Alatawi, F. Almasoudi, and M. Matin, "Performance Study of 1 Tbits/s WDM Coherent Optical OFDM System," Optics and Photonics Journal, vol. 03, pp. 330-335, 01/01 2013.

[10] A. T. Jaber, S. S. Ahmed, and S. A. Kadhim, "Next Generation of High-Speed Optical Communications Networks Using OFDM Technology," in Journal of Physics: Conference Series, 2020, p. 012092.

[11] R. Chhilar, J. Khurana, and S. Gandhi, "Modulation formats in optical communication system," IJCEM International Journal of Computational Engineering & Management, vol. 13, pp. 110-115, 2011.

[12] E. Lach and W. Idler, "Modulation formats for 100G and beyond," Optical Fiber Technology, vol. 17, pp. 377-386, 2011.

[13] A. J. Lowery, "Optical OFDM," in 2008 Conference on Lasers and Electro-Optics and 2008 Conference on Quantum Electronics and Laser Science, 2008, pp. 1-2.

[14] X. Luo, "The application of OFDM in optical fiber communication systems," IOP Conference Series: Earth and Environmental Science, vol. 332, p. 042010, 11/05 2019.

[15] F. Ali, E. A. A. A. Ali, and M. G. Tarbul, "Performance Analysis of Radio over Optical Fiber System with OFDM Using Multiplexing Techniques," 2018.

[16] Q. Yang, Y. Tang, Y. Ma, and W. Shieh, "Experimental demonstration and numerical simulation of 107-Gb/s high spectral efficiency coherent optical OFDM," Journal of Lightwave Technology, vol. 27, pp. 168-176, 2009.

[17] H. ALI, "Modeling and simulation of high speed optical fiber communication system with OFDM," Mémoire de Master, Université Normale Centrale de Chine, 2015.

[18] V. P. Patil and A. Tamboli, "Performance Evaluation of High Speed Coherent Optical OFDM System Using Wiener-Hammerstein Equalizer."

[19] I. R. Noé, P. Schreier, and D. EIM-E, "DSP based CD and PMD Equalization Techniques in PDM-QPSK and PDM-16-QAM Receivers."

[20] R. Sethi and A. Goel, "Dispersion compensation in optical communication system by employing 16-QAM modulation using OFDM," Int J Res Eng Technol, vol. 3, pp. 47-64, 2015.

[21] H. A. Fadhil, H. Y. Ahmed, and S. A. Aljunid, "Performance analysis of hybrid optical OFDM system with high order dispersion compensation," in The 17th Asia Pacific Conference on Communications, 2011, pp. 117-120.

[22] A. Güner, "Performance Analysis of 20 Gb/s QPSK Modulated Dual Polarization Coherent Optical OFDM Systems," Turkish Journal of Science and Technology, vol. 12, pp. 65-69, 2017.

[23] T. Jaemkarnjanaloha, R. Maneekut, and P. Kaewplung, "Long-haul Coherent Optical OFDM Point-to-Point Transmission using Optical Phase Conjugation," in OPTICS, 2016, pp. 43-47.

[24] R. Kamran, S. Naaz, S. Goyal, and S. Gupta, "High-Capacity Coherent DCIs Using Pol-Muxed Carrier and LO-Less Receiver," Journal of Lightwave Technology, vol. 38, pp. 3461-3468, 2020.

[25] Y. Bao, W. Lin, J. Fu, T. Gui, L. Yang, Z. Li, et al., "50Gbps DDO-OFDM transmission after 80km without DCF based on an electro-absorption modulator," in 10th International Conference on Optical Communications and Networks (ICOCN 2011), 2011, pp. 1-2.

[26] K. Borade and S. Kadlag, "The design of 100 Gb/s QAM modulated CO-OFDM system based on dual polarization," in 2016 International Conference on Communication and Signal Processing (ICCSP), 2016, pp. 2105-2108.

[27] X. Wang, B. Leible, W. Wang, D. Rörich, and S. ten Brink, "Joint IQ imbalance compensation and channel estimation in coherent optical OFDM systems," in 2016 10th International Conference on Signal Processing and Communication Systems (ICSPCS), 2016, pp. 1-6.

[28] S. A. H. Basha, D. Ghosh, and P. Sahu, "4-QAM and 16-QAM modulation employing single dual drive Mach-Zehnder modulator and FBG for OFDM-radio-over-fiber system," in 2017 International Conference on Communication and Signal Processing (ICCSP), 2017, pp. 1010-1012.

[29] Y. Tang, Y. Ma, and W. Shieh, "Performance impact of inline chromatic dispersion compensation for 107-Gb/s coherent optical OFDM," IEEE Photonics Technology Letters, vol. 21, pp. 1042-1044, 2009.

[30] M. S. Miah and M. M. Rahman, "The Performance Analysis Fiber Optic Dispersion on OFDM-QAM System," International Journal of Computer Networks and Wireless Communications (IJCNWC), vol. 1.

[31] D. R. Smith, "Fiber Optic Transmission Systems," in Digital Transmission Systems, ed: Springer, 2004, pp. 472-546.

[32] J. Juniet, "Fiber Optic Transmission Systems," in National Association of Broadcasters Engineering Handbook, ed: Routledge, 2017, pp. 1025-1034.

[33] S. Kumar and M. J. Deen, Fiber optic communications: fundamentals and applications: John Wiley & Sons, 2014.

[34] R. Shevgaonkar, "Fiber Optics," IIT Bombay, 2005.

[35] A. A. GHATAK, A. Ghatak, K. Thyagarajan, and K. Thyagarajan, An introduction to fiber optics: Cambridge university press, 1998.

[36] G. Breed, "A tutorial introduction to optical modulation techniques," High Frequency Electronics, 2007.

[37] A. Amari, O. A. Dobre, R. Venkatesan, O. S. Kumar, P. Ciblat, and Y. Jaouën, "A survey on fiber nonlinearity compensation for 400 Gb/s and beyond optical communication systems," IEEE Communications Surveys & Tutorials, vol. 19, pp. 3097-3113, 2017.

[38] C. Antonelli, A. Mecozzi, M. Shtaif, and P. J. Winzer, "Stokes-space analysis of modal dispersion in fibers with multiple mode transmission," Optics express, vol. 20, pp. 11718-11733, 2012.

[39] V. Bobrovs, S. Spolitis, and G. Ivanovs, "Comparison of chromatic dispersion compensation techniques for WDM-PON solution," in 2012 2nd Baltic Congress on Future Internet Communications, 2012, pp. 64-67.

[40] R. Udayakumar, V. Khanaa, and T. Saravanan, "Chromatic dispersion compensation in optical fiber communication system and its simulation," Indian Journal of Science and Technology, vol. 6, pp. 4762-4766, 2013.

[41] N. Kahlon and G. Kaur, "Various dispersion compensation techniques for optical system: A survey," Open journal of communications and software, vol. 1, pp. 64-73, 2014.

[42] M. O'Sillivan, K. Roberts, and C. Bontu, "Electronic dispersion compensation techniques for optical communication systems," in 2005 31st European Conference on Optical Communication, ECOC 2005, 2005, pp. 189-190.

[43] K. O. Hill and G. Meltz, "Fiber Bragg grating technology fundamentals and overview," Journal of lightwave technology, vol. 15, pp. 1263-1276, 1997.

[44] R. Sethi and A. Goel, "Performance analysis of optical communication systems using OFDM by employing QPSK modulation," International Journal on Recent and Innovation Trends in Computing and Communication, vol. 3, pp. 226-237, 2015.

[45] A. Barbieri, G. Colavolpe, T. Foggi, E. Forestieri, and G. Prati, "OFDM versus single-carrier transmission for 100 Gbps optical communication," Journal of Lightwave Technology, vol. 28, pp. 2537-2551, 2010.

[46] Q. Yang, A. Al Amin, and W. Shieh, "Optical OFDM basics," in Impact of nonlinearities on fiber optic communications, ed: Springer, 2011, pp. 43-85.

[47] J. Armstrong, "OFDM for optical communications," Journal of lightwave technology, vol. 27, pp. 189-204, 2009.

[48] P. J. Winzer and R.-J. Essiambre, "Advanced optical modulation formats," Optical Fiber Telecommunications VB, pp. 23-93, 2008.

[49] S. K. Mohapatra, "ANALOG AND DIGITAL MODULATION FORMATS OF OPTICAL FIBER COMMUNICATION WITHIN AND BEYOND 100 GB / S : A COMPARATIVE OVERVIEW," 2013.

[50] D. Kakati and S. C. Arya, "Performance of 120 Gbps single channel coherent DP-16-QAM in terrestrial FSO link under different weather conditions," Optik, vol. 178, pp. 1230-1239, 2019.

[51] A. H. Gnauck, P. J. Winzer, S. Chandrasekhar, X. Liu, B. Zhu, and D. W. Peckham, "10× 224-Gb/s WDM transmission of 28-Gbaud PDM 16-QAM on a 50-GHz grid over 1,200 km of fiber," in Optical Fiber Communication Conference, 2010, p. PDPB8.

[52] M. S. Alfiad, M. Kuschnerov, S. Jansen, T. Wuth, D. Van Den Borne, and H. De Waardt, "Transmission of 11× 224-Gb/s POLMUX-RZ-16QAM over 1500 km of LongLine and pure-silica SMF," in 36th European Conference and Exhibition on Optical Communication, 2010, pp. 1-3.

[53] J. R. Barry, E. A. Lee, and D. G. Messerschmitt, Digital communication: Springer Science & Business Media, 2012.

[54] A. Lowery and J. Armstrong, "Adaptation of orthogonal frequency division multiplexing (OFDM) to compensate impairments in optical transmission systems," in Proc. ECOC, 2007, pp. 121-152.

[55] K. Alatawi, "High Data Rate Coherent Optical OFDM System for Long-Haul Transmission," 2013.

[56] N. Albakay, "Design and Analysis of Binary Driven Coherent M-ary Qam Transmitter for Next Generation Optical Networks," 2018.

[57] J. M. Senior and M. Y. Jamro, Optical fiber communications: principles and practice: Pearson Education, 2009.

[58] K. Kikuchi, "Digital coherent optical communication systems: Fundamentals and future prospects," IEICE Electronics Express, vol. 8, pp. 1642-1662, 2011.

[59] E. Ip, A. P. T. Lau, D. J. Barros, and J. M. Kahn, "Coherent detection in optical fiber systems," Optics express, vol. 16, pp. 753-791, 2008.

[60] A. B. Dar and R. K. Jha, "Chromatic dispersion compensation techniques and characterization of fiber Bragg grating for dispersion compensation," Optical and Quantum Electronics, vol. 49, p. 108, 2017.

[61] D. Kakati and S. C. Arya, "A full-duplex pilot-assisted DP-16-QAM CO-OFDM system for high-speed long-haul communication," in 2019 2nd International Conference on Innovations in Electronics, Signal Processing and Communication (IESC), 2019, pp. 183-187.

[62] S. M. S. Kenshil, "Study of Optical OFDM System for Wireless LAN Applications," University of Denver, 2018.

[63] B. Sklar, "Digital communications : fundamentals and applications," 2020.

[64] E. Heras Miguel, "Fiber-based orthogonal frequency division multiplexing transmission systems," Universitat Politècnica de Catalunya, 2010.

[65] L. N. Binh, "Advanced Digital: Optical Communications," ed: CRC Press, 2015.

[66] G. Goldfarb, "Digital signal processing techniques for coherent optical communication," 2008.CCCCCCC

[67] M. Chakkour, O. Aghzout, B. Ait Ahmed, F. Chaoui, and M. El Yakhloufi, "Chromatic dispersion compensation effect performance enhancements using FBG and EDFA-wavelength division multiplexing optical transmission system," International Journal of Optics, vol. 2017, 2017.

[68] A. Sheetal, H. Singh, and A. Kumar, "Simulative Analysis of 10 Gb/s Coherent Detection Orthogonal Frequency Division Multiplexing Based Optical Communication System," in International Conference on Computing, Communication & Systems, 2014, pp. 242-246.